Structural, Thermal and Optical Study of Ge-Se-Sb Glassy System

A THESIS SUBMITTED TO
THE FACULTY OF PHYSICAL SCIENCES
HIMACHAL PRADESH UNIVERSITY

FOR THE AWARD OF
THE DEGREE OF

DOCTOR OF PHILOSOPHY
IN
PHYSICS

SUPERVISED BY

Dr. Vir Singh Rangra

SUBMITTED BY

Parikshit Sharma

DEPARTMENT OF PHYSICS
HIMACHAL PRADESH UNIVERSITY
SHIMLA-05

2010

Dedicated
To
His Holy Param Sant
Thakur Singh Ji Maharaj

Dr. Vir Singh Rangra
Associate Professor

HIMACHAL PRADESH UNIVERSITY
DEPARTMENT OF PHYSICS
SUMMER HILL, SHIMLA – 05

CERTIFICATE

Certified that Mr. Parikshit Sharma carried his research work on, **"Structural, Thermal and Optical Study of Ge-Se-Sb Glassy System"** under my supervision. The work is original and has not been submitted in part or full, for the other degree of this or any other university and is worthy of consideration for the award of the degree of Doctor of Philosophy in Physics.

Dated: 19 August, 2010

(Dr. Vir Singh Rangra)

ACKNOWLEDGEMENTS

I would never have been able to complete all this work just by myself and would like to truly acknowledge those who helped me along this way.

First of all I am heartily thankful to my esteemed Research Supervisor, ***Dr. Vir Singh Rangra****, Associate Professor, Department of Physics, Himachal Pradesh University, Shimla. His encouragement, guidance and support from the initial to the final level enabled me to develop an understanding of the subject. His benevolent and cordial attitude has always allowed me to express myself without hesitation.*

My sincere thanks to ***Dr. S. K. Dhiman****, Chairman, Department of Physics, for providing necessary facilities to carry out this work. I am thankful to entire laboratory and office staff of Department of Physics, Himachal Pradesh University, for their assistance at various stages of my work.*

I feel it my first and foremost duty to express my deep sense of gratitude and pay my sincere thanks to ***Dr. Pankaj Sharma****, Department of Physics, JUIT, Solan, for valuable guidance and requisite help in the present study. Without his kind help and proper guidance, it would not have been possible for me to complete this research work.*

My deepest gratitude goes to my family for the unflagging love and support throughout my life. This thesis was simply impossible without them. I am indebted to my mother ***Smt. Kusum Sharma****, for her tender care and love. She works whole heartedly to support the family and spare no effort to provide the best possible environment for me to grow up and study. I know she is the happiest person to see her son accomplishing his dream. I extend my gratitude to my dear Mamaji* ***Mr. Hem Raj Sharma*** *for always supporting me in my deeds and helping me to achieve my goals.*

There are moments in life when you feel directionless like heading nowhere. You get frustrated and demoralized and need a boost. The person, who deserves special mention here, is my dear fiancée ***Pooja****. She is like a backbone not letting me collapse during such gloomy hours. It is her affection and faith that gives me the courage to fulfill life's daunting jobs. This work would not have been possible without her valuable contribution.*

I express my sincere thanks to ***Prof S. C. Katyal, ADT Rakesh Verma, Asso. Prof. Raman Sharma*** *and* ***Dr. Raman Rana*** *for their invaluable help and necessary guidance throughout my research work.*

The completion of this work would not have been possible without the valuable contribution of my dear friends and well wishers ***Varun Mishra, Chander kant, Pawan, Dr. Kuldeep, Dr.Ajay Awasthi, Dr. Nikhilesh, Anamol, Vivek, Rajneesh , Vijay, Dheeraj, Ankit, Shivani, Ravi*** *and* ***Arun Poonchi.***

Finally, for completion of this work, I thank to the almighty GOD for fulfilling my desire to complete this study under HIS kind blessings.

Parikshit Sharma

Dated: ..19/08/10...

(Parikshit Sharma)

CONTENTS

LIST OF TABLES

LIST OF FIGURES

LIST OF PUBLICATIONS

Publications in International Journals:

1. **Parikshit Sharma**, V. S. Rangra, Pankaj Sharma and S. C. Katyal, "*Far Infrared Study of Amorphous $Ge_{0.17}Se_{0.83-x}Sb_x$ Chalcogenide Glasses*" **Journal of Alloys and Compounds**, (Elsevier: Netherlands) **480** (2009) 934-937

2. **Parikshit Sharma**, V. S. Rangra, Pankaj Sharma, S. C. Katyal, "*Effect of antimony addition on the optical behaviour of germanium selenide thin films*" **Journal of Physics D: Applied Physics 41** (2008) 225307.

3. **Parikshit Sharma**, V.S. Rangra, S.C. Katyal, Pankaj Sharma, "*Compositional dependence of physical parameters in $Ge_{17}Se_{83-x}Sb_x$ (x = 0, 3, 6, 9, 12, 15) glassy semiconductors*" **Optoelectron. Adv. Mater. – Rapid Commun. 1** (2007) 363.

4. V.Modgil, **Parikshit Sharma,** V.S.Rangra "*Structural study of Se-Te-Zn system using XRD spectra"* **Journal of Ovonic Research 6** (2010) 125-133.

Conferences (National/International):

1. **Parikshit Sharma**, V. S. Rangra, S. C. Katyal, Pankaj Sharma, "*Determination of refractive index and extinction coefficient for Ge-Se-Sb thin films*" National Conference – Semiconductor Materials and Technology **(NC – SMT 2008)** (Gurukula Kangri University Oct 16-18, 2008).

2. **Parikshit Sharma**, V. S. Rangra, S. C. Katyal, Pankaj Sharma. "*Optical energy gap study of $Ge_{0.17}Se_{0.83-x}Sb_x$ thin films*" **DAE – Solid State Physics Symposium** (BARC-Mumbai) **53** (2008).

3. **Parikshit Sharma**, V. S. Rangra, **Pankaj Sharma** and S. C. Katyal, "*Bonding arrangement study of amorphous $Ge_{0.17}Se_{0.83}$ and $Ge_{0.17}Se_{0.80}Sb_{0.03}$ chalcogenide glasses*" International Conference on Multifunctional Oxide Materials (**IC MOM, H.P. University, Shimla**) (2009).

Chapter-1

Introduction

1.1: Introduction

The material substances exist in three states of aggregation: the solid state, the liquid state and the gaseous state. In solids and liquids, the distance between the neighboring atoms is of the order of a few angstroms, while in gases the distance between the molecules or atoms is quite large as compared to solids and liquids. Solid materials are formed from densely-packed atoms, with intense interaction forces between them. These interactions are responsible for the mechanical (e.g. hardness and elasticity), thermal, electrical, magnetic and optical properties of solids. Depending on the material involved and the conditions in which it was formed, the atoms may be arranged in a regular geometric pattern (crystalline solids) or irregularly (amorphous solids). The forces between the atoms in a solid can take a variety of forms. For example, the crystal of sodium chloride is made up of ionic sodium and chlorine and held together with ionic bonds. In covalent solids the atoms share electrons and form covalent bonds. In metals electrons are shared by metallic bonding. Other solids, particularly including most organic compounds, are held together with Van der Waals forces resulting from the polarisation of the electronic charge cloud on each molecule. The differences between the types of solid result from the differences between their bonding.

In crystalline solids, the atoms or molecules that compose the solid are packed closely together. These constituent elements have fixed positions in space relative to each other. This accounts for the solid's structural rigidity. In mineralogy and crystallography, a crystal structure is a unique arrangement of atoms in a crystal. A

specific symmetry or crystal structure is composed of a Bravais lattice which is typically represented by a single unit cell. The unit cell is periodically repeated in three dimensions on a lattice. The spacing between unit cells in various directions is called lattice parameters. The symmetry properties of the crystal are embodied in its space group. A crystal's structure and symmetry play a role in determining many of its physical properties, such as cleavage, electronic band structure and optical properties.

An "amorphous solid" is a solid in which there is no long-range order of the positions of the atoms. Most classes of solid materials can be found or prepared in an amorphous form. For instance, common window glass is an amorphous solid, many polymers (such as polystyrene) are amorphous and even foods such as cotton candy are amorphous solids. Glasses do not exhibit the long-range order exhibited by crystalline substances. Strongly supercooled liquids behave partly as liquids and partly as glasses depending on the time scale of observation. Much work has been done to elucidate the primary microstructural features of glass forming substances (e.g. silicates) on both microscopic and macroscopic scales. One emerging school of thought is that a glass is simply the "limiting case" of a polycrystalline solid at small crystal size. Within this framework, domains exhibiting various degrees of short-range order become the building blocks of both metals and alloys as well as glasses and ceramics. The microstructural defects of both within and between these domains provide the natural sites for atomic diffusion and the occurrence of viscous flow and plastic deformation in solids [1].

In principle any liquid can be made into an amorphous solid by giving it a sufficiently high cooling rate. Cooling reduces molecular mobility. If the cooling rate

is faster than the rate at which molecules can organize into a more thermodynamically favorable crystalline state, then an amorphous solid will be formed. Because of entropy considerations, many polymers can be made amorphous solids by cooling even at slow rates. In contrast, if molecules have sufficient time to organize into a structure with two- or three-dimensional order, then a crystalline (or semi-crystalline) solid will be formed. Water is one example. Because of its small molecular size and ability to quickly rearrange, it cannot be made amorphous without resorting to specialized hyper quenching techniques. Amorphous materials can also be produced by additives which interfere with the ability of the primary constituent to crystallize. For example, addition of soda to silicon dioxide results in window glass and the addition of glycols to water results in a vitrified solid. Some materials such as metals are difficult to prepare in an amorphous state. Unless a material has a high melting temperature (as ceramics do) or low crystallization energy (as polymers tend to) cooling must be done extremely rapidly. As the cooling is performed, the material changes from a supercooled liquid, with properties one would expect from a liquid state material, to a solid. The temperature at which this transition occurs is called the glass transition temperature or T_g. The transition from the liquid state to the glass at a temperature below the equilibrium melting point of the material is called the glass transition. The glass transition temperature is approximately the temperature at which the viscosity of the liquid exceeds a certain value (about 10^{12} Pa s). The transition temperature depends on cooling rate, with the glass transition occurring at higher temperatures for faster cooling rates.

Amorphous phases are important constituents of thin films, which are solid layers of a few nm to some tens of μm thickness deposited upon an underlying substrate. So-called structure zone models were developed to describe the microstructure and morphology of thin films as a function of the homologous temperature T_h that is the ratio of deposition temperature over melting temperature [2,3]. According to these models, a necessary (but not sufficient) condition for the occurrence of amorphous phases is that T_h has to be smaller than 0.3 that is the deposition temperature must be below 30% of the melting temperature. For higher values, the surface diffusion of deposited atomic species would allow for the formation of crystallites with long range atomic order. Regarding their applications, amorphous metallic layers played an important role in the discussion of a suspected superconductivity in amorphous metals [4]. Today, optical coatings made from TiO_2, SiO_2, Ta_2O_5 etc. and combinations of them in most cases comprise of amorphous phases of these compounds. The technologically most important thin amorphous film is probably represented by few nm thin SiO_2 layers serving as isolator above the conducting channel of a metal-oxide semiconductor field-effect transistor (MOSFET). Also, hydrogenated amorphous silicon, a-Si:H in short, is of technical significance for thin film solar cells. In case of a-Si:H the missing long-range order between silicon atoms is partly induced by the presence by hydrogen in the percent range. The occurrence of amorphous phases turned out as a phenomenon of particular interest for studying thin film growth. Remarkably, the growth of polycrystalline films is often preceded by an initial amorphous layer, the thickness of which may amount to only a

few nm. The most investigated example is represented by thin multicrystalline silicon films, where such an initial amorphous layer was observed in many studies [5]. Wedge-shaped polycrystals were identified by transmission electron microscopy to grow out of the amorphous phase only after the latter has exceeded a certain thickness, the precise value of which depends on deposition temperature, background pressure and various other process parameters. The phenomenon has been interpreted in the framework of Ostwald's rule of stages [6] that predicts the formation of phases to proceed with increasing condensation time towards increasing stability. Experimental studies of the phenomenon require a clearly defined state of the substrate surface and its contaminant density etc., upon which the thin film is deposited.

Amorphous semiconductor is a solid state material that can be switched from one state to another. For example, the recording layer in phase change rewritable CDs and DVDs switches between an unstructured amorphous state that absorbs light and a structured crystalline state that allows light to pass. In phase change memory, the storage cell switches between states of low resistance to one of very high resistance. On the basis of difference in chemical bonding amorphous semiconductors can be broadly classified into three major categories viz: covalent non crystalline solids (including tetrahedral semiconductors and chalcogenide glasses), semiconducting oxide glasses and dielectric films.

Among these classifications our present work is mainly concerned with the study of chalcogenide glasses (CG).

1.2: Physical Properties of Chalcogenide Glasses

1.2.1: Structural properties

Crystalline solid state is characterized by strict order in the position of atoms even at large atomic distances. CGs could be characterized by short-range order (SRO) and partially by intermediate range order (IRO). That means that after changing the crystalline state of a crystal in vitreous or amorphous state, the shortest distance between neighboring atoms is almost the same as in the crystal, may be, only with small distortion, which certainly leads to destroying of the long-range order (LRO). For example, the first atomic coordination in the crystals and glasses of As_2S_3 and As_2Se_3 are almost the same [7]. Of course, this is not characteristic for all materials. The germinate glasses (Ge_xCh_{1-x}, where Ch=Se, Te, S) are a typical example of different SRO in crystals and glasses of the same composition [8, 9]. CGs bear some similarity to oxide glasses, since both oxygen and chalcogen belong to group VI in the Periodic Table. A CG can be regarded a kind of 'soft semiconductor', soft because its atomic structure is flexible and viscous (due to two-fold coordination of chalcogen atoms) and a semiconductor because it possesses a band gap energy (~2 eV) characteristic of semiconductor materials (1-3 eV). Accordingly, a CG may be characterized as being in between an oxide glass composed of three-dimensional networks and an organic polymer possessing one-dimensional chain structure [10]. Atomic bonding is, therefore, more rigid in CGs than that of organic polymers and more flexible that of oxide glasses (Fig. 1.1). Atomic structure and related properties in CGs depend upon preparation methods and history after preparation [11,12].

1.2.2: Electronic properties

CGs possesses electrical and optical band gaps of 1-3 eV and accordingly they can be regarded as amorphous semiconductors. Gap decreases in the sequence of S, Se and Te, reflecting enhanced metallic character. As a semiconductor, overall property of CGs can be grasped as the vertical sequence (Fig. 1.1). That is, with the change from organic semiconductors, chalcogenides, hydrogenated amorphous silicon films, to crystalline semiconductors, the electronic mobility becomes higher and a faster response is available. The material also becomes more rigid. Instead, material prices seem to increase with this sequence, which may reflect their typical preparation methods (coating, evaporation, glow discharge, and crystal-growth techniques).

Electrically CGs exhibit smaller conductivities than the corresponding crystals. This is because the electronic mobility is suppressed by band tail and gap states, which are manifestations of disordered structures. Glass can be regarded as a p-type semiconductor or, more exactly, hole conduction is greater than electron conduction [11,12]. In selenium at room temperature, holes exhibit conventional Gaussian transport with a mobility of 0.1 $cm^2 (Vs)^{-1}$. However, at low temperatures and, in several materials, at room temperature, holes exhibit so-called dispersive transport, and the effective mobility decreases to 10^{-5} $cm^2 (Vs)^{-1}$ or even less. Such hole motions are described in terms of multiple trapping with band-tail states or hopping transport in gap states. In general, the position of Fermi energy, which may be located near the center of the band gap, cannot be controlled by impurity doping. However, there are a few exceptions, such as Bi-Ge-Se, Pb-Ge-Se and Pb-In-Se, in which thermo power indicates n-type conduction [13-19].

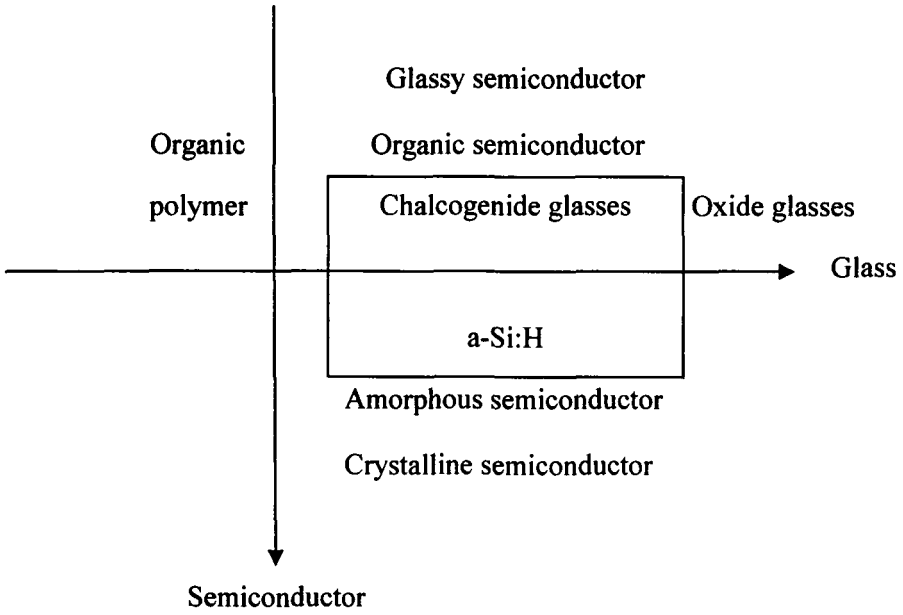

Fig. 1.1 Vertical sequence representing glasses

1.2.3: Optical properties

Extensive studies have been made on photo-induced phenomena in CGs [20,21]. At least seven distinct photo-induced phenomenon are observed in amorphous chalcogenides but not usually in crystalline chalcogenides. Photo-induced phenomena observed in CGs can be classified into two groups (Fig. 1.2): (i) It includes heat-mode phenomena, in which the heat generated through non-radiative recombination of photo-excited carriers triggers atomic structural changes; and (ii) Photon-mode, which can further be divided into the phenomena observed under illumination and after illumination. The best-known heat-mode phenomenon may be the optical phase change, or the optical Ovonic effect [20]. This phenomenon appears in tellurium compounds, which undergo thermal crystallization. A light pulse heats the film sample above crystallization temperature, resulting transformation from amorphous to crystalline phases. In some materials, this change is reversible. That is, a more intense light pulse heats the sample above melting temperature, and a successive temperature quenching can reproduce original amorphous structure. As for the photon-mode phenomena, reversible photo-darkening and related changes have been extensively studied [20,21]. Here, light illumination induces a red shift of the optical absorption edge, so that the sample becomes darker, while the red shift can be reversed with annealing at the glass-transition temperature. Refractive index in transparent wavelength regions increases with the red shift, which is consistent with the expectation obtained from the Kramers-Kronig relation. Sample volume, elastic, and

chemical properties also change with illumination and recover with annealing. As for the light, band gap illumination ($h\upsilon=E_g$) has been assumed to be effective. However, sub-gap light with photon energy lying in Urbach-tail region also produces some changes, which can be more prominent than those induced by band gap light [20]. Photo-darkening phenomenon continues to attract extensive interest, since this is a simple bulk phenomenon, which is characteristic of CG. That is, it does not appear in the corresponding crystal. Some structural studies have demonstrated that the amorphous structure becomes more disordered with illumination. However, it is difficult to identify explicitly the structural change in amorphous phases, and the mechanism is not yet elucidated. An example of photo-thermal bulk phenomena is the photo-induced anisotropy originally discovered by Fritzsche [20]. Macroscopically, untreated glasses are generally isotropic, while illumination with linearly polarized light can add some anisotropy such as dichroism, birefringence, and axial strains. Even unpolarized light can induce anisotropy if the light irradiates a side surface of a sample [20]. Photo-doping is a famous photo-thermal chemical reaction [20]. Consider a bilayer structure consisting of silver and AsS_2 films. When this bilayer is exposed to light, the silver film dissolves rapidly into the AsS_2. For instance, if the silver film is 10 nm in thickness, and the exposure is provided from the semitransparent silver side using a 100 W ultrahigh-pressure mercury lamp, the silver film will dissolve within few minutes.

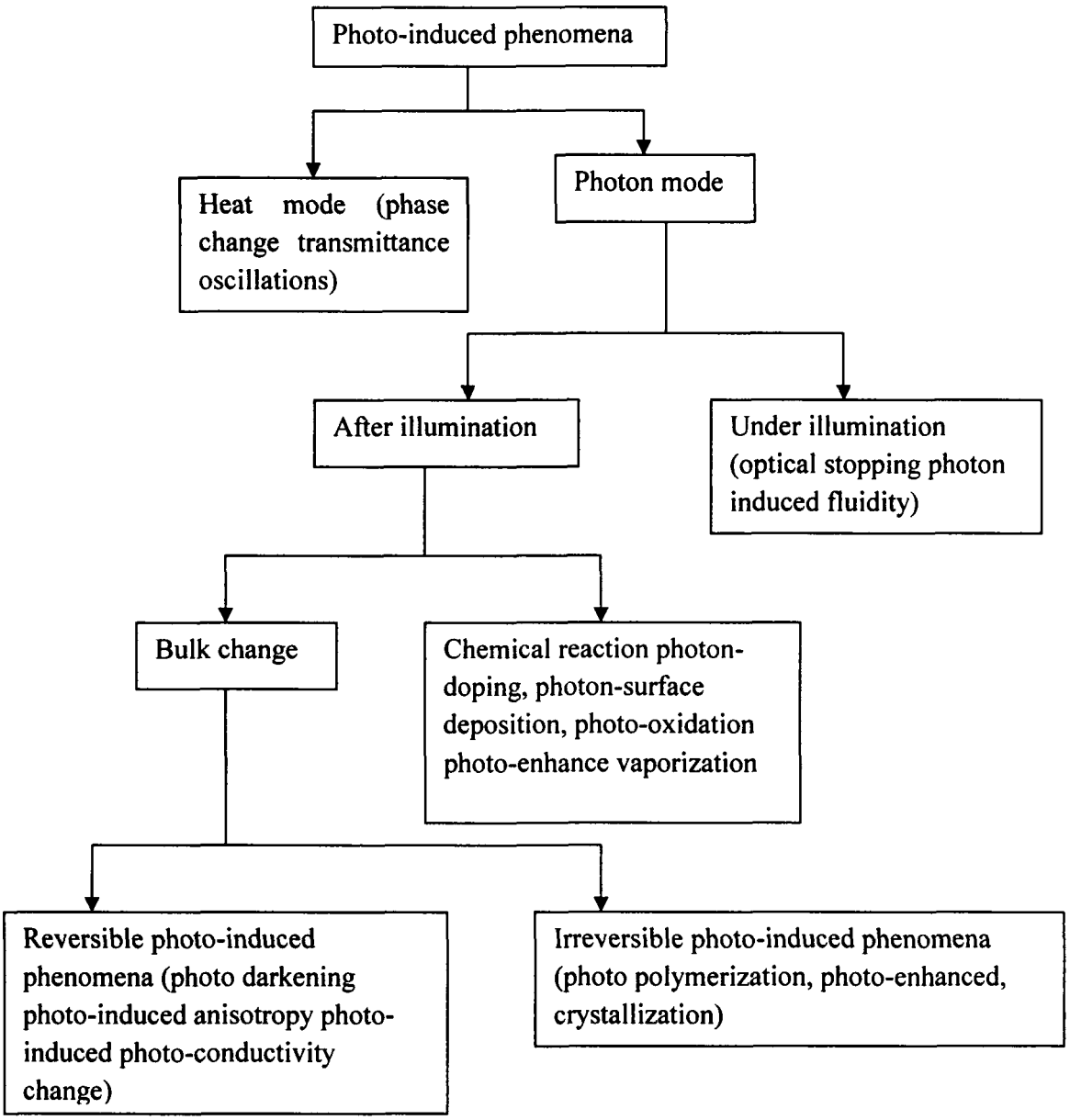

Fig. 1.2 Photo-induced phenomenon in chalcogenide glasses

Since the reaction becomes slower if the sample is illuminated at lower temperatures, this can be regarded as a photo-thermal phenomenon. However, it should be mentioned that temperature rise induced by illumination is not essential. There are also several irreversible and transitory changes. Examples are photo-polymerization and photo-induced fluidity [20]. Not only photons but also other excitations such as electrons can give rise to a variety of structural changes [22]. Some of these are similar to, but others are dissimilar from, the corresponding photon effects. For instance, electron beams can enhance silver doping into chalcogenide films like photons [22], while the beam can suppress crystallization of Se, in contrast to the photo- crystallization phenomenon. Studies using scanning tunneling microscopes etc. demonstrate nanometer scale structural changes in CGs.

1.2.4: Thermal properties

Many properties, especially that are time dependent, can be described from the enthalpic / temperature diagram (Fig. 1.3). When a CG is obtained from the liquid state and the cooling rate is high enough, enthalpy will follow the extrapolated liquid equilibrium curve and for a critical temperature, called the fictive equilibrium temperature (T_f), viscosity will increase drastically and enthalpy will leave the equilibrium curve and will reach a non-equilibrium state characterized by an excess of enthalpy [23]. This last state corresponds to the glassy state. Because of the lack of thermodynamic equilibrium, which characterizes these materials, two important phenomena will appear: i) Heating of a glass will lead to the appearance of a new transition called the glass transition, where the glass upon heating softens at a

characteristic temperature, known as the glass transition temperature, T_g, when molar volumes (V) and enthalpy (H) undergo a qualitative change; and ii) When the glass is maintained at a temperature lower than T_g, it will undergo structural relaxation (physical aging), observed by an enthalpic decrease.

T_g represents temperature above which an amorphous matrix can attain various structural configurations and below which the matrix is frozen into a structure, which cannot easily change to another structure. Therefore, it is reasonable to assume that T_g must be related to the magnitude of cohesive forces within the network since these forces must be overcome to allow for atom movement. Predictions of the T_g are generally based on simple models, in which it is assumed that T_g is proportional to another material parameter, which strongly depends on the cohesive forces or the rigidity of the network. Examples found in the literature of such parameters are average coordination number, enthalpy of atomization, overall mean bond energy, band gap or the average group number [24-26]. T_g is related to the average co-ordination number <z>. This relationship can be an exponential function as in [27] or follow the modified Gibbs–Dimarzio equation [28], which gives a reasonably good prediction of the T_g of CGs especially at low average coordination numbers. Physical quantities (melting temperature, magnitude of photo-darkening, mean atomic volume and width of the band tails in CGs) are also related with T_g [29-34]. Specific heat is another important thermal property of CGs, which is useful to understand the thermal relaxation process in these glasses. Specific heat is very sensitive to the way in which atoms or molecules are dynamically bound in a solid [35]. Thus measurement of such parameter like heat capacity will lead to an effective test for characterizing material as

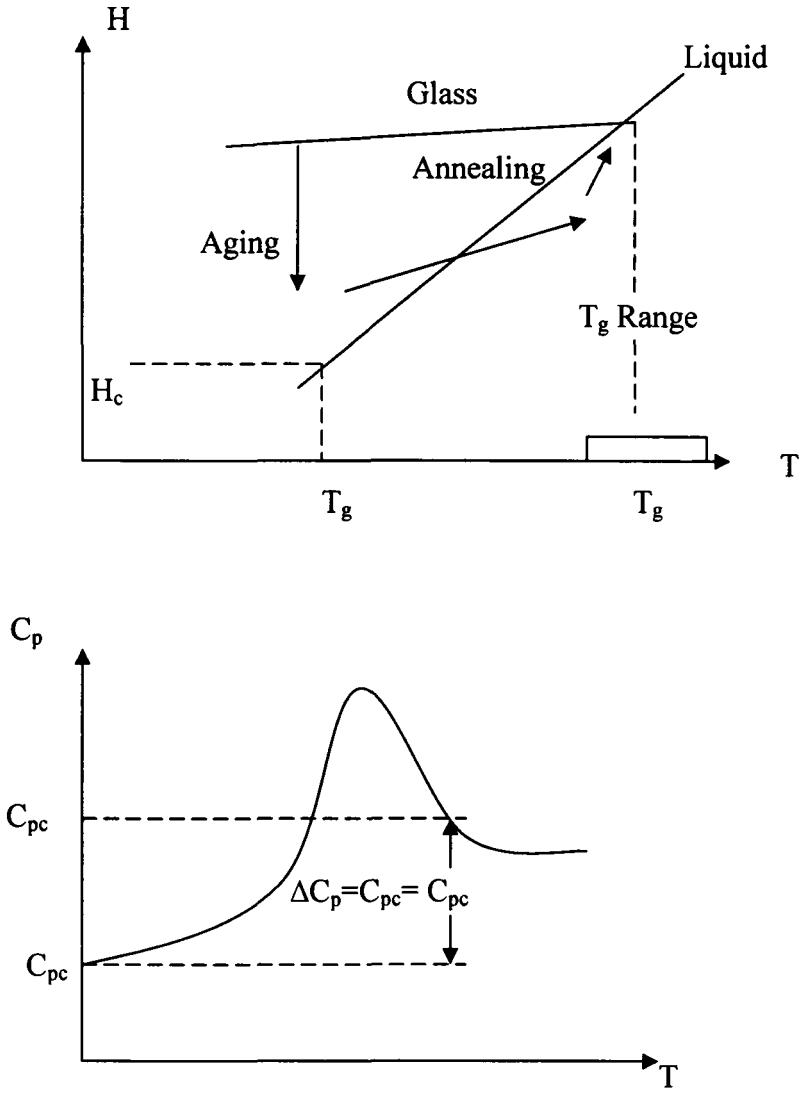

Fig. 1.3 Enthalpic / temperature diagram for chalcogenide glasses

glassy substance. An abrupt change in specific heat at the glass transition is characteristic of the all CGs. Below glass transition temperature, C_p is weakly temperature dependent (Fig. 1.3).

However, near glass transition temperature, C_p increases drastically with increase of temperature and shows maxima at glass transition temperature. After glass transition temperature, C_p attains a stable value, which is slightly higher as compared to C_p below glass transition temperature. The sudden jump in C_p value for each alloy at glass transition can be attributed [36] to anharmonic contribution to the specific heat. Overshoot in C_p at the upper end of "C_p jump" at glass transition is due to the relaxation effects. The time scale [37] for structural relaxation is highly dependent both on temperature and on the instantaneous structure itself. The observed peak in C_p at T_g may be due to the fact that the structural relaxation times at this temperature becomes of the same order as the time scale of experiment. Specific heat values after glass transition (equilibrium liquid specific heat, C_{pe}) and before glass transition (glass specific heat, C_{pg}) and their difference (C_p) are found useful for study of thermal relaxation in a particular CG.

1.3: Effects of chalcogenide glasses

One of the main properties of the chalcogenide materials is their sensibility to the action of light and other electromagnetic radiations. Therefore, many effects discovered in chalcogenide disordered materials are based on the action of light stated as below [38]:

1. The photo-darkening effect

It is defined as the shifts of the optical absorption edge towards longer wavelengths (lower energies), the so-called redshift. The effect appears when the chalcogenide glass (As_2S_3, As_2Se_3 or other chalcogenide alloys) is illuminated by light of energy above the band gap of the material.

2. The photo-bleaching effect

It is the reverse effect of photodarkening. In order to get photo- bleaching, it is important to illuminate the sample at a temperature a little bit larger than that, which favors the photo-darkening. The photo-bleaching is defined as the shift of the optical absorption edge of a chalcogenide material towards lower wavelengths (higher energies) when the sample is heated under T_g or illuminated with light of energy below the band gap.

3. The photo-plastic effect

This effect has been discovered and largely studied by Trunov and Bilanich . They observed that inorganic glasses are typically brittle materials at ambient temperature and this is due to the relatively low hardness as compared to their flow limit. By applying in-situ stress measurement to photostructural changes in chalcogenide films based on As-S(Se), Trunov and Bilanich have found essential dynamic changes in film plasticity, i.e. a reversible photo-induced transition from brittle to ductile state. The effect was explained in terms of the viscous flow of glasses under band gap illumination.

4. The photo-induced fluidity effect

It is the flow of a chalcogenide glass under illumination with sub-band gap light. The effect was discovered by Hisakuni and Tanaka.

5. The elongation effect

It was firstly reported by Vonwiller. He observed that the light influences the elongation speed in vitreous selenium fibers.

6. The photo-induced ductility effect

It was reported by Kastrissios et al.. The effect is related to fiber elongation under the action of light. The name of the effect reflects the presence of the combined action of illumination and application of an external stress.

7. The optomechanical effect

It was discovered by a group led by Elliott. The effect consists in the displacement of a cantilever with a chalcogenide film under the action of light. This displacement is the result of film internal stress relaxation or generation caused by increase or decrease in its plasticity (therefore is related to the photoplastic effect). Earlier B. V. Deryagin et al. reported an optomechanical effect in As-S films.

8. The polarization-dependent photoplastic effect

The polarization-dependent photoplastic effect in $As_{50}Se_{50}$ chalcogenide glasses has been discovered by Trunov and Bilanich. The authors have shown that band-gap linearly polarized light produces hardness anisotropy of the surface of the

$As_{50}Se_{50}$ films. The light induced decrease or increase of the plasticity of the glass depends on the polarization state of the incident light.

9. The light-stimulated interdiffusion effect

It was discovered by Kikineshi consists in the interdiffusion of the layers in multilayer structures based on chalcogenides (i.e. a-Se/As_2S_3) under the influence of light. An effective intermixing of components at short nanometer-size distances is produced and a volume increase is observed.

10. The photo-expansion effect

The photo-expansion effect consists in the increase of the volume of chalcogenide glasses under illumination. Sometimes a giant expansion effect is observed. In some films a photo-contraction effect is observed. The volume change during light induced diffusion in multilayers is due to the deviation from the Végard law during intermixing. The light stimulates the contraction- expansion effects, especially the giant photo expansion in nano-multilayers. Giant deformations (thickness changes up to 4-5 %) occurs under low-intensity laser illumination in a-Se/As_2S_3 nanolayer structures, similarly to the expansion effects observed in chalcogenide layers at high power illumination.

11. The photoinduced softening and hardening effect

The effect was observed in Ge-As-S films subjected to ultraviolet irradiation. This effect could be explained by the special property of chalcogenides: they are soft semiconductors, due to the two-fold coordinated chalcogen atoms, which are

susceptible to exhibit electro-atomic responses, and they behave as a flexible electron-lattice coupling system.

12. The photo-amplified oxidation effect

In ambient conditions the photo-oxidation is triggered during exposure to light. The composition $Ge_{35}S_{65}$ is the most sensible composition to this process.

13. The photo-dissolution and photo-doping effects

The first one consists in the photo- dissolution of the metals into a chalcogenide alloy. A metal layer deposited on the surface of a chalcogenide film diffuses in the chalcogenide under the influence of a light beam. The effect was discovered in 1966 by Kostishin et al. Silver diffuses very easily. A maximum silver concentration in a chalcogenide film is 29.1 %. The second one is related to the diffusion of various atoms at long distances, under the action of light.

14. The photo-polymerization effect

The polymerization of the glass during exposure to light, accompanied by a red shift of the optical absorption edge, is a typically irreversible phenomenon, which was observed both in evaporated arsenic-chalcogen films and simple chalcogenide films.

15. Photo-induced amorphisation effect

The amorphisation has not a thermal origin but an electronic one. The driving force of amorphisation is the presence of a small amount of amorphous phase and of strains.

1.4: Motivation and purpose of this research

Chalcogenide glasses have immense importance as they find applications in civil, medical and military areas to produce industrially electrical switches, xerographic and thermoplastic media, photo-resistant and holographic media, optical filters, optical sensors, thin films waveguides, nonlinear elements, etc. Application of chalcogenide glasses in infra-red optics includes energy management, thermal fault detection temperature monitoring and night vision. Chalcogenide infrared fibers are available today for spectroscopic applications but their applicability is still limited. Various other applications of the chalcogenide glasses will only be realized after much further study of their properties. All of the applications depend on our ability to engineer glass compositions to meet the specific requirement of the system. The tailoring of chalcogenide glasses for specific properties is possible but we do not know enough about most of the glassy systems to choose according to compositions. It is intent of this research to develop a basic understanding of the optical behavior of chalcogenides. These results may lead directly to the applications or more likely lay a foundation for other research into the optical behavior of chalcogenide glasses.

Chalcogenide glasses are having relatively high atomic mass and weak bond strength resulting low characteristic phonon energies (~50 – 450 cm^{-1}) even relative to fluoride glasses [39]. Thus, chalcogenide glasses are highly transparent in the mid to far infrared and they originally attract technological and commercial interest for use in IR windows and optics. The transparency window of sulphide glasses is 0.5-12 μm,

selenide glasses is approximately 0.8-15 μm while that of telluride glass transparency window extends to 20 μm wavelength range [40,41] . Related to their narrow band gaps and high linear refractive index, chalcogenide glasses exhibit high nonlinearities in the near IR wavelength region [42]. Key challenges for the use of chalcogenides (S, Se and Te) include disadvantages like short lifetime and low sensitivity etc. Due to high glass forming ability of Se it represents a good host matrix for the investigation of chalcogenide glasses in the bulk and in thin film forms [43-46]. Thus the above problems can be overcome by alloying Se with some impurity atoms (Bi, Sb, Ge, As, Pb etc), which gives higher sensitivity, higher crystallization temperature and smaller aging effects [47-49]. Here we have chosen Ge as an additive to Se. Since alloying of Se with Ge improves the thermal stability and gives smaller aging effects. The third element added is Sb as it improves thermal stability and enhances the IR transmission of Ge-Se glasses.

The present work deals with the systematic study of structural, physical, thermal and optical properties of $Ge_{17}Se_{83-x}Sb_x$ (x = 0, 3, 9, 12, 15) glassy system. Ge-Se system is the most studied system for its structural, electrical and optical properties. There is enough structural data on the Ge-Se systems but the structural study on the addition of Sb to Ge-Se for these particular compositions have not been performed well. So we have studied the effect of Sb addition on the structural properties of Ge-Se system using FTIR spectroscopy. On the other hand what happens to the Ge-Se system on account of its optical properties when Sb is alloyed to it? Also the glass transition temperature and thermal effects are studied.

1.5: Outline of thesis

Chapter I describes the general introduction of amorphous semiconductors and their classification. Various effects of chalcogenide glasses (CG) are described. A brief introduction of general properties of CG has also been given. Various applications of CG, motivation and objective of the thesis have also been included.

Chapter II includes the theoretical background of CGs. This includes topics like structural models for CG and a brief description of Wemple-DiDomenico single oscillator model.

Chapter III describes the experimental techniques used for the preparation of bulk glasses, cleaning of substrate, deposition of thin films, characterization of bulk and thin films for X-ray diffraction and FTIR spectroscopy. Method for optical studies of thin films using UV-Vis-NIR transmission spectra has been included.

Chapter IV contains the structural properties of Ge-Se-Sb system using far-infrared transmission spectra. This includes the study of bond energies, probability functions and the comparison of theoretical and experimental values of the wave numbers for the stretching vibrational modes.

Chapter V includes the study of physical parameters of $Ge_{17}Se_{83-x}Sb_x$ (x = 0, 3, 9, 12, 15) glassy system. The theoretical investigation of various physical parameters like average coordination number, number of constraints, average heat of atomization, mean bond energy and glass transition temperature have been studied.

Chapter VI includes thermal studies of $Ge_{17}Se_{83-x}Sb_x$ (x = 0, 3, 9, 12, 15) glassy system which includes the calculation of activation energy using Kissinger's model.

Chapter VII describes the optical properties of thin films of $Ge_{17}Se_{83-x}Sb_x$ (x = 0, 3, 9, 12, 15) glassy alloys. This includes the study of absorption coefficient, optical band gap, refractive index, extinction coefficient, dielectric constants and optical conductivity by using reflection and transmission spectra.

Chapter VIII includes the summary, discussion and suggestions for the future work of the present study.

References:

[1] J.C. Phillips, Physics Today **35** (1982) 27.

[2] B.A. Movchan and A.V. Demchishin, Phys. Met. Metallogr. **28** (1969) 83–90.

[3] J.A. Thornton, J. Vac. Sci. Tech. **11** (1974) 666–670.

[4] W. Buckel, Elektrische en Magnetische Eigenschappen van dunne Metallaagies. Leuven, Belgium (1961).

[5] M. Birkholz, B. Selle, W. Fuhs, S. Christiansen, H.P. Strunk, and R. Reich, Phys. Rev. B **64** (2001) 085402.

[6] W. Ostwald, Z. Phys. Chem. **22** (1897) 289–330.

[7] G. Lucovsky, Optic modes in amorphous As_2S_3 and As_2Se_3, Physical Rev B **6** (1972) 1480-1489.

[8] G.B. Fisher & Y. Tauc, Proc 5th Int Conf Amorphous and Liquid Semiconductors, edited by I Stuke & W Brenig (Taylor & Francis, London) (1974) 1259.

[9] M. Popescu, H. Stotzel & L. Vescan, Chisinau, Proc Int Conf Amorp Semicond' **80** (1980) 44.

[10] R. Zallen, The Physics of Amorphous Solids (John Willey & Sons, New York) (1983).

[11] S.R. Elliot, In Chalcogenide Glasses, edited by J Zarzycki (Materials Science and Technology, VCH, New York) (1991).

[12] A. Feltz, Amorphous Inorganic Materials and Glasses (VCH, Weinheim, Germany) (1993).

[13] K. Morigaki, Physics of Amorphous Semiconductors (Imperial College Press, London) (1999).

[14] N. Tohge, T. Minami & M. Tanaka, J Non-Cryst Solids **37** (1980) 23-30.

[15] P. Nagel, H. Ticha, L. Tichy & A. Triska, J Non-Cryst Solids **59-60** (1983) 1015-1018.

[16] N. Tohge, H. Matsuo & T. Minami, J Non-Cryst Solids **95-96** (1987) 809-816.

[17] K.L. Bhatia, G. Parthasarathy, E.S.R. Gopal & A.K. Sharma, Solid State Commun **51** (1984) 739-742.

[18] K.L. Bhatia, G. Parthasarathy, D.P. Gosain & E.S.R. Gopal, Phil Mag B **51** (1985) 63-68.

[19] S. Kohli, V.K. Sachdeva, R.M. Mehra & P.C. Mathur, Phys Stat Sol (b) **209** (1998) 389-394.

[20] H. Fritzsche, P. Boolchand (World Scientific, Singapore) 1993

[21] K. Shimakawa, A. Kolobov & S.R. Elliott, Adv Phys **44** (1995) 475-588.

[22] A. Kolobov & S.R. Elliott, Adv Phys **40** (1991) 625-684.

[23] A.Q. Tool & C. Eichlin, J Am Ceram Soc **14** (1931) 276-308.

[24] J.P. DeNeufville, H.K. Rockstad, J. Stuke & W. Brenig, In Proc 5th Int Conf Amorphous and Liquid Semiconductors, Edited by Stuke J & Brenig W (1974) 419.

[25] M. Lasocka, J Mater Sci **13** (1978) 2055-2059.

[26] L. Tichy & H. Ticha, J Non-Cryst Solids **189** (1995) 141-146.

[27] K. Tanaka, Solid State Commun **54** (1985) 867-869.

[28] A.N. Sreeram, A.K. Varshneya & D.R. Swiler, J Non-Cryst Solids **130** (1991) 225-235.

[29] S. Mahadevan & A. Giridhar, J Non-Cryst Solids **221** (1997) 281-289.

[30] S. Mahadevan & A. Giridhar, J Non-Cryst Solids **238** (1998) 225-233.

[31] M.K. Rabinal, J Non-Cryst Solids **188** (1995) 98-106.

[32] A. Giridhar & S. Mahadevan **248** (1999) 253-256.

[33] A. Giridhar & S. Mahadevan, J Non-Cryst Solids **258** (1999) 207-215.

[34] S. Mahadevan & A. Giridhar, J Non-Cryst Solids **275** (2000) 147-152.

[35] R.S. Tiwari, N. Mehta, P. Agarwal, R.K. Shukla & A. Kumar, Indian J Pure Appl Phys **43** (2005) 363-368.

[36] S. Mahadevan, A. Giridhar & A.K. Singh, J Non-Cryst Solids **88**(1986) 11-34.

[37] H.L. Ma, X.H. Zhang & J. Lucas, J Non-Cryst Solids **140** (1992) 209-214.

[38] M. Popescu, Journal of Optoelectronics and Advanced Materials **7** (2005) 2189 - 2210

[39] G. Gauglitz and T. Vo-Dinh, Handbook of Spectroscopy (Wiley-VCH Verlag: Wienheim) (2003).

[40] J.A. Savage, (London: Adam Hilger) (1985).

[41] S. Hocde, C. Boussard-Pledel, G. Fonteneau and J. Lucas, Solid State Sciences **3** (2001) 279.

[42] R.E. Slusher, G. Lenz, J. Hodelin, J. Sanghera, L.B. Shaw and I.D. Aggarwal, J.Opt. Soc. Amer. B **21** (2004) 1146.

[43] K.V. Reddy, A.K. Bhatnagar and V. Srivastava, J. Phys.: Condens. Matter **4** (1992) 5273.

[44] A.A. Othman, K. Tahon and M.A. Osman, Physica. B **311** (2002) 356.

[45] N.F. Mott and E.A. Davis, (Oxford: Clarendon) (1979).

[46] A.A. Othman, Thin Solid Films **515** (2006) 1634.

[47] K. Shimakawa, J. Non Cryst. Solids **77-78** (1985) 1253.

[48] J.Y. Shim, S.W. Park and H.K. Baik, Thin Solid Films **292** (1997) 31.

[49] J.M. Saitar, J. Ledru, A. Hamou and G. Saffarini, Physica B **245** (1998) 256.

Chapter-2

Theoretical Background

2.1: History of chalcogenide glasses

Chalcogenide glasses which are semiconducting in nature contain one or more of the chalcogen elements (group VI elements S, Se, Te) as alloy elements. They behave as semiconductors, or more precisely, they exhibit amorphous semiconductor behavior with band gap energies from 1 to 3 eV. Chalcogenide glasses possess properties intermediate between those of organic polymers and oxide glasses. The term glass was developed in the late Roman Empire. It was in the Roman glassmaking center at Trier, now in modern Germany, that the late-Latin term 'glesum' originated, probably from a Germanic word for a transparent, lustrous substance [1] .

It is difficult to define with accuracy when mankind first fabricated its own glass but some sources go back 10,000 years in time [2]. It is also difficult to point in time when the field of chalcogenide glasses started. For the vast majority of time the vitreous glassy state was limited to oxygen compounds and their derivatives. Schulz-Sellack was the first to report data on oxygen-free glass in 1870 [3]. Though vitreous selenium and arsenic selenide and sulfide were synthesized for the first time at the end of the 19^{th} century, scientists were not attracted to these new materials. Vitreous selenium became of interest for the scientific community at the beginning of the 20^{th} century when Wood [4] and Meier [5] reported the first research on the subject.

The rising of infrared (IR) optics in the 20^{th} century lead to the need of new IR materials. Classical oxide glasses covered a transparency region from 3 μm to 5 μm

while the heavy oxide materials helped to extend that region up to 8 μm. The interest for the chalcogens comes from the attempt of scientists to extend the IR transparency region in glasses past 8 μm. The first works on CG were attributed to Frerichs in the early 50's on As_2S_3 glass [6, 7], and As_2Se_3 by Fraser [8] and Dewulf [9]. Frerichs was also at the instigation of the development of selenium glasses and binary compounds with sulfur [7]. Another important investigator of vitreous around that time was Winter-Klein [10]. At this point, two major research groups from Saint-Petersburg started the first developed research program on CG: one was led by B.T. Kolomiets and N.A. Goryunova from the "A.F. Joffe Physico-Technical Institute" who were reported to discover the first semiconducting glass [11], while the other group from the University of Saint-Petersburg was led by R.L. Myuller.

Another famous contributor to the knowledge on CG is S.R. Ovshinsky who worked at Energy Conversion Devices in Michigan. His most famous discovery is the memory and switching effect in CG [12,13]. This led to the development of non-crystalline CG in various fields such as xerography or computer memories. Around the same period in the 1970's, Sir N. F. Mott (a former Nobel Prize winner in Physics in 1977) and E.A. Davis developed the theory on the electronic processes in non-crystalline CG [14]. Several review books were published in the following years on glasses and with an interest on CG: "The Chemistry of Glasses" by A. Paul in 1982, "The Physics of Amorphous Solids" by R. Zallen in 1983 or "Physics of Amorphous Materials" by S. R. Elliott in 1983. However, the first review entirely dedicated to CG

materials entitled "Chalcogenide Semiconducting Glasses" was published in 1983 by Z.U. Borisova who previously worked with Myuller in Saint-Petersburg. G.Z. Vinogradova from Moscow followed the next year with her monograph "Glass Formation and Phase Equilibrium in Chalcogenide Systems". More recently, A.M. Andriesh dedicated a book to some specific applications of CG entitled "Glassy Semiconductors in Photo-electric Systems for Optical Recording of Information". Finally, M.A. Popescu gave a large and detailed account on the physical and technological aspects of chalcogenide systems in his book called "Non-Crystalline Chalcogenides" published in 2001. Most recently a compendium of monographs on the subject of photo-induced processes in CG entitled "Photo-induced Metastability in Amorphous Semiconductors" was compiled and edited by A. Kolobov (2003).

2.2: Classification of Amorphous Semiconductors

Amorphous semiconductors can be classified into different categories depending upon their physical and chemical properties, and techniques employed for their preparation. Thermodynamically, these materials are unstable and tend to relax with time towards a stable or metastable phase. As shown in Fig. 2.1, amorphous solids, like crystalline materials, can be ionic, metallic, covalent, Van der Waals and hydrogen bonded [15].

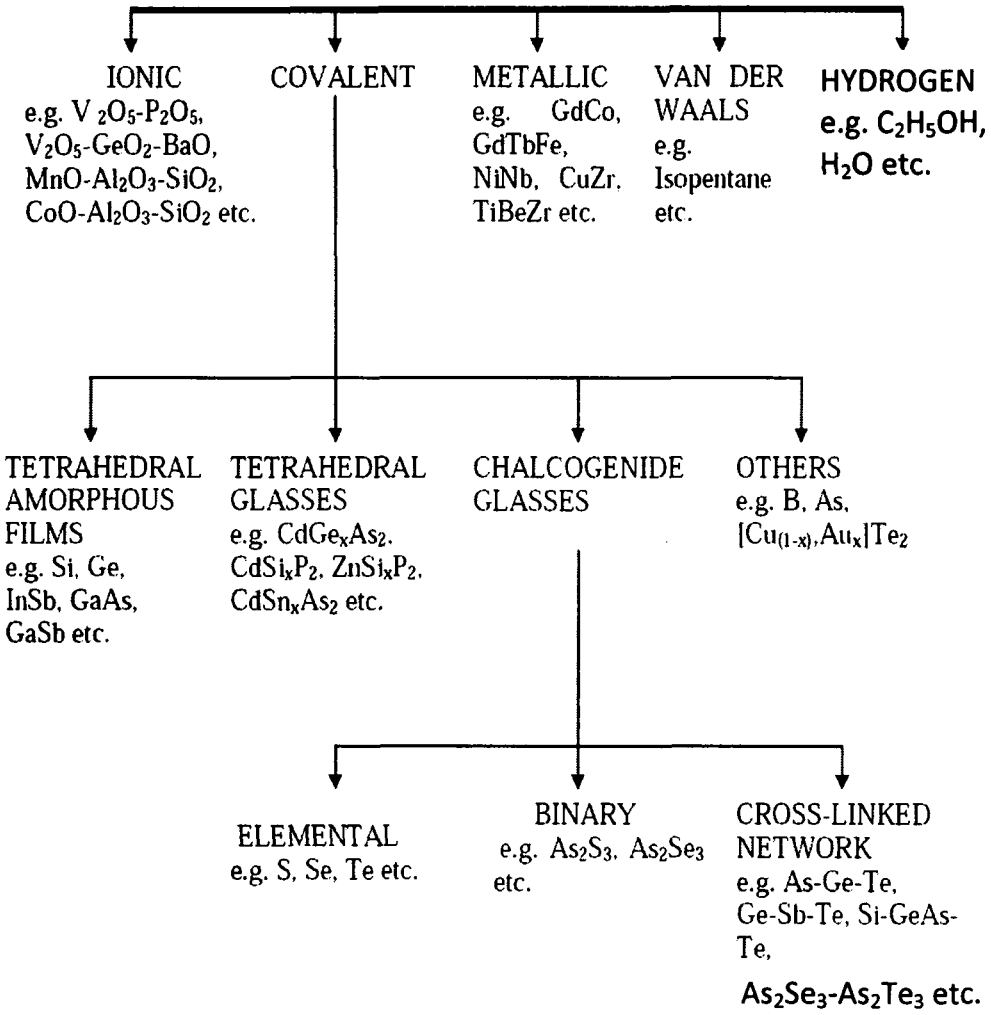

Fig 2.1 Classification of Amorphous Semiconductors

A brief description of some of these categories is given below:

1. Ionic Solids:

The ionic solids are inorganic glasses consisting of mixtures of silicates with strong ionic bonds, also called as Semiconducting Oxide Glasses. These glasses are widely used in everyday applications like window glasses, glass tubing and optical instruments. These include halide and oxide glasses, vanadium phosphate and iron phosphate glasses [15-17]. The hopping of electrons between ions contributes to the electrical conductivity of glasses. The electrical conduction in transition metal oxide glasses has been explained on the basis of bipolaron hopping between two sites [18].

2. Metallic Amorphous Solids:

The most widely used metallic solids are, metglass alloys which consist of base metals such as Fe, Ni, Al, Co, Mn, Cr and Cu together with inexpensive metalloids B, C, Si, P, N, Ge and As. Metglass alloys with Fe, Ni and Co are amorphous solids. In addition, there are rare earth-transition metal amorphous alloys like GdCo, GdFe, GdTbFe which have good magnetic properties. Because of high quenching rate required, these materials are prepared by melt- spinning and sputtering [19]. These materials are found to have superior magnetic properties than their crystalline counterparts [20].

3. Covalent Amorphous Semiconductors:

The covalently bonded amorphous semiconductors can be subdivided into three different parts

(a) Tetrahedral Amorphous Semiconductors (TAS):

These are group IV and III-V semiconductors. Being metallic, above their melting point they can be prepared either by thin film deposition or by amorphisation.

They cannot be prepared by quenching the melt, because the melt has a structure characterized by higher co-ordination number.

(b) Tetrahedral Glasses (TG):

They may be represented by the general formula

$A^{II}B^{IV}$ X_2^{V}, where the suffix gives the group of the periodic table. The interesting feature of the tetrahedral glasses is that although the Fermi level lies always near the middle of the gap, still some of them are n-type or p-type materials [21].

(c) Chalcogenide Glasses (CG):

Sulphur (S), Selenium (Se) or Tellurium (Te) group VI elements of the periodic table are called Chalcogenide glasses. Like Silicon (Si), the best known and most widely used in IC technology, chalcogenides as Germanium Selenide (GeSe) and Arsenic Sulphide (As_2S_3) are poor conductors of electricity, unless some impurities are added to these materials. This process of impurity addition is called doping. However unlike Silicon, which has to be manufactured in an extremely pure crystalline state for use in most electronic devices, chalcogenide glasses do not have extended order in the arrangement of their atoms. This means that they can be deposited very easily, using any of number of well-known thin film manufacturing techniques, and are not nearly as susceptible to the presence of contamination or defects in their structure as Silicon (Si). Chalcogenides are also known as Lone Pair semiconductors, because of their distinct feature of having two non-bonding p-orbitals of the group VI chalcogen in two fold coordination, which accounts for many of their unique properties.

Chalcogenide glasses are predominantly electronic with conductivities ranging from 10^{-13}-10^{-3} Ω^{-1} cm^{-1}. These can be either elemental semiconductors such as S, Se,

etc.; binary such as As_2S_3, As_2Se_3 etc. or multi-component mixtures as Si-Ge-Te-As, As_2Se_3:Tl_2Se_3, As_2Se_3:As_2Te_3 etc. The elemental and binary chalcogenides have chain or layer structure with considerable order extending locally in one or two dimensions, whereas, the multi-component alloys possess three dimensional network structure. The range of short order in elemental and binary chalcogenides is longer as compared to multi-component chalcogenides. These glasses are therefore, said to have comparatively incomplete structural or positional disorder. These glasses were investigated in the early 1950's as possible infrared materials [22,23]. The interest in these materials increased when Kolomiets [24] showed that chalcogenide glasses behaved like intrinsic semiconductors and their electrical conductivity could not be increased by adding certain dopants.

The field livened considerably with the observation of switching and memory effects in these materials [25]. In 1975, Mott and his collaborators [26,27] proposed that the important localized states in chalcogenide glasses are not because of the disorder in the material, but because of well-defined defects much like those in a crystalline semiconductor. They further explained the unique properties of these glasses using the concept of dangling bonds. Presently various models [28-30] have been proposed to explain transport mechanism in chalcogenides but the recombination kinetics and transport phenomena, of both pure and doped materials, have not been clearly understood. Further, the incorporation of impurity (e.g. Ag, Ni, Mn, Al, Ga, Tl etc.) in some chalcogenides (e.g. As_2Se_3, As_2S_3) has revealed interesting results. Heat or light energy can be used to dissolve metals such as Silver (Ag) or Copper (Cu) into the chalcogenides to form a Solid Solution. During dissolution, a simple chemical reaction takes place; Ag atom looses an electron in the process to form Ag+ ions,

$$Ag - e^{-} = Ag^{+}$$

which are relatively free to move in a ternary compound. This reaction will go on till an equilibrium state is achieved in this process.

2.3: Band Models for Amorphous Semiconductors

The band model, which has been proved helpful in explaining the behavior of crystalline materials, is not directly applicable to the highly disordered materials. However, the band models used to explain the behaviour of amorphous materials assume a band of extended states along with the localized states. Extended states are quantum-mechanical states of motion in which an electron may be found anywhere in space with equal probability. Due to large variation in the nature, properties and constituents of amorphous semiconductors, various models and their modifications are proposed to give a fair amount of understanding of the essential features of these semiconductors. Three basic models are discussed below to describe the properties of amorphous materials.

2.3.1: Cohen, Fritzsche and Ovshinsky (CFO) Model

This model has been developed by Cohen, Fritzsche and Ovshinsky [31], in which they have suggested that in case of disordered covalent alloys, such as chalcogenide glasses, the valence and conduction band tails overlap each other close to the center of forbidden gap. The mobility of the carriers has finite value in high-density states but it decreases abruptly in the tail states. These boundaries are called mobility edges. The critical energies at mobility edges define mobility gap. CFO model discussed above is shown in Fig. 2.2.

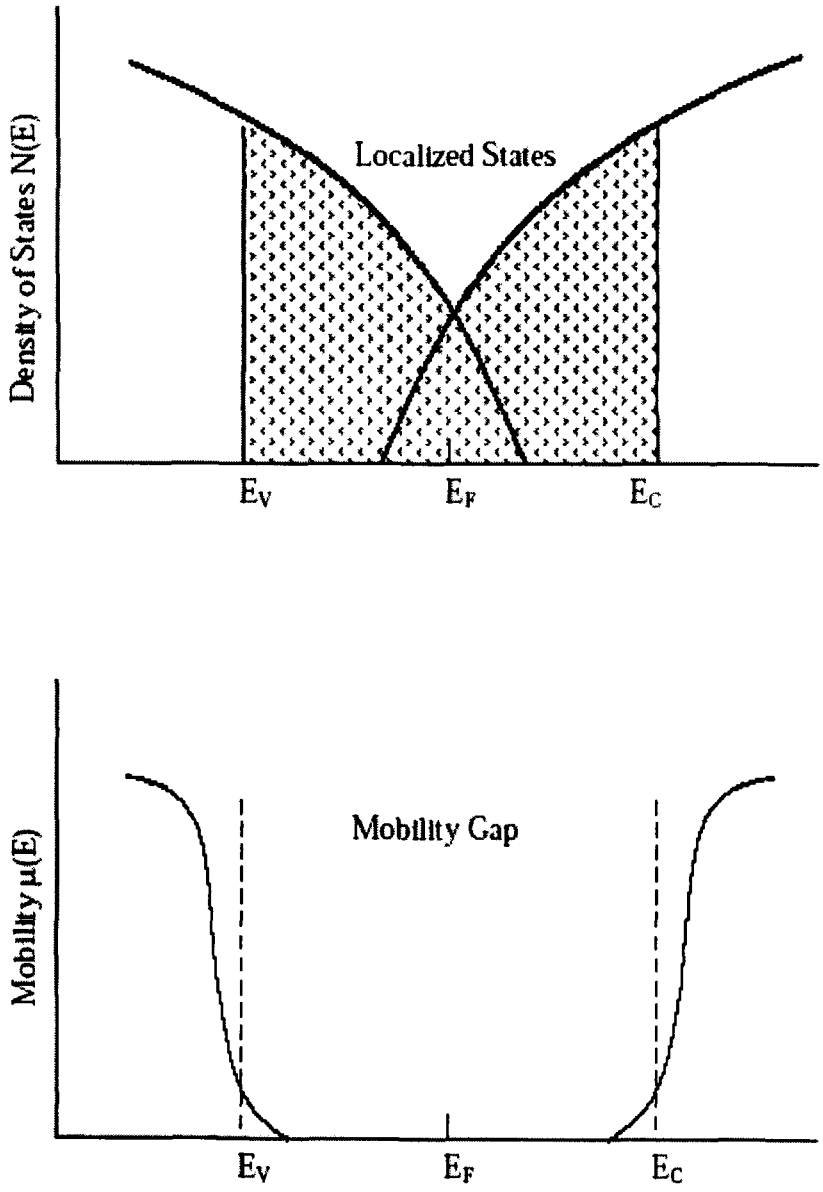

Fig 2.2 Cohen, Fritzsche and Ovshinsky (CFO) Model

2.3.2: Davis and Mott (DM) Model

This model has been developed by Davis and Mott [32]. They proposed that there is a narrow band of compensated localized states which pins the Fermi level between the two tails. The mobility edges for electrons and holes are at E_c and E_v as shown in Fig. 2.3. This model suggests that hopping conduction can take place in the localized states. The model that explains the behaviour of crystalline materials is based upon the assumption that band edges are sharp.

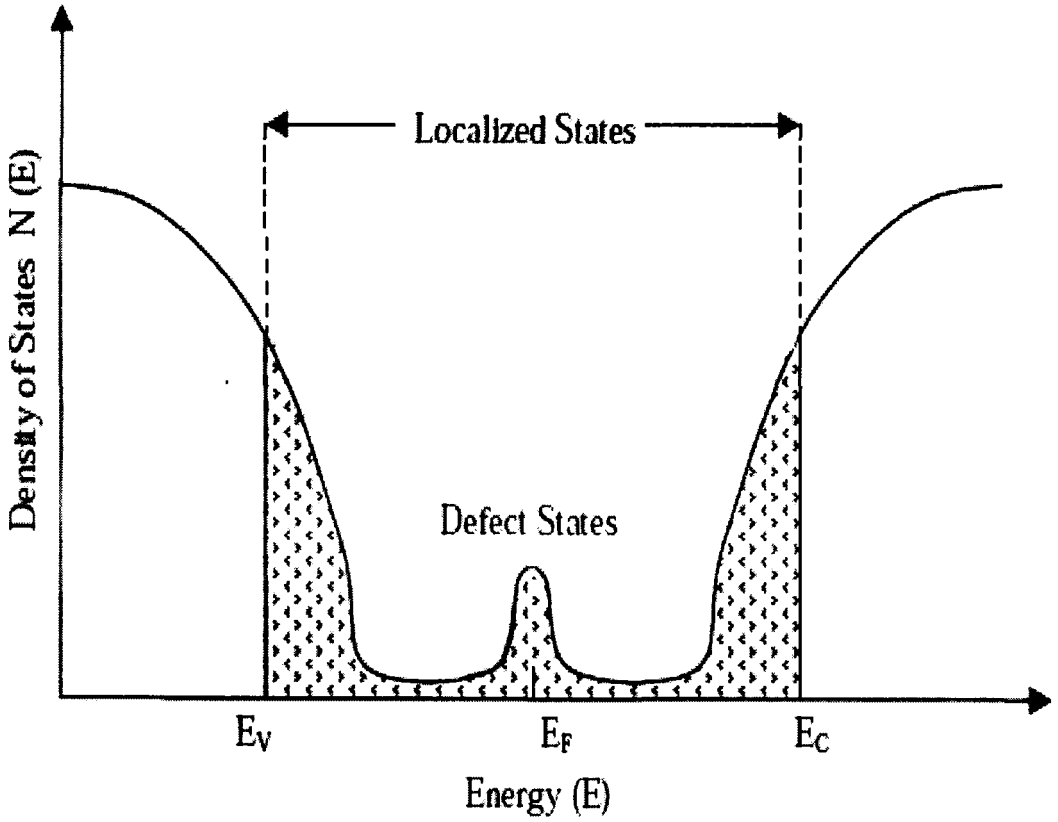

Fig 2.3 Davis and Mott (DM) Model

2.3.3: Mott, Davis and Street (MDS) Model

Mott-Davis and Street (MDS) proposed a band model in 1975 to explain the behavior of amorphous semiconductors [25,27]. The mobility edges for electrons and holes are at Ec and Ev. The localized states originate due to lack of long-range order while the defect states are due to various kinds of defects in the structure. The center band splits into two levels forming donor and acceptor bands as shown in Fig. 2.4. They considered the states near Fermi level due to defects, particularly, dangling bonds. Their model is based on Anderson's idea [33] that paired electron states are preferred in chalcogenide glasses i.e., D^- and D^+. In some structural configurations, the atoms are not able to share the electrons and the bond breaks. Hence, a dangling bond emerges out of this unstable situation. If a dangling bond is singly occupied, it is neutral (D^0) indicating that an Electron Spin Resonance (ESR) signal is expected. In some cases, a dangling bond can attract an additional electron and, thus providing a lone pair, it is designated as D^-, indicating that there will be no ESR signal, and D^+, when the bond loses even the single electron it has, giving rise to a hole representing a bond without any spin.

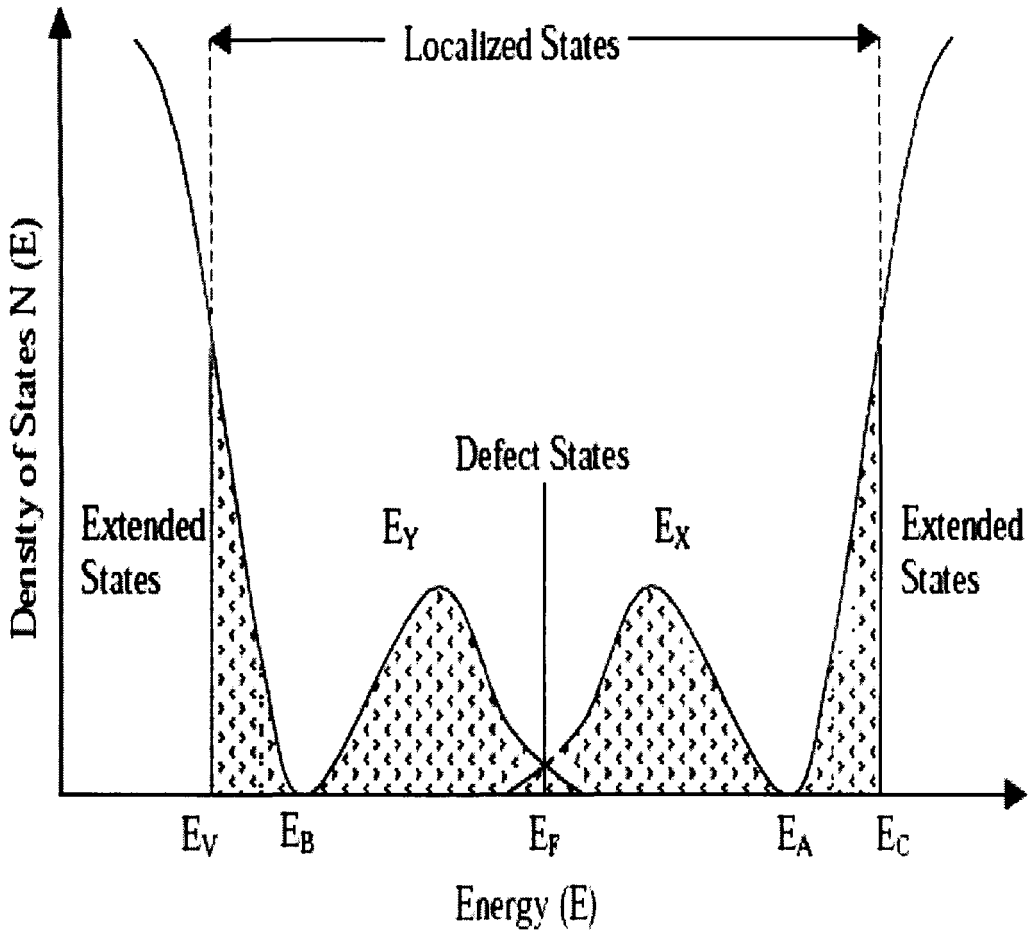

Fig 2.4 Mott, Davis and Street (MDS) Model

This model predicts no ESR, paramagnetism and can explain many other properties of chalcogenide glasses.

2.4: Wemple-DiDomenico (WDD) Model

According to single oscillator model proposed by Wemple DiDomenico (WDD) model [34], the optical data could be described to an excellent approximation by the following expression:

$$n^2(h\nu) = 1 + \frac{E_0 E_d}{E_0^2 - (h\nu)^2} \qquad [1]$$

Where n is the refractive index, hν is photon energy, E_o is single oscillator energy and E_d is dispersion energy which is the measure of the average strength of interband optical transitions (interband transition energy or also called dispersion energy). Experimental verification of equation (1) can be obtained by plotting $(n^2-1)^{-1}$ against $(h\nu)^2$. The resulting straight line yields values of parameters E_o and E_d. Moreover an important achievement of WDD model is that it relates the dispersion energy E_d to other physical parameters of the material through a simple empirical relation:

$$E_d = \beta N_c Z_a N_e \qquad [2]$$

where N_e is the effective number of valence electrons per anion, N_c is the effective coordination number of the cation nearest neighbor to the anion, Z_a is the chemical valence of the anion and β is a two valued constant with either an ionic or covalent value (for ionic materials $\beta = 0.26 \pm 0.03$ eV and for covalent materials $\beta = 0.37 \pm 0.04$ eV [35]).

2.5: Defect States in Chalcogenide Glasses

In chalcogenide glasses, the absence of Electron Spin Resonance (ESR) [36], curie para- magnetism at low temperature [37] and Variable Range Hopping (VRH) [38] indicates non-crystalline structure. Despite all this, ample evidences are there that these materials contain high concentration of \defect states" such as \broken bonds" or \dangling bonds", which can be proved from photoluminescence [39-41], field effects [42], photoconductivity [43], drift mobility [44] and pinned Fermi energy levels [38]. In these glasses, the top of the valance band is derived from lone pair orbital of the chalcogen atom [45]. Thus, significant rearrangement in chemical bonding may take place within the glass and utilizing the lone pair orbitals, the chalcogen atoms can become over-coordinated, giving rise to doubly occupied defect states and additional degrees of freedom into the network, with a consequent diminution in rigidity. Anderson [33,46] further extended the Cohen-Fritzsche-Ovshinsky (CFO) model by developing a theory which describes the nature of defect states within a glass. He concluded that, under certain conditions, the formation of doubly occupied states (pair spin) is energetically favoured at the expense of singly occupied states. This reaction is favoured if the elastic energy gained through a lattice distortion in forming the doubly occupied center, is greater than the Columbic repulsion between the electrons. Electron pairing due to the electron-phonon interaction is strong enough to over- come the Columbic repulsion between two electrons placed on the same site [33,46]. Electron therefore experiences a negative Columbic energy U_{eff}.

Pair Spin Model of Anderson [46] formed the basis of Charged Defects Model put forward by Street and Mott [25], who introduced the concept of charged dangling bonds in chalcogenide glasses. The dangling bonds may be occupied by zero or two electrons and are designated as D^+ and D^- respectively. The superscripts denote the total charge of the center. These dangling bonds have no unpaired spins; half the dangling bonds have two anti parallel spin of half zone. Considering the lone pair electrons, the spin pairing at the dangling bonds defects can be explained in the following manner [25,27]. The unpaired electron from one defect site moves to another similar site producing a spin paired negatively charged defect D^-. The empty orbital produces a positively charged site which bonds with a lone pair, resulting in a threefold coordinated defect results. These charged defect states successfully account for the absence of an Electron Spin Resonance (ESR) signal in the dark, the luminescence spectra, an ESR signal and absorption at midgap induced by irradiation with light of slightly sub-band-gap energy, and lack of the $T^{1/4}$ variable range hopping, the dominant d.c. conduction mechanism. Following Anderson [33,46], the total distortion of electron cloud occurs when the electron occupation of the dangling bond changes and it is sufficiently strong for the reaction illustrated in Fig. 2.5 (a), i.e.,

$$2D^0 \rightarrow D^+ + D^- \qquad [3]$$

Mott et al. [25,27] presumed that the whole process is exothermic as a result of strong electron-phonon interaction, associated with relaxation of these centers. Kastner, Adler and Fritzsche [46,47] applied chemical bond approach to explain the reason for the above reaction to be exothermic and emphasized that both D^+ and D^0 centers in chalcogenide glasses are three-fold-coordinated. Mathematically, if B is the optical

band gap, W_1 is the energy required (distortion plus electronic) to take an electron from the valance band and place it on D^0 center thereby turning it into D^-, and W_2 is the total energy necessary to take an electron from a D^0 center and place it in conduction band as shown in Fig.2.5 (b). Reaction (Eq. 3) will be exothermic when

$$W_1 + W_2 < B \qquad [4]$$

Furthermore, the thermal energy required to take two electrons out of the D_i center and place them in conduction band is

$$W_m = B - W_1 + W_2 \qquad [5]$$

where W_m can be taken to be simply twice the energy difference between the Fermi level and conduction band, assuming that there is no distortion energy associated with the D^- center. Fermi energy is the average energy per electron to take an electron out of highest occupied state D^- and places it in the lowest occupied state. Since chalcogenide glasses are, in general, p-type, exhibiting simply activated d.c. conduction with activation energy ΔE, W_m can also be written as

$$W_m \cong 2(B - \Delta E) \qquad [6]$$

The Fermi energy is pinned as stated by Anderson [33,46].

Since $W_1 \cong W_2$ (to first order approximation), the Fermi level will lie near the mid gap i.e., $E \cong \frac{1}{2}B$ for chalcogenide materials. Hence $W_m \cong B$, within 10% approximation [48].

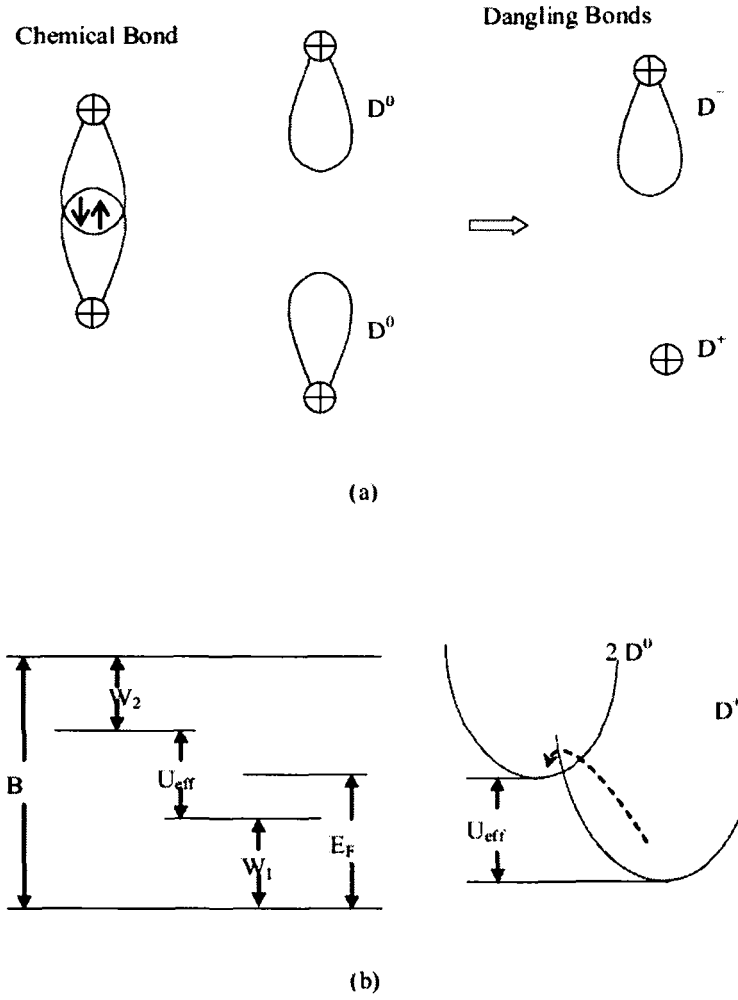

Fig 2.5 (a) Formation of Charged Dangling Bonds. (b) Thermal Energy Levels Associated with Electronic Transition between D^+ and D^- centers.

References:

[1] R.W. Douglas, G T Foulis & Co Ltd. ISBN 0854291172 (1972).

[2] H. Fritzche, Proc. of the Kyoto Summer Institute, p.1, Kyoto, Japan (1980) 8-11.

[3] C. Schultz-Sellack, Ann.Phys. **139** (1870) 182.

[4] R.W. Wood, Phil. Mag. **3** (1902) 607.

[5] W. Meier, Ann. Phys. **31** (1910) 1017.

[6] R. Frerichs, Phys. Rev. **78** (1950) 643.

[7] R. Frerichs, J. Opt. Soc. Am. **43** (1953) 1153.

[8] W.A. Fraser, J. Opt. Soc. Am. **43** (1953) 823.

[9] G. Dewulf, Rev. Opt. **33** (1954) 513.

[10] A. Wnter Klein, Verres et Réfractaires **9** (1955) 147.

[11] N.A. Goriunova, B.T. Kolomiets, Zhurnal Tekhnicheskoi Fiziki (Russian) **25** (1955) 2069.

[12] S.R. Ovshinsky, Phys. Rev. Lett. **21** (1968) 1450.

[13] S.R. Ovshinsky, J. Non-Cryst. Solids **2** (1970) 99.

[14] N.F. Mott and E.A. Davis, In Oxford University Press, Second Edition (1979).

[15] D.A. Adler, Amorphous Semiconductors, CRC Press, Cleveland, Ohio (1971).

[16] N.F. Mott, Adv. Phys. **16** (1967) 49.

[17] A.E Owen, Contemp. Phys. **11** (1970) 227.

[18] N.F. Mott, J. Non-Cryst. Solids **1** (1968) 1.

[19] C.M. Srivastva and C. Srinivasan, Science of Engg. Materials, Wiley Eastern Ltd. (1987).

[20] Edited by A. Levy and R. Hasegana, Amorphous Magnetism II, Plenum, New York (1977).

[21] R. Callaerts, M. Denayer, F.H. Hashmi and P. Nagels, Discussion of Faraday Soc. **50** (1970) 27.

[22] R. Frerichs, Phys. Rev. Lett. **78** (1950) 643.

[23] R. Frerichs, J. Opt. Soc. Soc. Am. **43** (1950) 1153.

[24] B.T. Kolomiets, Phys. Stat. Sol. 7 **359** (1964) 713.

[25] R.A. Street and N.F. Mott, Phys. Rev. Lett. **35** (1975) 1293.

[26] S.R. Ovshinsky, Phys. Rev. Lett. **21** (1968) 1450.

[27] N.F. Mott, E.A. Devis and R.A. Street, Phil. Mag. **32** (1975) 961.

[28] A.R. Long, Adv. Phys. **31** (1982) 553.

[29] S.R. Elliot, Adv. Phys. **36** (1987) 135.

[30] N.F. Mott and A. Davis, Claren-don Press, Oxford, England (1971).

[31] M.H. Cohen, H. Fritzsche and S.R. Ovshinsky, Phys. Rev. Lett. **22** (1969) 1065.

[32] E.A. Davis and N.F. Mott, Phil. Mag. **22** (1970) 903.

[33] P.W. Anderson, Phys. Rev. Lett. **34** (1975) 953.

[34] S.H. Wemple, M.Di Domenico, Phys. Rev. B **3** (1971) 1338.

[35] S.H. Wemple, Phys. Rev. B **7** (1973) 3767.

[36] S.C. Agarwal, Phys. Rev. B **7** (1973) 685.

[37] F.J. Disalvo, A. Menth, J.V. Easzczak and J. Tauc, Phys. Rev. B **6** (1972) 4574.

[38] N.F. Mott, Phil. Mag. **19** (1969) 835.

[39] R.A. Street, T.M. Searle and I.G. Austin, J. Phys. C: Solid State Phys. **6** (1973) 1830.

[40] R.A. Street, T.M. Searle and I.G. Austin, Phil. Mag. **30** (1974) 1185.

[41] R.A. Street, I.G. Austin, T.A. Searle and B.A. Smith, J. Phys. C: Solid State Phys. **7** (1974) 4185.

[42] Edited by J.M. Marshall, F.D. Fisher and A.E. Owen, Proc. of Vth Int. Conf. on Amorphous and Liquid Semiconductors, Garmisch-Partenkirchen, Germany (1973) 1305.

[43] C. Main, Ph.D. Thesis, Edinburgh (1974).

[44] J.M. Marshall and A.E. Owen, Phil. Mag. **24** (1971) 1281.

[45] M. Kastner, D. Adler and H. Fritzsche, Phys. Rev. Lett. **28** (1972) 355.

[46] P.W. Anderson, J. de Physique **37** (1976) 339.

[47] M. Kastner and H. Fritzsche, Phil. Mag. B **37** (1978) 199.

[48] S.R. Elliot, Solid State Communications **28** (1978) 939.

Chapter-3

Experimental Techniques

3.1: Preparation Techniques of Chalcogenide Glasses

3.1.1: Quenching Technique:

Chalcogenide materials are prepared by rapid cooling from the melt. For preparation of glasses, required composition is prepared by weighing the constituent elements in desired atomic percentages and then sealed in quartz ampoules under high vacuum. Sealed ampoules are kept in a furnace at a temperature which makes the components to melt. Inside furnace, ampoules are frequently rocked for 12 h to make the melt homogeneous. Quenching is done by dropping the quartz ampoules suddenly in ice-cooled water or liquid nitrogen depending upon the requirement. In some cases, air quenching is sufficient where an air blower blows air on the heated ampoules. Not all the materials can be made in glassy form even at the fastest cooling rates. In case of alloys also, there are certain range of constituent elements in which they can be glassy. A systematic study is made to find out phase diagram for a specific series for making glassy alloys by preparing small amount of sample and checking glassy nature by X-ray diffraction.

3.1.2: Thermal Evaporation Technique:

Chalcogenide materials are made amorphous in the form of thin films by creating high vacuum in the bell jar and heating the filament containing the material by passing electricity. Substrate used may be glass or any other suitable material. Substrate temperature can also be varied by mounting a heater inside the bell jar. Standard coating units are available in the market for making thin films by this technique.

3.1.3: Flash Evaporation Technique:

This technique is similar to Thermal Evaporation except that the material is dropped on already heated filament. In addition to the coating unit, an AC magnetic field is established to produce vibration in a magnetic strip containing material.

3.1.4: Sputtering Technique:

It consists of bombardment of a target by energetic ions from low-pressure plasma, causing erosion of material, either atom by atom or as clusters of atoms, and subsequently depositing of film on the substrates. Simplest way to induce sputtering is to apply a high negative voltage to the target surface, thereby attracting positive ions from the plasma. However, DC sputtering process is feasible only when target is sufficiently conducting so that target can act as electrode.

3.1.5: Glow Discharge Decomposition Technique:

This technique, like sputtering, relies on the production of plasma in a low-pressure gas, but instead of ions from the plasma ejecting material from the target, a chemical decomposition of the gas itself takes place, leading the deposition of a solid film on a substrate kept in the plasma. The plasma is produced by the application of a radio frequency field, either using inductive coupling or capacitive coupling. The films deposited depend upon gas pressure, flow rate, substrate temperature and chamber geometry.

3.1.6: Chemical Vapor Deposition Technique:

It is analogous to the glow discharge method in that both depend on the decomposition of a vapor species. This method relies on the thermal energy for the decomposition and the applied radio frequency field simply serves to heat up the substrate upon which the vapor decomposes.

3.2: Thin film deposition

Thin films can be prepared from a variety of materials such as metals, semiconductors, insulators or dielectrics etc. and for this purpose various preparative techniques have been developed. Techniques involved in general are

(i) Thermal deposition in vacuum by resistive heating, electron gun or laser gun evaporation, etc. from suitable sources.

(ii) Sputtering of cathode materials in presence of inert or active gases either at low or medium pressure.

(iii) Chemical vapour deposition (CVD) by pyrolysis, dissociations, reactions in vapour phase.

(iv) Chemical deposition from solutions including electro-deposition, chemical displacement, chemical reaction etc.

In the present work, we have dealt with thermal deposition in vacuum by resistive heating. This is the most commonly used technique adopted for deposition of metals, alloys and also many compounds. The primary requirement for this method is a high vacuum deposition system at a pressure of about 10^{-4} Pa or even less.

Fine powder of the material to be deposited was put into the flash cleaned boat. Flash cleaning was done by passing a heavy current through the boat so as to make it white hot or incandescent for a short period. Then the system was evacuated to a base pressure of 10^{-4} Pa. A shutter was incorporated in between the source and the substrate so that no vapour stream of the material can reach the substrate directly prior to attaining the required deposition conditions. After establishing required source temperature, substrate temperature and vacuum in the chamber, the shutter was removed to start the deposition of film on the cleaned substrate. When the required film thickness was obtained the shutter was brought back to the original position.

Cleaning of the substrate was done in three steps: (i) soap solution cleaning and (ii) cleaning with acetone (vapour cleaning) and (iii) with methanol. Soap solution cleaning basically involves scrubbing the substrate in the soap solution, then rinsing it thoroughly with distilled water. This procedure was repeated 3 - 4 times for cleaning the single substrate. Soap solution cleaning was used to remove any visible oil, grease and dust impurities. Vapour cleaning procedure was used to remove the organic impurities, which may be present on the surface of substrate. Acetone was used for the removal of organic impurities. For the removal of inorganic impurities methanol was used. After all this cleaning the substrates are subjected to dry in an oven at a temperature approximately 110^0C and then put into deposition chamber.

Thin films were kept in the deposition chamber in the dark for 24 h to attain thermodynamic equilibrium as stressed by Abkowitz et al [1]. The vacuum evaporation process was carried out in a coating system (HINDHIVAC model 12A4D India). The rate of evaporation of deposited thin films and thickness of the films deposited has been measured by thickness monitor (Model DTM-101).

3.3: X-ray Powder Diffraction (XRD)

X-ray powder diffraction (XRD) is a rapid analytical technique primarily used for phase identification of a crystalline material and can provide information on unit cell dimensions. The analyzed material is finely ground, homogenized, and average bulk composition is determined.

Max von Laue, in 1912, discovered that crystalline substances act as three-dimensional diffraction gratings for X-ray wavelengths similar to the spacing of planes in a crystal lattice. X-ray diffraction is now a common technique for the study of crystal structures and atomic spacing.

X-ray diffraction is based on constructive interference of monochromatic X-rays and a crystalline sample. These X-rays are generated by a cathode ray tube, filtered to produce monochromatic radiation, collimated to concentrate, and directed toward the sample. The interaction of the incident rays with the sample produces constructive interference (and a diffracted ray) when conditions satisfy Bragg's Law ($n\lambda=2d \sin \theta$) [2]. This law relates the wavelength of electromagnetic radiation to the diffraction angle and the lattice spacing in a crystalline sample. These diffracted X-rays are then detected, processed and counted. By scanning the sample through a range of 2θ angles, all possible diffraction directions of the lattice should be attained due to the random orientation of the powdered material. Conversion of the diffraction peaks to d-spacings allows identification of the mineral because each mineral has a set of unique d-spacings. Typically, this is achieved by comparison of d-spacings with standard reference patterns.

All diffraction methods are based on generation of X-rays in an X-ray tube. These X-rays are directed at the sample, and the diffracted rays are collected. A key component of all diffraction is the angle between the incident and diffracted rays. Powder and single crystal diffraction vary in instrumentation beyond this. X-ray diffractometers consist of three basic elements: an X-ray tube, a sample holder, and an X-ray detector.

X-ray powder diffraction is most widely used for the identification of unknown crystalline materials (e.g. minerals, inorganic compounds). Determination of unknown solids is critical to studies in geology, environmental science, material science, engineering and biology.

Other applications include:

- characterization of crystalline materials
- identification of fine-grained minerals such as clays and mixed layer clays that are difficult to determine optically
- determination of unit cell dimensions
- measurement of sample purity

With specialized techniques, XRD can be used to:

- determine crystal structures using Rietveld refinement
- determine of modal amounts of minerals (quantitative analysis)
- characterize thin films samples by:

- determining lattice mismatch between film and substrate and to inferring stress and strain
- determining dislocation density and quality of the film by rocking curve measurements
- measuring superlattices in multilayered epitaxial structures
- determining the thickness, roughness and density of the film using glancing incidence X-ray reflectivity measurements

- make textural measurements, such as the orientation of grains, in a polycrystalline sample

The powder method was used to check the nature (i.e. amorphous or polycrystalline or crystalline) of the bulk samples. The bulk samples were crushed to fine powder with a pestle and mortar and then this powder was used for taking XRD pattern. Philips PW 1710 X-ray diffractometer (Cu-Kα radiation, $\lambda = 1.540598\ \overset{0}{A}$, 40 KV and 25 mA was used to take the XRD patterns of the samples. Data acquisition was made in the 2θ range from 10^{o} to 100^{0}. Step size was set to 0.05^{0} was employed. Thin films of the fabricated bulk samples deposited on the microscopic glass slides were also characterized to check the nature of the films.

3.4: Transmission spectroscopy

Ultraviolet-Visible-Near-Infrared (UV-Vis-NIR) spectroscopy is useful to characterize the absorption, transmission, and reflectivity of a variety of technologically important materials, such as pigments, coatings, windows, and filters.

Transmission Spectroscopy is highly interrelated to Absorption Spectroscopy. This technique can be used for solid, liquid, and gas sampling. Here, light is passed through the sample and compared to light that has not. The output depends on the path length or sample thickness, the absorption coefficient of the sample, the reflectivity of the sample, the angle of incidence, the polarization of the incident radiation, and, for particulate matter, on particle size and orientation.

This application usually requires recording at least a portion of the spectrum for characterization of the optical or electronic properties of materials. No material is fully transparent in all optical frequencies and hence there is always some absorption in some region of the spectra. When light is incident on a thin film some of its energy is reflected, some is absorbed and rest is transmitted. Thin films are studied more accurately by acquiring transmission instead of absorption as is the case for bulk glasses. The transmission spectra of the thin films in the spectral range 400 – 2000 nm were obtained using a double beam ultraviolet - visible - near infrared spectrophotometer (Hitachi-330 and Perkin Elmer Lambda-750). The spectrophotometer was set with a slit width of 1 nm. Therefore it was unnecessary to make slit width corrections because of a small slit width value in comparison with different line widths [3].

3.5: Fourier-Transform infrared spectroscopy

FTIR is most useful for identifying chemicals that are either organic or inorganic. It can be utilized to quantitate some components of an unknown mixture. It can be applied to the analysis of solids, liquids, and gasses. The term Fourier

Transform Infrared Spectroscopy (FTIR) refers to a fairly recent development in the manner in which the data is collected and converted from an interference pattern to a spectrum. Today's FTIR instruments are computerized which makes them faster and more sensitive than the older dispersive instruments.

3.5.1: Qualitative Analysis

FTIR can be used to identify chemicals from spills, paints, polymers, coatings, drugs, and contaminants. FTIR is perhaps the most powerful tool for identifying types of chemical bonds (functional groups). The wavelength of light absorbed is characteristic of the chemical bond as can be seen in this annotated spectrum.

By interpreting the infrared absorption spectrum, the chemical bonds in a molecule can be determined. FTIR spectra of pure compounds are generally so unique that they are like a molecular "fingerprint". While organic compounds have very rich, detailed spectra, inorganic compounds are usually much simpler. For most common materials, the spectrum of an unknown can be identified by comparison to a library of known compounds. We have several infrared spectral libraries including on-line computer libraries. To identify less common materials, IR will need to be combined with nuclear magnetic resonance, mass spectrometry, emission spectroscopy, X-ray diffraction, and/or other techniques.

3.5.2: Quantitative Analysis

Because the strength of the absorption is proportional to the concentration, FTIR can be used for some quantitative analyses. Usually these are rather simple types

of tests in the concentration range of a few ppm up to the percent level. For example, EPA test methods 418.1 and 413.2 measure the C-H absorption for either petroleum or total hydrocarbons. The amount of silica trapped on an industrial hygiene filter is determined by FTIR using NIOSH method 7602 spectroscopy, X-ray diffraction, and/or other techniques.

3.5.3: Physical Principles

Molecular bonds vibrate at various frequencies depending on the elements and the type of bonds. For any given bond, there are several specific frequencies at which it can vibrate. According to quantum mechanics, these frequencies correspond to the ground state (lowest frequency) and several excited states (higher frequencies). One way to cause the frequency of a molecular vibration to increase is to excite the bond by having it absorb light energy. For any given transition between two states the light energy (determined by the wavelength) must exactly equal the difference in the energy between the two states i.e. ground state and the excited state. The energy corresponding to these transitions between molecular vibrational states is generally 1-10 kilocalories/mole which corresponds to the infrared portion of the electromagnetic spectrum.

Fourier - Transform infrared (FT-IR) spectroscopy combines the advantages of IR spectroscopy and Fourier -Transform to allow the identification of functional groups and the detection of the presence of impurities. When a molecule absorbs specific frequencies of IR radiation, vibration or rotations of the functional groups are created and an absorbance spectrum regrouping the absorbed frequencies can be

observed. This spectrum is specific to each molecule which allows an experimenter to know with precision the functional groups forming the sample. In addition the radiation absorbed is proportional to the concentration of each compound. This electronic process is combined with Fourier transform, named after Jean-Baptiste Joseph Fourier, which converts time based signals into frequency domain. The IR beam used in FT-IR is split into two components in an interferometer, one component traveling to a mirror placed at a distance and other one to a moving mirror, thus creating constructive and destructive interference [4]. The resulting interference pattern is a time based function that is translated as a function of frequency after Fourier transform.

The far IR transmission spectra of different alloys were recorded on a Fourier transform IR (NICOLET 5700) used in conjunction with the KBr disc technique, over the spectral range of 500–200 cm^{-1} at room temperature. Powdered samples of 4 mg were thoroughly mixed and ground with 200 mg KBr; after which the mixtures were pressed at 10 tons cm^{-2} for 5 min. under vacuum.

3.6: Differential Thermal Analysis (DTA)

Differential thermal analysis (or DTA) is a thermoanalytic technique, similar to differential scanning calorimetry. In DTA, the material under study and an inert reference are made to undergo identical thermal cycles, while recording any temperature difference between sample and reference [5]. This differential temperature is then plotted against time, or against temperature (DTA curve or thermogram). Changes in the sample, either exothermic or endothermic, can be

detected relative to the inert reference. Thus, a DTA curve provides data on the transformations that have occurred, such as glass transitions, crystallization, melting and sublimation. The area under a DTA peak is the enthalpy change and is not affected by the heat capacity of the sample.

A DTA consists of a sample holder comprising thermocouples, sample containers and a ceramic or metallic block; a furnace; a temperature programmer; and a recording system. The key feature is the existence of two thermocouples connected to a voltmeter. One thermocouple is placed in an inert material such as Al_2O_3, while the other is placed in a sample of the material under study. As the temperature is increased, there will be a brief deflection of the voltmeter if the sample is undergoing a phase transition. This occurs because the input of heat will raise the temperature of the inert substance, but be incorporated as latent heat in the material changing phase.

DTA experiments were carried out on a Perkin Elmer (Pyris Diamond) in Nitrogen atmosphere (200 ml/min). All measurements were referenced to Alumina powder in an Alumina-pan, and carried out in a nitrogen atmosphere flowing at 50 ml/min.

References:

[1] M. Abkowitz, G.M.T. Foley, J.M. Markovics and A.C. Palumbo, (AIP Conf. Proc.) ed P C Taylor and S G Bishop (New York: American Institute for Physics) **120** (1984) 117–124.

[2] C. Suryanarayana and M.G. Norton, X-Ray Diffraction – A Practical Approach (New York: Plenum Press) (1998).

[3] E. Marquez, J. Ramirez-Malo, P. Villares, R. Jimenez-Garay, P.J.S. Ewen, and A.E. Owen, J. Phys. D: Appl. Phys. **25** (1992) 535.

[4] J.W. Goodman, Introduction to Fourier Optics (New York: McGraw-Hill) (1996).

[5] H.K.D.H. Bhadeshia, University of Cambridge, Material Science and Metallurgy (2002).

Chapter-4

Structural Study of Ge-Se-Sb System

This chapter includes the structural study of $Ge_{17}Se_{83-x}Sb_x$ (x = 0, 3, 9, 12, 15) glassy system by using FTIR.

4.1: Introduction

Chalcogenide glasses have drawn colossal attention over the past three decades because of their potential in photoresist [1,2], microelectronic [3-5], optoelectronic [6-9], holographic [10,11] applications and especially their ability to transmit light in the mid to far-infrared region. Impurity effects in chalcogenide glasses may have importance in fabricating glassy semiconductors. The infrared transparency of chalcogenide glasses allows their use in optical fibers for transmission of light generated by CO and CO_2 lasers operating in infrared region and such fibers are applied towards high-precision tools in surgery, industrial cutting and welding etc. The study of the IR spectra of chalcogenide glasses provides a pave way into the molecular structure of these glasses. Recently several workers have reported [12-15] vibrational spectroscopic studies of these glasses and have tried to assign the observed absorptions to the different chemical bonds in the system.

Amorphous solids display a characteristic extreme far infrared (FIR) and microwave absorption as a result of phonon coupling to modes which are not active in the corresponding crystalline counterpart material. For many years infrared spectroscopy is used as an important tool for investigating chemical processes and structure. The combination of infrared spectroscopy with the theories of reflection has made advances in surface analysis possible. Specific IR reflectance techniques are

divided into the areas of specular reflectance, diffuse reflectance and internal reflectance [16-19]. The latter is often termed as attenuated total reflectance. Recent advances in low frequency IR and Raman spectroscopy and Brillouin scattering have given a great stimulus to studies on vibrations in solids and liquids and in providing data which supplement that obtained from measurements of elastic properties from the velocities of acoustic waves and by neutron and X-ray inelastic scattering. It is important to have the low frequencies for two reasons: they are needed to complete the vibrational assignments and they are essential for calculating the thermodynamic properties. Sometimes the low frequencies cannot be obtained from the Raman spectrum because the selection rules forbid them, the sample is unsuited for the experiment because of colour or instability or the Raman bands are just too weak. The only source of data may be the far infrared [20].

Optical transmission is among one of the major applications of Ge–Se–Sb thin films which generally offer IR transparency in the wavelength (λ) regions of 3–5 μm and 4–14 μm [21]. Ge–Se–Sb thin films family is emerging as one of the most promising families which feed the material requirements for the fabrication of optical fibers, such as large band gap, low material dispersion, low light scattering and long wavelength multiphonon edge along with good thermal, mechanical and chemical properties. These properties of Ge–Se–Sb thin films makes several groups [22,23] to work on these glasses to prepare IR optical fibers for the 2–14 μm regions. Structural properties of both amorphous and crystalline solids can be explained with topological models [24], chain crossing model (CCM) [25], random covalent network model

(RCNM) [26] and chemical bond approach (CBO) [27]. In these models, some of the properties can be discussed in terms of the average coordination number, which is indiscriminate of the species or valence bond. The glass network has either a mechanical threshold or critical composition, at which the network changes from an elastically floppy (polymeric glass) mode to a rigid (amorphous solid) mode. The particular base composition of our study $Ge_{17}Se_{83}$ is the bearer of short range order of initial components and also exhibit compound short range order formed from both the initial components [28].

In the present work far-IR absorption studies have been carried out on $Ge_{17}Se_{83-x}Sb_x$ (x = 0, 3, 9, 12, 15) thin films. The results are discussed in the light of probabilities and the bond energies of various chemical bonds possible in this glass.

4.2: Experimental Details

Glassy alloys of $Ge_{17}Se_{83-x}Sb_x$ (x = 0, 3, 9, 12, 15) system were prepared by melt quench technique. Materials (99.999% purity) were weighed according to their atomic percentages and sealed in evacuated (at~10^{-4} Pa) quartz ampoules. The sealed ampoules were kept inside a furnace where the temperature was increased up to 950°C at a heating rate of 3-4°C/min and then the ampoules were frequently rocked for 8 h at the highest temperature to make the melt homogeneous. Ice cold water was used for quenching. The bulk samples were characterized by X-ray diffraction technique and found to be amorphous in nature as no prominent peak was observed in the spectra [29].

The far IR transmission spectra of different alloys were recorded on a Fourier transform IR (NICOLET 5700) used in conjunction with the KBr disc technique, over the spectral range of 500–200 cm^{-1} at room temperature. Powdered samples of 4 mg were thoroughly mixed and ground with 200 mg KBr; after which the mixtures were pressed at 10 tons cm^{-2} for 5 min. under vacuum.

4.3: Results

Far IR transmission study provides valuable information about the atomic configuration of glasses. The IR spectra of $Ge_{17}Se_{83-x}Sb_x$ (x = 0, 3, 9, 12, 15) glassy system is shown in Fig 4.1.

The bond energies of Ge-Ge, Se-Se, Sb-Sb, Ge-Se, Ge-Sb and Se-Sb bonds have been calculated on the basis of the relation postulated by Pauling [30]:

$$D(A-B) = [D(A-A) \times D(B-B)]^{\frac{1}{2}} + 30(X_A - X_B)^2$$

where X_A and X_B are the electronegativities of atoms A and B, and D(A-A) and D(B-B) are the bond energies of A-A and B-B bonds, respectively.

The relative probabilities of the different bonds have also been calculated using the probability function $\exp\left(D/k_BT\right)$ at room temperatures as well as at the temperature of 950°C at which the sample was prepared. The results are shown in Table 4.1

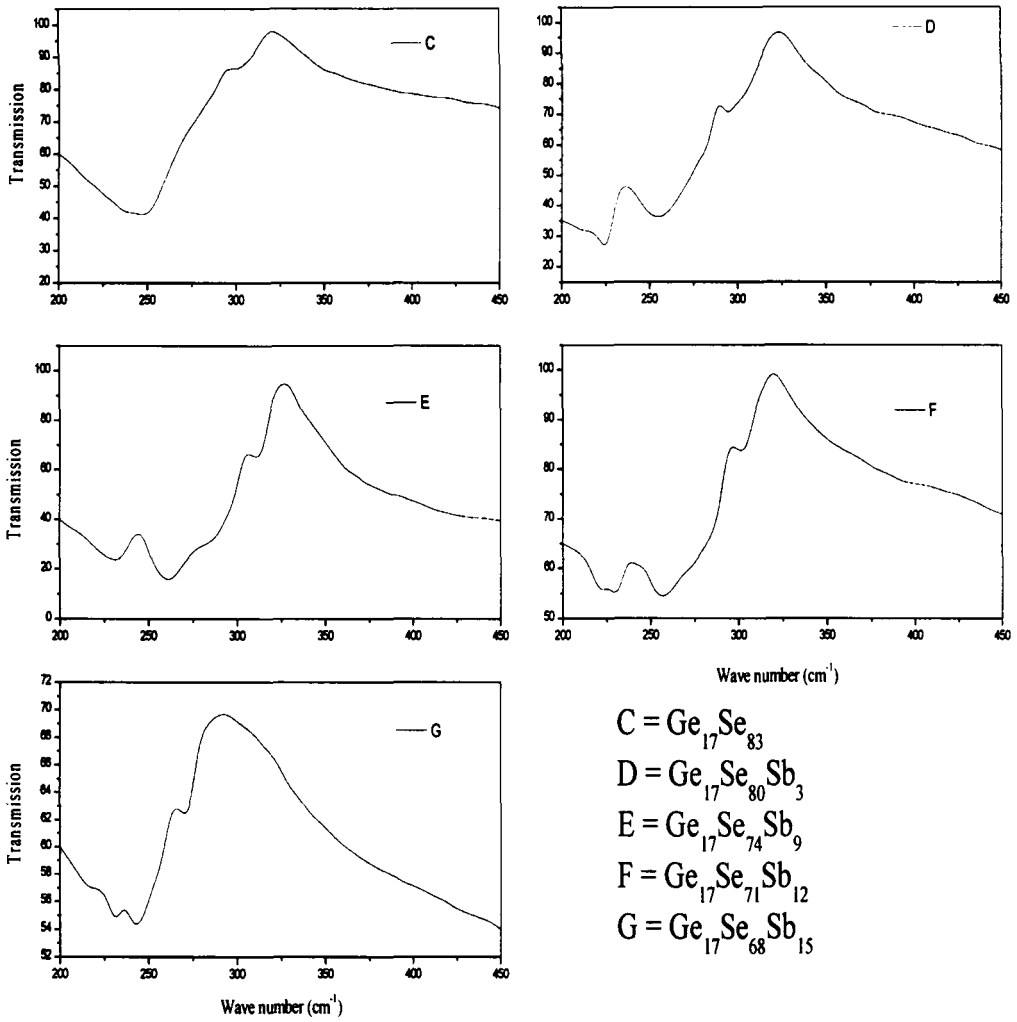

Fig. 4.1 Far IR transmission spectra of amorphous $Ge_{17}Se_{83-x}Sb_x$ glassy alloys.

Table 4.1 Bond energies and their relative probabilities of formation at 27^0C and 950^0C of $Ge_{17}Se_{83-x}Sb_x$ (x = 0, 3, 9, 12, 15) glassy alloys.

Bond	Bond energy (kcal mol^{-1})	Relative probability of bond formation	
		27°C	950°C
Ge-Se	49.4	1	1
Se-Se	44.0	1.18×10^{-4}	1.08×10^{-1}
Se-Sb	43.9	1.08×10^{-4}	1.06×10^{-1}
Ge-Sb	39.7	9.31×10^{-8}	1.88×10^{-2}
Ge-Ge	37.6	2.57×10^{-9}	7.78×10^{-3}
Sb-Sb	30.2	1.06×10^{-14}	3.70×10^{-4}

4.4: Discussion

Researchers have applied various methods and models to explain the structure of amorphous solids. Chain crossing model and random covalent model has been proposed for the structural analysis of Ge-Se amorphous glasses [25,26]. In chain crossing model the fourfold tetrahedrally coordinated Ge atoms acts as chain crossing points in the Se chain structure. In random covalent model the tetrahedrally coordinated Ge atoms bond to the other Ge atoms as readily as to the twofold coordinated Se atoms.

From an energy point of view heteropolar bonds are preferred over homopolar bonds. This can be largely explained on the basis of CBO proposed by Biecerano and Ovshinsky [27]. In this approach, the glass structure is assumed to be composed of cross linked structural units of the stable chemical compounds (heteropolar bonds) of the system and excess if any, of the elements (homopolar bonds). Due to the chemical ordering, features like extremum, a change in slope or kink [32], occur for the various properties at the tie line or stoichiometric compositions. In this case the glass structure is made up of cross linked structural units consisting of heteropolar bonds only. Heteropolar bonds thus have preeminence over homopolar bonds and bonds are formed in the sequences of decreasing bond energy until all the available valances of the atoms are saturated. Each constituent is coordinated by 8-N atoms, where N is the number of electrons in outer shell and this is equivalent to neglecting the dangling bonds and the other valence defects.

In the $Ge_{17}Se_{83}$ bulk glass the main absorption bands appear at ~ 250 cm^{-1} and 300 cm^{-1}. The existence of the absorption band at 250 cm^{-1} is assigned due to the presence of Se_8 (A_1, E mode) and the absorption band appearing at 300 cm^{-1} is due to the presence of Ge-Se-Ge (ν_1 mode). These results are in good agreement with Goyal and Mann [22]. On addition of Sb to the base sample it is seen that the Se-Se absorption band is bifurcated into 228-231 cm^{-1} and 250-260 cm^{-1}. The new absorption band appearing at 228-231 cm^{-1} having lower bond energies is assigned to Se-Sb and the absorption band at 250-260 cm^{-1} is assigned due to the presence of Se_8. The absorption band near 250-260 cm^{-1} in the spectra corresponds well to the value of 250 cm^{-1} calculated by Somayayulu [33]. As the amount of Sb goes on increasing heteropolar Se-Sb bonds starts forming on the expense of Se-Se bonds [34]. So formation of Se-Sb bonds reduces the average energy of the system which consequently supports the decrease in optical band gap [29].

From Table 4.2, the order of bond energies and the probability functions indicate that the Se atoms will preferentially first saturate Ge atoms and thereafter Se-Sb and Se-Se bonds will be formed. The result also shows that there is least probability of forming Ge-Ge, Sb-Sb and Ge-Sb bonds. The Se atoms will form chain like structures and these chains will be interlinked by Ge and Sb atoms. The bond energy results exclude the random covalent model structure where germanium atoms can be linked with other germanium atoms. These leads to the exemption of bonds like Ge-Sb and Sb-Sb whose bond energies are very low.

Table 4.2 Experimentally and theoretically calculated values of wave number (ν), reduced mass and force constant of the probable bonds.

Bond	Reduced mass 10^{-26} (kg U^{-1}) (μ)	Bond length (nm) (d)	Force constant K_{AB} (eV)	Wave number	
				Experimental (cm^{-1})	Theoretical (cm^{-1})
Ge-Ge	6.060	0.224	1.29	-	231
Ge-Sb	7.584	0.263	1.07	-	206
Ge-Se	6.301	0.239	1.93	300	277
Sb-Sb	10.129	0.282	0.87	-	173
Se-Sb	7.962	0.258	1.54	226	201
Se-Se	6.559	0.234	1.91	250-260	270

4.5: Theoretical justification of some absorption bands

Two assumptions are generally employed for discussing the IR transmission measurements for Ge-Se-Sb materials: (1) The valence force field model (VFF) [35]; (2) The position of the intrinsic IR features is influenced mainly by stretching force constants of corresponding chemical bonds.

The wave number of the vibration modes in the IR spectra is determined by the mass of the atoms and the interatomic force within the groups of the atoms comprising the glass network. The wave number is given by the following formula:

$$\nu = \left(\frac{K_r}{\mu} \right)^{\frac{1}{2}}$$

where K_r is the bending or stretching force constant of the bond and μ is the reduced mass of the molecule and is given by the following relation:

$$\mu = \frac{M_1 M_2}{M_1 + M_2}$$

where M_1 and M_2 are the atomic masses of two atoms. The force constant K_r can be calculated by the following relation obtained by Gordy [36]:

$$K_r = aN \left(\frac{\chi_A \chi_B}{d^2} \right)^{\frac{3}{4}} + b$$

Here a and b are constants which depend on the structural unit type, d is the bond length, χ_A and χ_B are the electronegativities (Ge=1.8, Se=2.4, Sb=1.9) in Pauling scale [37] and N is the bond order, which can be determined from the expression [30]

$$N = \frac{d + 2r_1 - 3r_2}{2d + r_1 - 3r_2}$$

where r_1 and r_2 are the covalent radii for the single bond and double bond respectively. By using the elemental covalent force constant electronegativities Somayayulu [33] has developed a method for predicting the force constant as follows:

$$K_{AB} = (K_{AA} K_{BB})^{\frac{1}{2}} + (\chi_A - \chi_B)^2$$

where K_{AB} is the force constant between the elements A and B and K_{AA} and K_{BB} are the force constants for bonds A-A and B-B respectively the values of which are (10^5 dyne cm^{-1}) 1.29 eV for Ge-Ge, 0.87 eV for Sb-Sb and 1.91 eV for Se-Se.

Both the experimental and theoretical values of wave number (ν) are listed in Table 4.2, together with the calculated reduced mass and the force constants of the probable bonds. From the Table 4.2 it can be seen that the experimental values of the wave number for the stretching vibrational modes for Ge-Se and Se-Sb bonds are greater than the theoretically observed values but the wave number for the stretching vibrational modes for Se-Se bond the experimental values are lesser than the theoretically observed one. This could happen because of the existence of more closely lying modes which leads to the broadening in the absorption bands.

4.6: Conclusions

The structure of the taken glassy system is based on the chain structure of selenium atoms interlinked by the tetrahedrally coordinated germanium and conceivably trivalent antimony atoms. The bond energies and probability functions conclude the least existence of bonds like Ge-Ge, Sb-Sb and Ge-Sb whose bond energies are very low. The comparison of theoretical and experimental values of the wave numbers for the stretching vibrational modes shows that the experimental wave number value for Ge-Se bond and Se-Sb bonds are greater than their corresponding theoretical values but it is just reverse for the Se-Se bonds. This may be due to the existence of more closely lying modes which leads to the broadening in the absorption bands.

References:

[1] P. Sharma, M. Vashistha, V. Ganesan, I.P. Jain, J. Alloys Compd. **462** (2008) 452.

[2] L. Petit, N. Carlie, K. Richardson, Y. Guo, A. Schulte, B. Campbell, B. Ferreira, S. Martin, J. Phys. Chem. Solid **66** (2005) 1788.

[3] O.V. Marchuk, I.D. Olekseyuk, A.G. Grebenyuk, J. Alloys Compd. **457** (2008) 337.

[4] S.R. Ovshinsky, J. Non-Cryst. Solids **141** (1992) 200.

[5] V.M. Lyubin, V.K. Tikhomirov, J. Non-Cryst. Solids **164-166** (1993) 1211.

[6] M. Mitkova, T. Petkova, R. Markovski, V. Mateev, J. Non-Cryst. Solids **164-166** (1993) 1247.

[7] P.J.S. Ewen, A. Zekak, C.W. Slinger, G. Dale, D.A. Pain, A.E. Owen, J. Non 8 Cryst. Solids **164-166** (1993) 1203.

[8] P.M. Nikolic, D. Lukovic, S.S. Vujatovic, K.M. Paraskevopoulos, M.V. Nikolic, V. Blagojevic, T.T. Zorba, B. Stamenovic, W. König J. Alloys Compd. **466** (2008) 319.

[9] B.G. Aitken, R.S. Quimby, J. Non-Cryst. Solids **213&214** (1997) 281.

[10] D. Pathinettam Padiyan, A. Marikani, K.R. Murali J. Alloys Compd. **365** (2004) 8.

[11] K. Tai, E. Ong, R.G. Vadimsky, Proc .Electrochem. Society **9** (1995) 82-89.

[12] G.J. Ball and J.M. Chamberlain, J. Non-Cryst. Solids **29** (1978) 239.

[13] V.P. Izvekov, M. Koos and K. Somogyi, J. Non-Cryst. Solids **59/60** (1983) 1011.

[14] P.M. Bridenbaugh, G.P. Espinosa, J.E. Griffiths, J.C. Phillips and J.P. Remeika, Phys. Rev. B **20** (1979) 4140.

[15] J.M. Chamberlain, S.S. Sirbegovic and P.M.Nikolic, J. Phys. C 7 (1974) L150.

[16] F.M. Mirabella, Principles, Theory, and Practice of Internal Reflection Spectroscopy, Inc. New York, 1993.

[17] A.V. Prokofiev, A.I. Shelykh, A V. Golubkov, I A. Smirnov, J. Alloys Compd. (1995) 172.

[18] R.H. Renard, J.Opt. Soc. America **54** (1964) 1190.

[19] T. Hirschfield, Appl. Spectroscopy. **31** (1977) 243.

[20] Peter Hepple, Molecular Spectroscopy, The Institute of Petroleum, 6r New Cavendish Street, London 1968.

[21] J.A. Savage, Infrared Optical Materials and Their Antireflection Coatings, Adam Hilger, Bristol, 1985.

[22] D.R. Goyal and A.S. Maan, J. Non-Cryst. Solids **183** (1995) 182.

[23] S.M. EI-Sayed, Semiconductor Science and Technology **18** (2003) 337-341.

[24] J.C. Phillips, J. Non-Cryst. Solids **34** (1979) 153; **43** (1981) 37.

[25] P. Tronc, M. Bensoussan, A. Brenac and C. Sebenne, Phys. Rev. B **8** (1973) 5947.

[26] G. Lucovsky, F.L. Galeener, R.C. Keezer, R.H. Geils and H.A. Six, Phys. Rev. B **10** (1974) 5134.

[27] J. Biecerano, S.R. Ovshinsky J. Non Cryst. Sol. **74** (1985) 75.

[28] R. Fairman, B. Ushkov, Semiconducting Chalcogenide Glass I Elsevier, Amsterdam, 2004.

[29] P. Sharma, V.S. Rangra, P. Sharma and S.C. Katyal, J. Phys. D: Appl. Phys. **41** (2008) 225.

[30] L. Pauling, The Nature of the Chemical Bonds, Cornell University Press, 1962.

[31] M.Fadel, Vacuum **52** (1999) 277.

[32] S. Mahadevan, A. Giridhar and A.K. Singh, J. Non-Cryst. Solids **103** (1988) 179.

[33] G.R. Somayayulu, J. Chem. Phys. **28** (1958) 814.

[34] S.S. Fouad, A.H. Ammar, M. Abo-Ghazala, Physica B **229** (1997) 249.

[35] L. Tichy, H. Ticha, A. Pacesova and J. Petzlt, J. Non-Cryst. Solids **128** (1991) 191.

[36] W. Gordy, J. Chem. Phys. **14** (1946) 305.

[37] L. Pauling, Uniones Quimicas, Buenos Aires, Kapelusz (1969).

Chapter-5

Physical Study of Ge-Se-Sb System

This chapter includes the study of physical parameters of $Ge_{17}Se_{83-x}Sb_x$ (x = 0, 3, 9, 12, 15) glassy system. The theoretical investigation of various physical parameters like average coordination number, number of constraints, average heat of atomization, mean bond energy and glass transition temperature have been studied.

5.1: Introduction

Prior investigative studies of physical properties in chalcogenide glasses have gain immense importance in technological [1] and commercial field [2]. Chalcogenide glasses are considered as promising materials for infrared optical elements, infrared optical fibres, information transfer, xerography, switching and memory devices, photolithography, fabrication of inexpensive solar cells and for reversible phase change optical records [3-11]. The Ge_xSe_{1-x} system is of special interest in view of the fact that it forms glasses over a wide domain of composition [12,13]. Addition of third element like As, Sb, Te, In etc. increases the glass forming region as well as creates the compositional and configurationally disorder in the system. Since, each impurity may satisfy its valence requirements by adjusting its nearest neighbour's environment, so it was believed that properties of amorphous semiconductors are weakly affected by the addition of impurities [14], but recently this has been reported that the addition of metal impurities [15] increases the refractive index and lowers the optical band gap significantly. The addition of Sb in the Ge-Se system may change its optical and electrical properties significantly. This stimulated to us to study the Ge-Se-Sb system which varies from floppy mode to rigid mode.

The aim of the present work is to examine the system $Ge_{17}Se_{83-x}Sb_x$ (x = 0, 3, 9, 12, 15) theoretically for various physical parameters. The physical parameters viz. coordination number, number of constraints, number of lone pair electrons, bond energies of the different bonds formed in the system, heat of atomization, average single bond energy (which is a measure of cohesive energy [16]), mean bond energy and glass transition temperature. The glass transition temperature has been theoretically investigated using the model proposed by Tichy and Ticha [17,18].

5.2: Experimental details

Bulk samples $Ge_{17}Se_{83-x}Sb_x$ (x = 0, 3, 9, 12, 15) were prepared by conventional melt quenching technique. High purity (99.999%) elements Ge, Se and Sb in the appropriate weight proportion, were vacuum sealed (10^{-4} Pa) in quartz ampoules and heated upto 950°C in a rocking furnace at a heating rate of 3-4°C/min, the ampoules were frequently rocked at the highest temperature for 8 hrs. The quenching was done in ice-cold water immediately after taking out the ampoules from the furnace. The detailed experimental technique has been given elsewhere [19]. The amorphous nature of the bulk samples was confirmed by the X-ray diffraction technique as no sharp peak was observed in spectra.

5.3: Results and discussion

5.3.1: Calculation of coordination number (m) and number of constraints in glassy network

Nearest neighbour coordination number (m) in the ternary system $Ge_{17}Se_{83-x}Sb_x$ (x = 0, 3, 9, 12, 15) is suitable for testing the validity of topological

concepts [20,21] because of its large glass forming domain. The average coordination number in our system has been calculated using the relation

$$m = \frac{\alpha N_{Ge} + \beta N_{Se} + \gamma n_{Sb}}{100} \qquad [1]$$

where α, β and γ are the at % of Ge, Se and Sb respectively and N_{Ge}, N_{Se} and N_{Sb} are their respective coordination numbers. The calculated coordination numbers (m) lie in the range $2.34 \leq m \leq 2.49$ and are given in Table 5.1.

The covalent bonded glassy networks are influenced by mechanical constraints (N_c) i.e. bond stretching (N_a) and bond bending (N_b) which are associated with atomic bonding and effective coordination number $< m_{eff} >$. The number of constraints per atom arising from bond bending can be calculated by $N_b = 2m - 3$ and from bond stretching by $N_a = m/2$ for the atomic species having coordination number (m). For different compositions of the glassy system $Ge_{17}Se_{83-x}Sb_x$ (x = 0, 3, 9, 12, 15), knowing the average number of constraints i.e. $N_c = N_a + N_b$ and the average coordination number (m), the effective coordination number $< m_{eff} >$ can be calculated

$$< m_{eff} >= \frac{2}{5}(N_c + 3) \qquad [2]$$

The calculated values of N_a, N_b, N_c and $< m_{eff} >$ for the glassy system $Ge_{17}Se_{83-x}Sb_x$ (x = 0, 3, 9, 12, 15) are listed in Table 5.1. According to Thorpe [21], in the range of the glassforming compositions, the system should contain floppy and rigid regions. In a-$Ge_{17}Se_{83-x}Sb_x$ compositions the average coordination number varies from 2.34 to 2.49.

Table 5.1: Values of the average coordination number (m), number of constraints arising from bond stretching (N_a), number of constraints arising from bond bending (N_b), average number of constraints (N_c), effective coordination number $<m_{eff}>$ for $Ge_{17}Se_{83-x}Sb_x$ (x = 0, 3, 9, 12, 15) glassy alloys.

Composition	M	N_a	N_b	N_c	$<m_{eff}>$
$Ge_{17}Se_{83}$	2.34	1.17	1.68	2.85	2.34
$Ge_{17}Se_{80}Sb_3$	2.37	1.185	1.74	2.925	2.37
$Ge_{17}Se_{74}Sb_9$	2.43	1.215	1.86	3.075	2.43
$Ge_{17}Se_{71}Sb_{12}$	2.46	1.23	1.92	3.15	2.46
$Ge_{17}Se_{68}Sb_{15}$	2.49	1.245	1.98	3.225	2.49

According to Zachariasen [22] heteropolar bonds have supremacy over the formation of homopolar bonds. This condition is equivalent to assuming the maximum amount of chemical ordering possible. This means that bonds between like atoms will only occur if there is an excess of a certain type of atom, so that it is not possible to satisfy its valence requirements by bonding it to atoms of different kinds alone, so bonds are formed in the sequence of decreasing bond energy until all available valences of the atoms are saturated. The possible bond distribution at various compositions is expressed using chemically ordered network (CON) model by Ovshinsky et al [23].

The model assumes that (a) atoms combine more favorably with atoms of different kinds than with the same and (b) bonds are formed in the sequence of decreasing bond energy until all available valences of the atoms are saturated. The bond energies E_{A-B} for heteronuclear bonds have been calculated by using the relation [24]

$$E_{A-B} = (E_{A-A} \times E_{B-B})^{0.5} + 30\,(\chi_A - \chi_B)^2 \qquad [3]$$

where E_{A-A} and E_{B-B} are the bond energies of the homonuclear bonds and χ_A and χ_B are the electronegativities of the atoms involved. The values of the electronegativities of Ge, Se and Sb are 2.01, 2.55 and 2.05 respectively. The calculated values for different bonds are given in Table 5.2.

Table 5.2: The number of lone pair electrons and bond energies of different bonds possible in $Ge_{17}Se_{83-x}Sb_x$ (x = 0, 3, 9, 12, 15) glassy alloys.

Composition	m	V	L = V-m	Bonds	Bond energy (eV/bond)
$Ge_{17}Se_{83}$	2.34	5.66	3.32	Ge-Se	2.144
$Ge_{17}Se_{80}Sb_3$	2.37	5.63	3.26	Se-Se	1.908
$Ge_{17}Se_{74}Sb_9$	2.43	5.57	3.14	Ge-Sb	1.724
$Ge_{17}Se_{71}Sb_{12}$	2.46	5.54	3.08	Ge-Ge	1.631
$Ge_{17}Se_{68}Sb_{15}$	2.49	5.51	3.02	Sb-Sb	1.309

5.3.2: Role of lone pair electrons in the glass forming ability

The introduction of average coordination number proposed by Phillips [20] leads to the calculation of the number of lone pairs of a chalcogenide glass system. The number of lone pair electrons is equal to the difference of all the valence electrons of the system and the shared electrons i.e.

$$L = V - m \qquad [4]$$

where L and V are lone pair electrons and valence electrons respectively. For the glassy system $Ge_{17}Se_{83-x}Sb_x$ the number of lone pair electrons is obtained by using equation (4) and are listed in Table 5.2. It is inferred from the above table and from Figure 5.1 that with the increase in content of Sb the number of lone pair of electrons decreases continuously for $Ge_{17}Se_{83-x}Sb_x$ (x = 0, 3, 9, 12, 15) glassy system. This result is caused by the interaction between the Sb ion and the lone pair electrons of a bridging Se atom. The interaction decreases the role played by the lone-pair electrons in the glass formation. Zhenhua [25] introduced a simple criterion for computing the ability of a chalcogenide system to retain its vitreous state; the criterion contains the number of lonepair electrons which is necessary for obtaining the system in its vitreous state. For a binary system the number of lone-pair electrons must be larger than 2.6 and for ternary system it must be larger than 1. In our case the values of lone pair electrons lie in the range $3.02 \leq L \leq 3.32$. This explains the fact that the system can be obtained in glassy state.

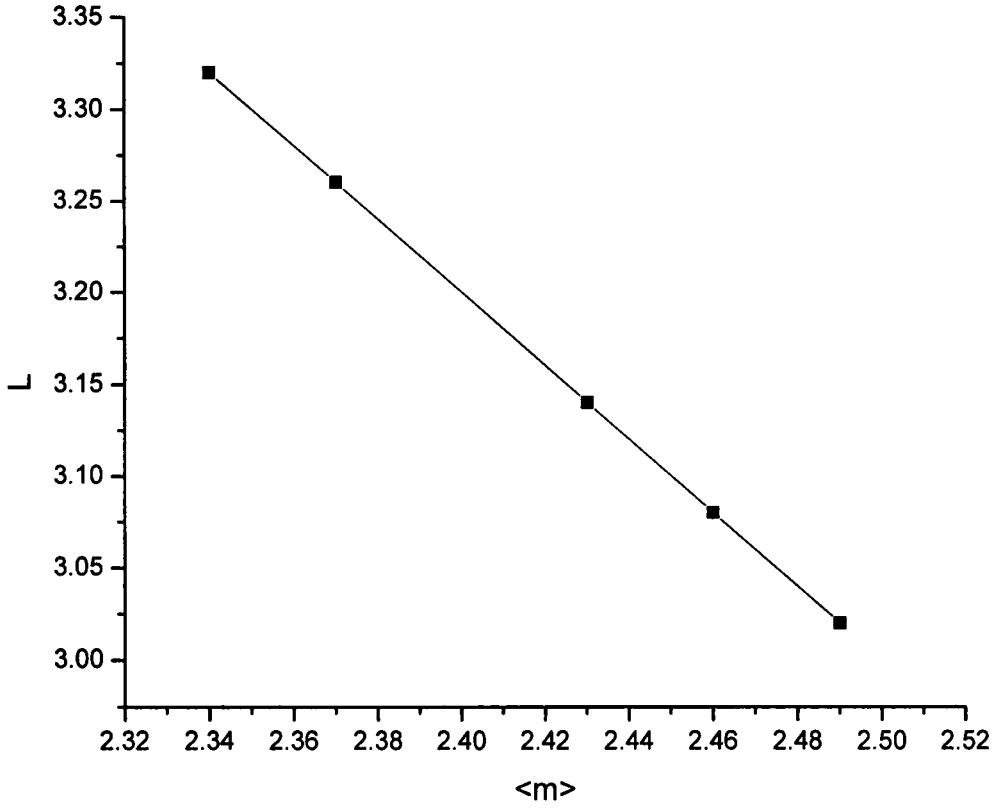

Fig. 5.1: Variation of lone pair of electrons (L) with average coordination number <m> for the glassy alloys $Ge_{17}Se_{83-x}Sb_x$ (x = 0, 3, 9, 12, 15).

5.3.3: Average heat of atomization

In chalcogenide glasses containing a high concentration of group VI element the lone-pair form the top of the valence band and the antibonding band forms the bottom conduction band [26]. The optical gap corresponds closely to the energy difference between the top of the valence band and the bottom of the conduction band. Metal atoms can form a dative bond with group VI atoms (lone pair with empty orbital) without any cost of energy, due to the presence of high-energy lone pair on the latter. Dative bonds correspond to (empty) antibonding levels which give localized acceptors states in the gap [27].

It is interesting to relate the optical band gap with the chemical bond energy. According to Pauling [28] the heat of atomization H_S (A − B) at standard temperature and pressure of a binary semiconductor formed from atoms A and B is the sum of the heat of formation ΔH and the average of the atomization H_S^A and H_S^B that corresponds to the average non polar bond energy of the two atoms

$$H_S(A-B) = \Delta H + \frac{1}{2}\left(H_S^A + H_S^B\right) \qquad [5]$$

The first term in the above equation is proportional to the square of the difference between the electronegativities χ_A and χ_B of the two atoms

$$\Delta H \propto (\chi_A - \chi_B)^2 \qquad [6]$$

In order to extend this idea to ternary and higher order semiconducting compounds, the average heat of atomization $\overline{H}_S$ (in kcal per gram-atom) is defined for a compound. $A_\alpha B_\beta C_\gamma$ is considered a direct measure of the cohesive energy and thus of average bond strength, as

$$\overline{H}_S = \frac{\alpha H_S^A + \beta H_S^B + \gamma H_S^C}{\alpha + \beta + \gamma} \qquad [7]$$

Obviously the $\overline{H}_S$ values do not contain the heat of formation (ΔH) as part of cohesive energy; however $\overline{H}_S$ is a useful parameter for correlating the physical properties of semiconducting compounds. In case of chalcogenide glasses the heat of formation contributes very little towards the average heat of atomization because the electronegativities of the constituent elements i.e. Ge, Se, Sb are very similar and in most of the cases of chalcogenide glasses the heat of formation is unknown. In the few materials for which heat of formation is known it accounts only 10% for the heat of atomization and is therefore neglected. Hence for binary chalcogenide glasses H_S (A – B) is given by

$$H_S(A-B) = \frac{1}{2}\left(H_S^A + H_S^B\right) \qquad [8]$$

whereas for ternary and higher order compounds, $\overline{H}_S$ is given by equation (7). The values of heat of atomization for Ge, Se and Sb elements are 373.8 kJ/mol, 226.0 kJ/mol and 262.04 kJ/mol, respectively, and the calculated average heat of atomization $\overline{H}_S$ and average single bond energy ($\overline{H}_S/m$) is given in Table 5.3, where m is the average coordination number. From Table 5.3 it is found that heat of atomization increases with the increase of Sb content while the average single bond energy ($\overline{H}_S/m$) which is a measure of cohesive energy decreases with the increase of Sb content. This decrease in the average single bond energy with the increase of Sb content may cause the decrease of optical band gap [16].

Table 5.3: Values of average heat of atomization ($\overline{H}_S$), average single bond energy ($\overline{H}_S/m$), mean bond energy < E > and glass transition temperature T_g (K) for $Ge_{17}Se_{83-x}Sb_x$ (x = 0, 3, 9, 12, 15) glassy alloys.

Composition	$\overline{H}_S$ (eV/bond)	$\overline{H}_S/m$ (eV/bond)	<E>	T_g (K)
$Ge_{17}Se_{83}$	2.61	1.115	2.257	422.03
$Ge_{17}Se_{80}Sb_3$	2.62	1.105	2.297	434.68
$Ge_{17}Se_{74}Sb_9$	2.64	1.086	2.388	462.99
$Ge_{17}Se_{71}Sb_{12}$	2.65	1.077	2.438	478.59
$Ge_{17}Se_{68}Sb_{15}$	2.66	1.068	2.491	495.09

5.3.4: Mean bond energy and glass transition temperature

The covalent bond approach of Tichy and Ticha [17,18] may be considered as a first approximation in the case of chalcogenide glasses. The glass transition temperature is considered to be proportional to the mean bond energy <E>, which depends on factors like average coordination number, degree of cross linking, bond energy and the nature of the bonds. Taking account of all these factors, they have examined 186 chalcogenide glasses with T_g ranging from 320 to 760 K, and obtained a good correlation between T_g and <E> in the form

$$T_g = 311[\langle E \rangle - 0.9] \qquad [9]$$

which satisfies the Arrhenius relation for viscosity. The mean bond energy of the system may be calculated using the relation

$$< E >= E_C + E_{rm} \qquad [10]$$

where E_c is the overall contribution towards bond energy arising from strong bonds and E_{rm} is the contribution arised from weaker bonds that remain after the number of strong bonds will become maximum. For $Ge_xSe_ySb_z$ system (where x+y+z = 1),

In the selenium rich region,

$$E_c = 4xE_{Ge-Se} + 3zE_{Sb-Se} \qquad [11]$$

and

$$E_{rm} = \frac{[2y - 4x - 3z]}{< r >} E_{Se-Se} \qquad [12]$$

The calculated values of the mean bond energy are given in Table 5.3. This is clear from mean bond energy data that when Sb content increases, the mean bond energy of the system increases. Figure 5.2 shows the variation of glass transition temperature with mean bond energy. The glass transition temperature increases with the increase of mean bond energy. The glass transition temperature for the various compositions of the system $Ge_{17}Se_{83-x}Sb_x$ (x = 0, 3, 9, 12, 15) have been calculated using equation (9) and is listed in Table 5.3. The glass transition temperature of the system under consideration shows that it increases with the increase of the Sb content. This increase in the value of the glass transition temperature with increasing Sb content in glass forming alloys may be due to the accumulation in them of three dimensional structural units $SbSe_{3/2}$ and $GeSe_{4/2}$, and to the decrease of the content of chain like formation of excess Se.

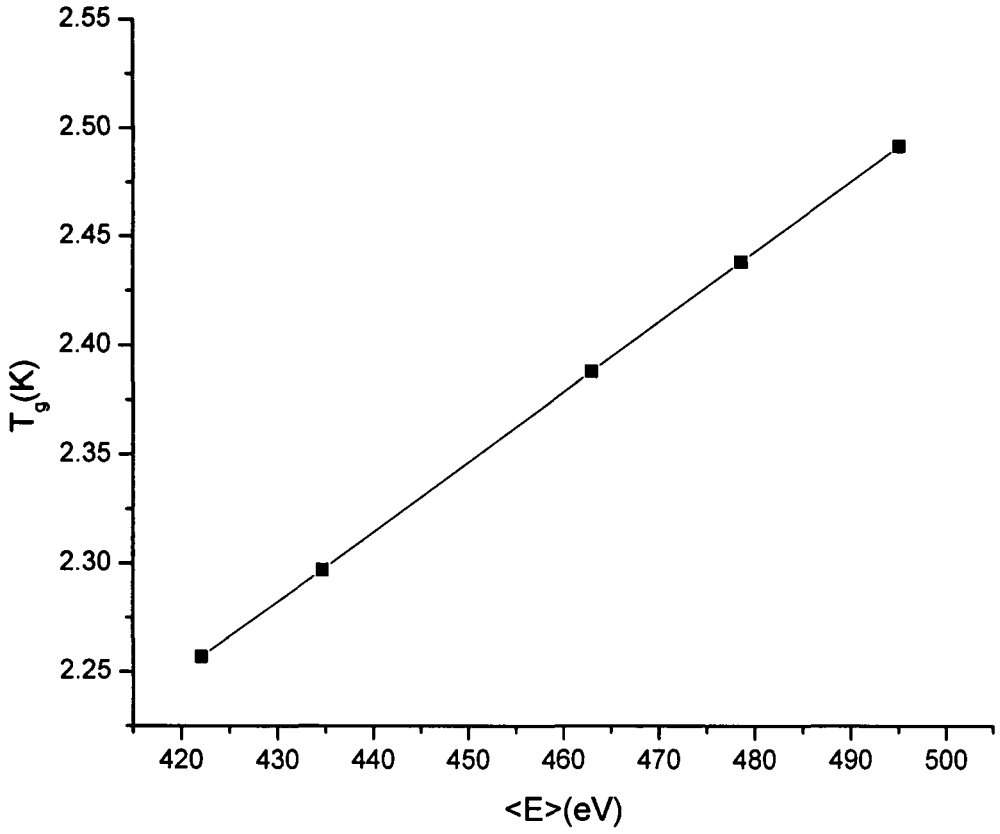

Fig. 5.2: Variation of glass transition temperature (T_g) with mean bond energy (<E>) in $Ge_{17}Se_{83-x}Sb_x$(x = 0, 3, 9, 12, 15) glassy alloys.

5.4: Conclusions

The theoretical investigation of various physical parameters for $Ge_{17}Se_{83-x}Sb_x$ (x = 0, 3, 9, 12, 15) glassy system leads to the conclusion that the average coordination number, number of constraints, average heat of atomization, mean bond energy and glass transition temperature increases with the increase of Sb content while the number of lone pair of electrons decreases. The increase of glass transition has been explained on the basis of accumulation of Sb in Se-chain.

References:

[1] K. Tanaka, Phys. Rev. B **39** (1989) 1270.

[2] A.B. Seddon, J Non-Cryst Solids **44** (1995) 184.

[3] J.A. Savage, in "Infrared Optical Materials and their Antireflection Coatings" (Hilger, London, 1985).

[4] S.R. Ovshinsky, Phy. Rev. Lett. **21** (1986) 1450.

[5] V.S. Shiryaev, C. Boussard-Pl´edel, P. Houizot, T. Jouan, J.L. Adam, J. Lucas, Materials Science and Engineering B **127** (2006) 138.

[6] M. Popescu, in "Non-Crystalline Chalcogenides" Kluwer Academic, Boston (2001).

[7] B. Cole, L.B. Shaw, P.C. Pureza, R. Mossadegh, J.S. Sanghera, I.D. Aggarwal, J. Non-Cryst. Solids **256 & 257** (1999) 253.

[8] J.S. Sanghera, I.D. Aggarwal, J. Non-Cryst. Solids **256 & 257** (1999) 6.

[9] B. Cole, L.B. Shaw, P.C. Pureza, R. Mossadegh, J.S. Sanghera, I.D. Aggarwal, J. Non-Cryst. Solids **256 & 257** (1999) 253.

[10] L. Le Neindre, F. Smektala, K. Le Foulgoc, X.H. Zhang, J. Lucas, J. Non-Cryst. Solids **242** (1998) 99.

[11] J. Fusong, M.Okuda, Jpn. J. Appl. Phys. **30** (1991) 97.

[12] M.M. Wakkad, E. Kh. Shokr, S.H. Mohamed, J. Non-Cryst. Solids **265** (2000) 157.

[13] S.S. Fouad, Physica B **213** (1995) 215.

[14] G. Saffarini, A. Schlieper, App. Phys. A **61** (1995) 29.

[15] M.M. El-Samanoudy, Thin Solid Films **423** (2003) 201.

[16] M. Yamaguchi, Phil. Mag. B **41(6)** (1985) 651.

[17] L. Tichy, H. Ticha, J. Non-Cryst. Solids **189** (1995) 141.

[18] L. Tichy, H. Ticha, Mater. Lett. **21** (1994) 313.

[19] P. Sharma, S.C. Katyal, J. Phys. D: Applied Physics **40** (2007) 2115.

[20] J.C. Phillips, J. Non-Cryst. Solids **34** (1979) 153.

[21] M.F. Thorpe, J. Non-Cryst. Solids **57** (1983) 355.

[22] W.H. Zachariasen, J. Am. Chem. Soc. **54** (1932) 3841.

[23] J. Bicerno, S.R. Ovshinsky, J. Non-Cryst. Solids **74** (1985) 75.

[24] S.C. Katyal, R.C. Verma, J. Phys.: Condens. Matter **5** (1993) 3469.

[25] L. Zhenhua, J. Non-Cryst. Solids **127** (1991) 298.

[26] M. Kastner, Phys. Rev. Lett. **28** (1972) 355.

[27] S.R. Ovshinsky, Selected papers, "Disordered Materials: Science and Technology", D. Adler (Ed.) Amorphous Institute Press, USA (1982) 83.

[28] L. Pauling, "The Nature of Chemical Bond", Cornell University Press, New York (1963).

Chapter-6

Thermal Study of Ge-Se-Sb System

This chapter includes the Thermal study of $Ge_{17}Se_{83-x}Sb_x$ (x = 0, 3, 9, 12, 15) glassy system.

6.1: Introduction

The chalcogenide glasses are one of the most widely known families of amorphous materials and have been studied extensively over the past few decades because of their interesting fundamental properties and wide commercial applications. The physical properties and compositional dependence of chalcogenide glasses have attracted much interest due to their wide technical applications [1-3]. Among various applications of these glasses the most important applications are in the field of fabricating technological important devices like IR detector, electronic and optical switches and optical recording media, laser fiber amplifiers, ultra low loss telecommunication links, radiation resistant telecommunication links, flexible CO_2 laser power guides [4,5], absorption filters, image bundles form detector array dissection, temperature, pressure and chemical sensors, non-linear components and many other optical elements [6,7].

Thermal studies on chalcogenide glasses including glass transition and kinetics of crystallization are of particular interest from fundamental and practical view points. The glass transition, one of the characteristic features of glasses, was firstly observed during the thirties of the last century and since that time, it has been the subject of the intensive study [8]. The glass transition was originally observed during the melt

cooling and for this reason; it is very often associated with gradual freezing of the melt structure during cooling. According to this approach, it is generally assumed that when a melt is sufficiently quickly cooled to avoid crystallization, an abrupt increase of structural relaxation time occurs and a melt gets into the structural non-equilibrium. Such a material, denoted as a glass, is still regarded as a melt. Until recently the glass transition is thus frequently considered to be a pure kinetic effect [9,10]. This view is commonly supported by the following findings: the value of the glass transition temperature depends on both applied technique of measurement and the process by which the glass is formed, it means on its thermal history [9-13].

Two methods are generally employed to study the crystallization kinetics – an isothermal one and a non isothermal one [14]. In the first case, the sample is subjected to a thermal treatment. At $T \approx T_{crystalline}$ for a short time and the physiochemical properties are studied as a function of time. According to the second method, the sample is heated with a constant rate and the investigated characteristics are measured as a function of the temperature.

The study of glass forming region is of great interest so it is quite important to know the glass stability and chemical durability of these materials. However no simple way presently exists to formulate the correlation between ideal composition and stability of these glasses. With object to evaluate the level of stability of the vitreous alloys, different simple quantitative methods have been suggested. Most of these

methods [15-19] are based on characteristic temperatures such as the glass transition temperature (T_g), the crystallization temperature (T_c) or the melting temperature (T_m). Some of them [20,21] are based on the reaction constant (K) some of others [22-24] are based on the crystallization activation energy. These thermal parameters are easily and accurately obtained by differential thermal analysis (DTA) during the heating process.

Differential thermal analysis is known to demonstrate with ease the characteristic difference between a structurally stable material (exhibiting switching phenomena) and a reversible material (exhibiting memory phenomena). This communication reports a systematic investigation of the compositional dependence (Ge:Se:Sb) of different thermal properties for $Ge_{17}Se_{83-x}Sb_x$ (x = 0, 3, 9, 12, 15) glassy system.

6.2: Experimental Details

Glassy alloys of $Ge_{17}Se_{83-x}Sb_x$ (x = 0, 3, 9, 12, 15) system were prepared by melt quench technique. Materials (99.999% purity) were weighed according to their atomic percentages and sealed in evacuated (at ~ 10^{-4} Pa) quartz ampoules. The sealed ampoules were kept inside a furnace where the temperature was increased up to 950°C at a heating rate of 3-4°C/min. The ampoules were frequently rocked for 8 h at the highest temperature to make the melt homogeneous. The quenching was done in ice cold water. Thin films of glassy alloys were prepared on glass substrates by vacuum

evaporation technique at room temperature and base pressure of ~10^{-4}Pa. The glassy substrates were firstly cleaned by soap solution at room temperature using ultrasonic cleaner then with double distilled water, a dip in acetone followed by ethyl alcohol, dried in an oven at approximately 110°C. The bulk as well as thin films of the samples prepared were characterized by X-ray diffraction technique and found to be amorphous in nature as no prominent peak was observed in the spectra.

DTA experiments were carried out on a Perkin Elmer (Pyris Diamond) in Nitrogen atmosphere (200 ml/min). All measurements were referenced to Alumina powder in an Alumina-pan, and carried out in a nitrogen atmosphere flowing at 50 ml/min.

6.3: Results and discussion

DTA measurements provide quantitative and qualitative information about physical and chemical changes that involve endothermic or exothermic processes or changes in heat capacity. The vitreous or glass transition is an endothermal reaction, specify to glassy materials. All the modifications which take place in the region of glass transition are essential for all the processes in glasses and influence directly the glass properties. The $Ge_{17}Se_{83-x}Sb_x$ (x = 0, 3, 9, 12, 15) glassy system is measured repeatedly over the glass transition region by Perkin Elmer (Pyris Diamond) in Nitrogen atmosphere (200 ml/min)DTA using considerable different heating/cooling step rates. DTA thermograms of $Ge_{17}Se_{83-x}Sb_x$ (x = 0, 3, 9, 12, 15) glassy system are studied for different heating rates viz. 10^0, 15^0, 20^0 and 25^0.

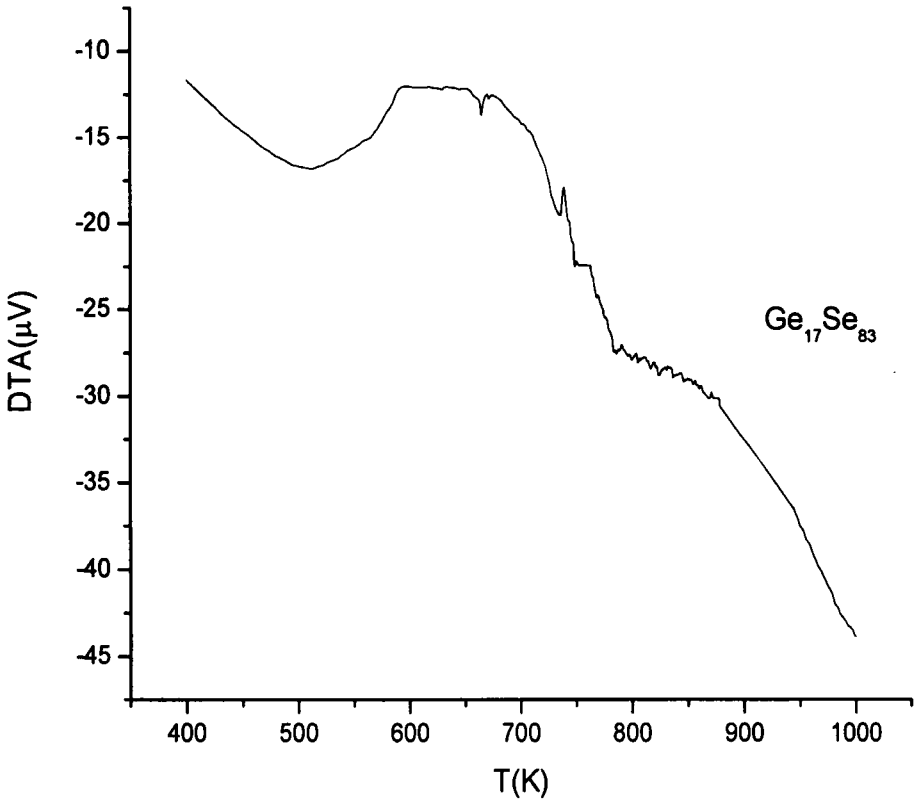

Fig 6.1 DTA traces of $Ge_{17}Se_{83}$

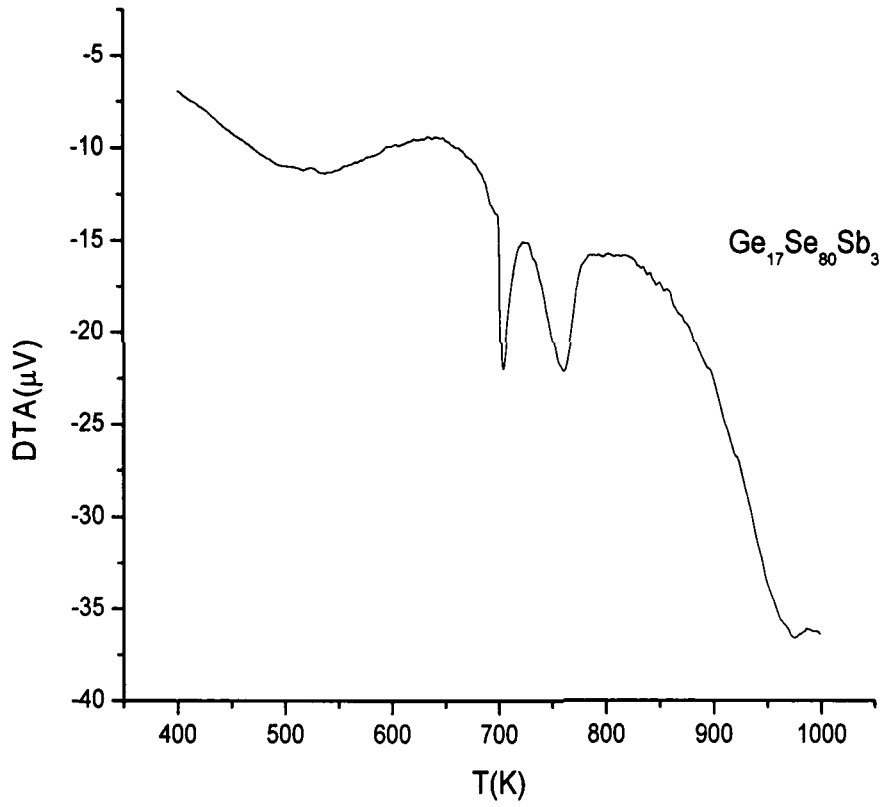

Fig 6.2 DTA traces of $Ge_{17}Se_{80}Sb_3$

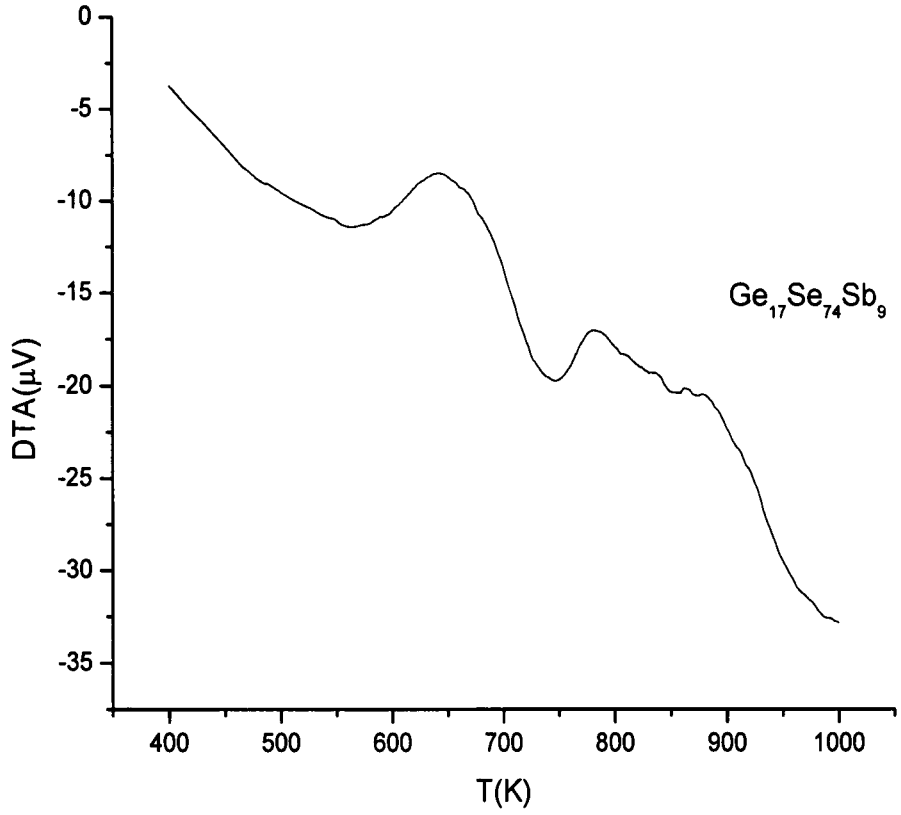

Fig 6.3 DTA traces of $Ge_{17}Se_{74}Sb_9$

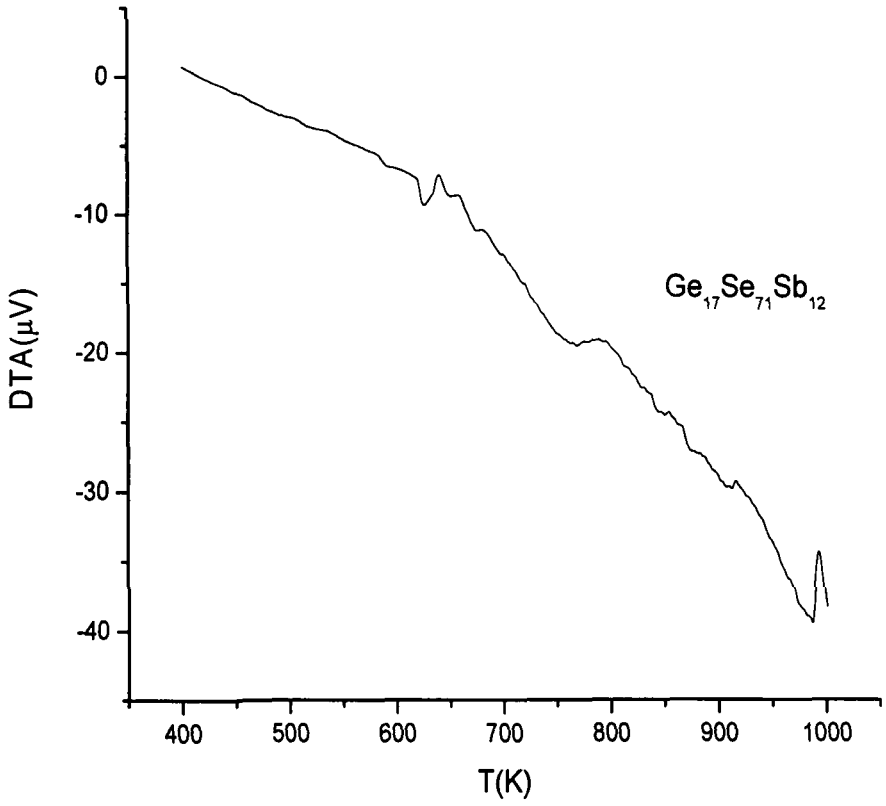

Fig 6.4 DTA traces of $Ge_{17}Se_{71}Sb_{12}$

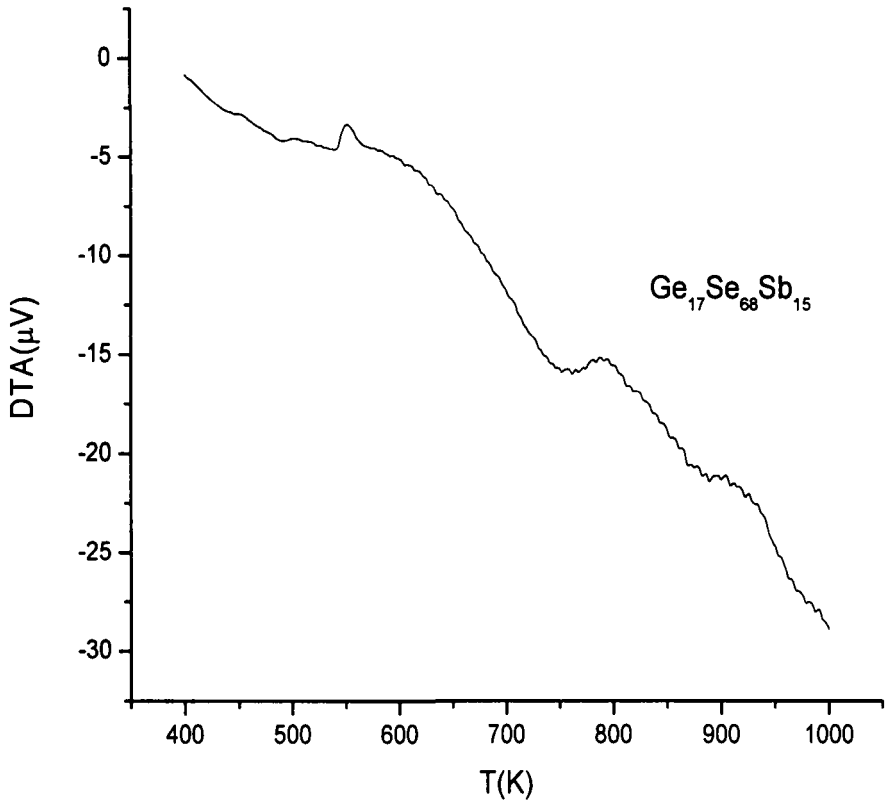

Fig 6.5 DTA traces of $Ge_{17}Se_{68}Sb_{15}$

DTA thermograms of Ge-Se-Sb at the heating rate of 10^0C are shown in Figures 6.1-6.5. It can be seen from the figures that glass transition temperature (T_g) and glass crystallization temperature (T_c) shift towards higher temperature with increase in antimony content. This increase in the value of glass transition temperature (T_g) can be explained on the basis of CONM, according to which the heteropolar bond is favoured over the homopolar bond. The various types of bonds involved in the present system are Se-Se, Se-Ge, Se-Sb, Ge-Sb, Ge-Ge and Sb-Sb. When the percentage of antimony is increased, antimony is expected to form bonds with selenium rather than germanium because the bond energy of Se-Sb (43.9 Kcal/mol) is larger than the bond energy of Ge-Se (39.7 Kcal/mol) [25]. This explains the increase in glass transition temperature (T_g) with increase in antimony content.

6.3.1: Glass forming ability

In the differential thermal analysis (DTA) technique, the sample is heated at the same heating rate as an inert reference sample and temperature difference (ΔT) between these two samples is plotted against the temperature of the glass. Second order transformations (viz, changes in specific heat, thermal expensivity, etc.) produce vertical displacement of the otherwise horizontal ΔT curve (base line). The range of temperature over which this transition takes place is called the glass transition or glass transformation temperature T_g. The magnitude of this endothermic effect is sensitive to the thermal history of the glass [26]. A slowly cooled glass yields a larger area under

the endothermic peak (a quantity proportional to the energy which is absorbed by the relaxation of glass structure) than one rapidly chilled [27]. As the glass is heated through the temperature T_g, enough vibrational energy is present to help relaxation of glass structure and to break some of the weaker (highly strained) bonds, thus introducing some degrees of freedom into the system. These additional degrees of freedom result in an increase in the heat capacity.

The glass transition is not at a precisely defined temperature. The glass transition is not sharp but occurs over a range of temperature. T_g is sensitive to the total thermal history of the glass, i.e. to rate of cooling from the liquid as well as to the subsequent heat treatment in the neighbourhood of T_g [28,29]. As glass is heated above T_g, one may observe an exotherm for the re-crystallization point T_c, and on still further heating another endothermic effect for the melting point T_m of the glass [30].

The glass transformation temperature T_g alone does not give any direct information in the determination of the glass-forming tendency of a melt as it is connected with the chemical composition of glass [31]. Nevertheless, it is a quantity of fundamental importance since all glasses have, approximately, equal values of viscosity ($\sim 10^{-13}$ poise) at T_g, and are in an. intermediate state between the solid and liquid phase, where binding forces of molecular character vanish [32]. However, coupled with T_c and T_m, T_g can probably assist in the evaluation of glass-forming tendency.

The temperature dependence of viscosity is of decisive importance in determining the behaviour of glass on its heating above glass transition temperature (T_g). Provided the viscosity drops rapidly, the rate of diffusion increases accordingly. The latter is one of the factors relevant to the rate of crystallization. In this case crystallization occurs close to T_g. This happens for substances that form glasses with difficulty. A short interval $T_c - T_g$ signifies that glass contains structural units with high crystallization tendency, i.e. with high liquidus temperature of the melt which is unfavourable to the glass formation [33]. A short interval T_m - T_c in its turn indicates that the original melt has relatively low temperature of solidification (solidus). Therefore, this circumstance is favourable to the glass formation.

Several attempts have been made in the past to enable one to estimate or predict the glass-forming ability of a melt on the basis of structural and kinetic factors [33-40]. As a result of this several rules or models have been worked out and they serve as a guide for preparation of new amorphous materials [32]. Dietzel [33] defines 'glassiness' as the reciprocal rate of crystallization of the melt. Sarjeant and Roy [34] use the critical rate of cooling as a criterion of glass-forming tendency. These models seem to have only a limited applicability. Haverman et al [35] compared the Dietzel's criterion with critical rate of cooling in the system of sodium and lithium silicates and found that no definite relation between these two criteria existed. Kautzman [36] dealt in detail with the significance of the relation between T_g and T_m. He gives the criterion of glass-forming tendency expressed by the relation:

$$T_{cg} = \frac{T_g}{T_m}$$

where T_{cg} is the reduced temperature of transformation T_g / T_m which he puts in a direct relation with the temperature dependence of the viscosity.

The value obtained obey the two-thirds rule which states

$$\frac{T_g}{T_m} = \frac{2}{3}$$

However, according to Turnbull [37] this relation has limited applicability when confronted with experimental data. Cohen and Turnbull [38] have in turn suggested a semiquantitative criterion of glass-forming tendency expressed by:

$$\tau = \frac{R - T_m}{H_n}$$

where H_n is the molar heat of evaporation that they directly relate to the cohesion energy and the asymmetry of molecules. R is the gas constant and T_m the melting temperature. This criterion is valid only for/certain type of substances and certain rate of cooling. Its wider applicability is hindered by the loose concept of melting temperature, as the interval between the solidus and liquidus may be rather large for more complex system [39].

Hruby [40] has proposed another criterion of evaluation of glass-forming ability of a melt. This model assumes that glass has already been prepared. Therefore,

this is not applicable for hitherto unknown melts. Nevertheless, it is useful to compare different kinds of liquids (glasses) and find connections in a certain specific system. Also like that of Kautaman's model, this model can yield a relatively fast technique of evaluation of the glass-forming ability of melts. This criterion is based on the following three rules:

1. All glasses are in a comparable state at T_g.

2. The interval T_c - T_g is directly proportional to the glass-forming tendency.

3. The interval T_m - T_c is directly proportional to the glass-forming tendency.

The numerical measure of the glass-forming tendency according to this model is given by:

$$K_{gl} = \frac{T_c - T_g}{T_m - T_c}$$

According to this model if the value of K is about 0.1, the preparation of glass is very difficult. For K_{gl} = 0.5, glass is easily formed merely by free cooling of the melt in air. For K_{gl} above 1.0 only a glass of high-molecular polymer type is possible. The larger the value of K_{gl} the greater is the stability of glass against crystallization. Hruby parameter (Table 6.1) of the investigated glass is indicating not high stability against crystallization and also indicating the formation of glass of high-molecular polymer type.

Table 6.1 Glass transition temperature, glass crystallization temperature, glass melting temperature, glass forming ability of $Ge_{17}Se_{83-x}Sb_x$ (x = 0, 3, 9, 12, 15) glassy system.

Sample	T_g (^{O}K)	T_c (^{O}K)	T_m (^{O}K)	T_g/T_m	K_{gl}
$Ge_{17}Se_{83}$	786.4885	925.4934	1007.59	0.780564	1.693182
$Ge_{17}Se_{80}Sb_3$	812.6102	973.0723	1071.029	0.758719	1.638095
$Ge_{17}Se_{74}Sb_9$	840.5978	998.2611	1105.547	0.760346	1.469565
$Ge_{17}Se_{71}Sb_{12}$	899.3717	1022.517	1124.205	0.800007	1.211009
$Ge_{17}Se_{68}Sb_{15}$	813.5432	999.9927	1163.388	0.699288	1.141098

6.3.2: Calculation of Activation Energy by Kissinger's model:

DTA thermograms of $Ge_{17}Se_{83-x}Sb_x$ (x = 0, 3, 9, 12, 15) glassy system are studied for different heating rates 10^0, 15^0, 20^0 and 25^0. The activation energies of above glassy system are calculated by Kissinger model [41] using the formula:

$$\ln\frac{b}{T_c^2} = -\frac{E_a}{RT_c} + const$$

Where b is the heating rate, E_a is the activation energy of the glass transition for homogeneous crystallization with spherical nuclei and R is the gas constant. The values of activation energies are given in Table 6.2 and the related plots of ln (b/T_c^2) vs $1000/T_c$ are shown in figures 6.6-6.10.

Table 6.2 Activation energy of $Ge_{17}Se_{83-x}Sb_x$ (x = 0, 3, 9, 12, 15) glassy system.

Sample	Kissinger's model(E_a)(KJ/mol)
$Ge_{17}Se_{83}$	0.309
$Ge_{17}Se_{80}Sb_3$	1.095
$Ge_{17}Se_{74}Sb_9$	1.105
$Ge_{17}Se_{71}Sb_{12}$	1.671
$Ge_{17}Se_{68}Sb_{15}$	1.141

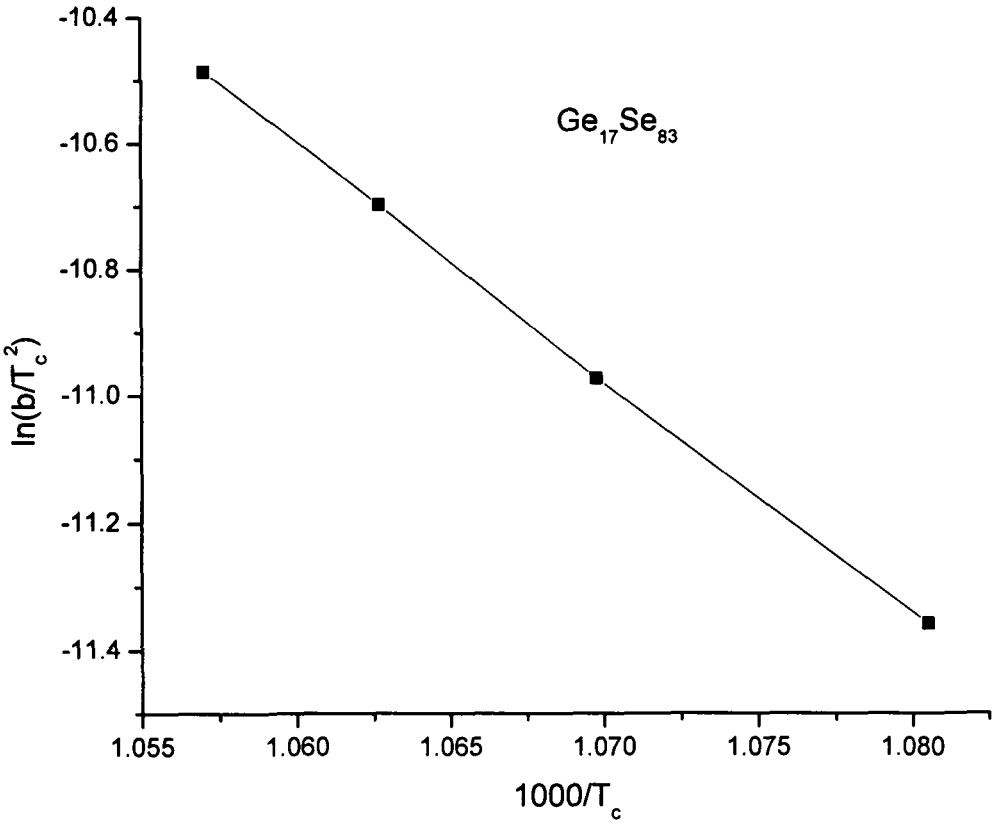

Fig 6.6 Plot of $\ln(b/T_c^2)$ vs $1000/T_c$ for $Ge_{17}Se_{83}$

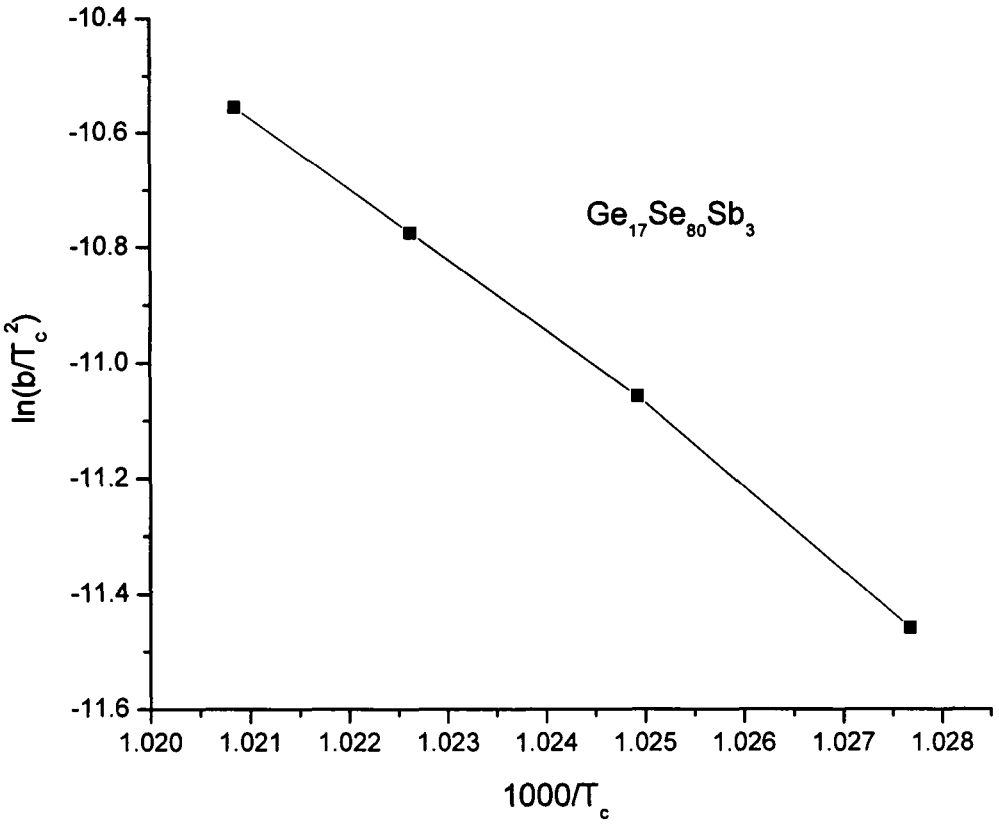

Fig 6.7 Plot of $\ln(b/T_c^2)$ vs $1000/T_c$ for $Ge_{17}Se_{80}Sb_3$

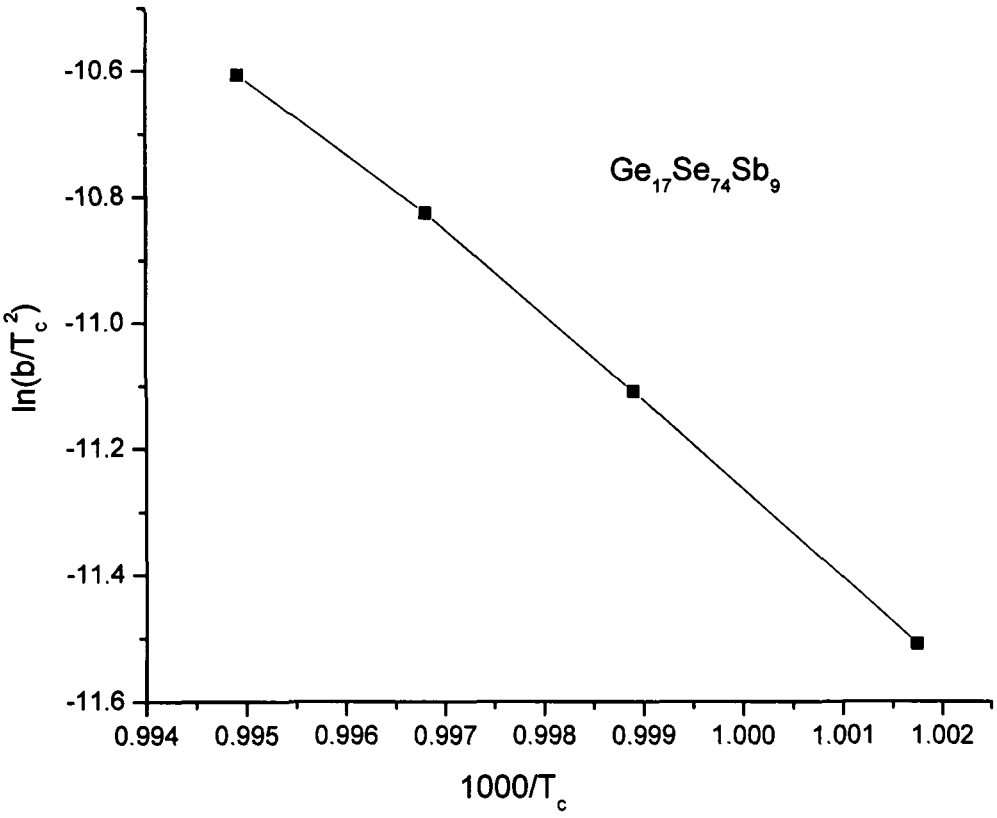

Fig 6.8 Plot of $\ln(b/T_c^2)$ vs $1000/T_c$ for $Ge_{17}Se_{74}Sb_9$

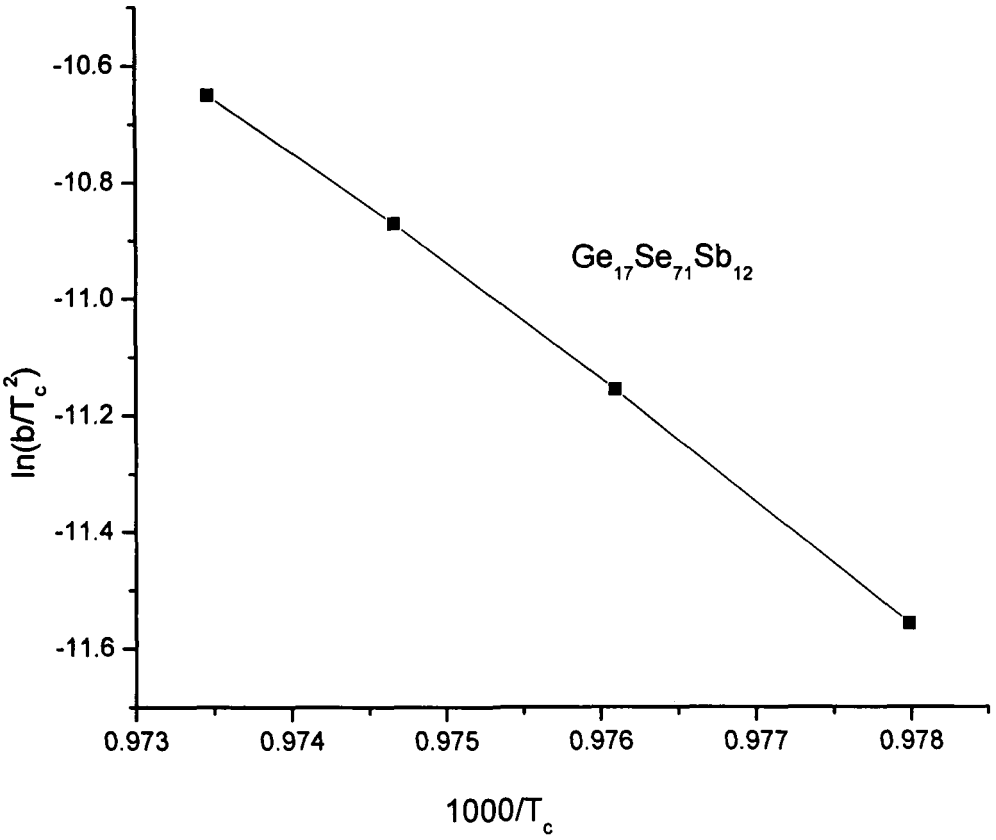

Fig 6.9 Plot of $\ln(b/T_c^2)$ vs $1000/T_c$ for $Ge_{17}Se_{71}Sb_{12}$

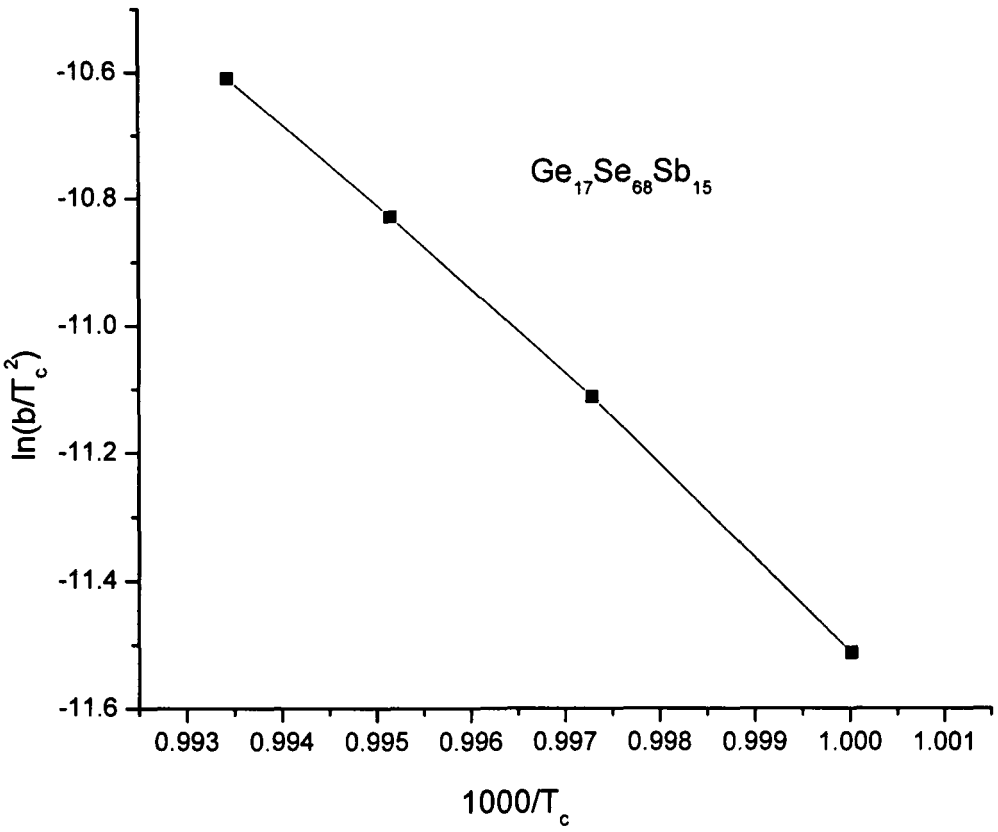

Fig 6.10 Plot of $\ln(b/T_c^2)$ vs $1000/T_c$ for $Ge_{17}Se_{68}Sb_{15}$

6.4: Conclusions

Hruby parameter calculated from the DTA study of the investigated glassy system $Ge_{17}Se_{83-x}Sb_x$ (x = 0, 3, 9, 12, 15) is indicating not high stability against crystallization and also indicating the formation of glass of high-molecular polymer type. Also it can be seen that glass transition temperature (T_g) and glass crystallization temperature (T_c) shift towards higher temperature with increase in antimony content. This increase in the value of glass transition temperature (T_g) can be explained on the basis of CONM, according to which the heteropolar bond is favoured over the homopolar bond.

References:

[1] S.A. Khan, M. Zulfequar, M. Husain, Physica B **324** (2002) 336–343.

[2] M.B. Elden, M.M. El-Nahass, Opt. Laser Technol. **35** (2003) 335–340.

[3] Z.H. Khan, M. Zulfequar, Arvind Kumar, M. Husain, Con. J. Phys. **80** (2002) 19–27.

[4] J. Nishi, S. Morimoto, I. Ingawa, R. Lizuka, T. Yamashita, J. Non- Cryst. Solids **140** (1992) 199.

[5] X. Zhang, H. Ma, J. Lucas, J. Optoelectron. Adv. Mater. **5(5)** (2003) 1327.

[6] S.R. Elliot, Physics of Amorphous Materials, Longman, New York (1990).

[7] P. Sharlandjev, B. Markova, J. Optoelectron. Adv. Mater. **5(1)** (2003) 39.

[8] H. Suga, J. Therm. Anal. Cal. **60** (2000) 57.

[9] I.M. Hodge, J. Non-Cryst. Solids **169** (1994) 211.

[10] J.M. Hutchinson, Thermochimica Acta **324** (1998) 165.

[11] C.T. Moynihan, A.J. Easteal, M.A. DeBolt, J. Tucker, J. Am. Ceram. Soc. **59** (1976) 12.

[12] A.J. Kovacs, J.M. Hutchinson, J. Polym. Sci. **17** (1979) 2031.

[13] S.R. Elliott, in: Physics of amorphous materials, 2nd edition, Longman Scientific & Technical, Essex, UK (1990) 33.

[14] N. Mehta, M. Zulfequar, A. Kumar, JOAM **2** (2004) 441.

[15] A. Dietzel, Glasstech. Ber. **22** (1968) 41.

[16] D.R. Uhlmann, J. Non-Cryst. Solids **7** (1972) 337.

[17] D.R. Uhlmann, J. Non-Cryst. Solids **25** (1977) 43.

[18] A. Hruby, Czech. J. Phys. B **22** (1972) 1187.

[19] M. Saad, M. Poulain, Mater. Sci. Forum **19/20** (1987) 11.

[20] S. Surinach, M.D. Baro, M.T. Clavaguera-Mora, N. Clavaguera, J. Mater. Sci. **19** (1984) 3005.

[21] L. Hu, Z. Jiang, J. Chin. Ceram. Soc. **18** (1990) 315.

[22] A. Marotta, A. Buri, F. Branda, J. Non- Cryst. Solids **95/96** (1987) 593.

[23] X. Zhao, S. Sakka, J. Non- Cryst. Solids **95/96** (1987) 487.

[24] F. Branda, A. Marotta, A. Buri, J. Non- Cryst. Solids **134** (1991) 123.

[25] J. Biecerano, S. R. Ovshinsky, J. Non Cryst. Sol. **74** (1985) 75.

[26] A. Winter, J. Canad. Ceram. Soc **41** (1972) 27.

[27] W. Wilbum and J. Dawson, in: Differential thermal analysis, Ed.: R.C. Mackenzie (Academic Press, London, 1972).

[28] A.E. Owen, in: Electrical and structural properties of amorphous semiconductors, Eds. G. LeComber and J" Mort (Academic Press, London, 1973) 161.

[29] W. Espe, Materials of high vacuum technology, vol.2 (Pergamon> Oxford, 1968).

[30] R.C. Mackenzie, Ed.: Differential thermal analysis, vol. I&II Academic Press, London, (1970, 1972).

[31] M.B. Meyers and E.J. Pelty, Mat. Res. Bull. **6** (1967) 535.

[32] H. Scholae, Glass (F. Vieweg &Sohn, Braunschweig (1965).

[33] A. Dietzel, Glastech. Ber. **22** (1968) 41.

[34] P.T. Sarjeant and R. Roy, Mat. Res. Bull. **3** (1968) 265.

[35] A.C.J. Kaverman, N. H. Stein and J.M. Stevels, J. Non-cryst. Sol. **5** (1970) 66.

[36] W. Kautxman, Chem. Rev. **43** (1948) 219.

[37] D. Turnbull, Contempt. Phys. 10 No. **5** (1969) 488.

[38] M. H. Cohen and D. Turnball, Nature **189** (1961) 131.

[39] H. Rawson, Inorganic glass forming systems (Academic Press, New York, London) (1967).

[40] H. Hruby, Czech. J. Phys. B **22** (1972) 1187.

[41] H.E. Kissinger, Anal. Chem. **29** (1957) 1702.

Chapter-7

Optical Study of Ge-Se-Sb System

This chapter includes the optical study of $Ge_{17}Se_{83-x}Sb_x$ (x = 0, 3, 9, 12, 15) thin films.

7.1: Introduction

Chalcogenide glasses are formed from group VI elements (S, Se and Te) of the periodic table. Oxides are excluded by convention, largely due to early and extensive development of this field. Chalcogenide glasses are similar to oxides but they exhibit pronounced optical properties [1–4]. They have attracted the attention of many investigators due to their potential in IR optics, photonics device, reversible optical recording, memory switching, inorganic photo resists, antireflection coatings, optical imaging, optical data storage, Raman amplification, optical limiter, frequency doubling, etc [5–12]. Among chalcogenides, selenide materials have been identified as possible materials for non-linear optical applications [13]. Because of large atomic radius compared with oxygen in oxide glasses and sulfur in sulfide glasses, selenium plays an important role in the non-linear optical properties in selenide glasses. Working with Se causes some problems like the ageing effect and low sensitivity. Hence in order to produce changes in the properties of new complex glass, it is worth adding more than one component into the selenium matrix to get rid of these problems. To overcome these problems, several workers [14–17] have used certain additives (Ge, Bi, As, etc) to make binary alloys with selenium, which in turn give high sensitivity, a high crystallization temperature and smaller ageing effects. Germanium based chalcogenide containing heavy metal species such as Sb has shown

their potential as glasses with high non-linear optical properties [18]. In this work we have chosen the Ge–Se–Sb system. The well-known glass-forming system Ge–Se–Sb has been chosen because of the relatively lower vapour pressure compared with the Ge–As–Se [19] system. Moreover, working with Sb in comparison with As is less hazardous to health. The particular base composition of our study $Ge_{17}Se_{83}$ is the bearer of short range order of initial components and also exhibit compound short range order formed from both the initial components [20]. No work has been reported so far on optical, structural and electrical properties of the system under investigation as per our knowledge. Earlier we have reported the physical properties (coordination number, lone pair of electron, bond energy, heat of atomization, glass transition temperature) of this system [21].

Most of the applications of chalcogenide glasses depend on our ability to engineer their compositions to meet the specific requirements. The tailoring of chalcogenide glasses for specific properties is possible but we do not know enough about most of the glass systems to choose according to compositions. It is the intent of this paper to develop a basic understanding of the optical behaviour of $Ge_{17}Se_{83-x}Sb_x$ (x = 0, 3, 9, 12, 15) system. These results may lead directly to applications in non-linear optics or lay a foundation for other research into the optical behaviour of the $Ge_{17}Se_{83-x}Sb_x$ system. Optical properties viz. refractive index (n), extinction coefficient (k) and optical energy gap $\left(E_g^{opt}\right)$ has been reported for $Ge_{17}Se_{83-x}Sb_x$ (x = 0, 3, 9, 12, 15) thin films. Transmission and reflection spectra have been used for the

study of optical properties. The dispersion of refractive index has been studied using the Wemple–DiDomenico (WDD) single oscillator model. Some allied parameters (dielectric constant, dielectric loss and optical conductivity) have also been determined using n, k and absorption coefficient (α).

7.2: Experimental details

Glassy alloys of the $Ge_{17}Se_{83-x}Sb_x$ (x = 0, 3, 9, 12, 15) system were prepared by the melt quench technique. Materials (99.999% purity, Sigma Aldrich) were weighed (4 g for each batch using a Mettler Toledo PL83-S) according to their atomic weight percentage and sealed in evacuated (at ~ 10^{-4} Pa) quartz ampoules. The sealed ampoules were kept inside a furnace where the temperature was increased up to 950°C at a heating rate of 3–4°C min^{-1}. The ampoules were frequently rocked for 8 h at the highest temperature to make the melt homogeneous. The quenching was done in ice cold water. Films of bulk glasses were deposited on microscopic glass substrates using the vacuum evaporation technique at a base pressure of ~10^{-4} Pa (Hindhivac Model No. 12A4D). The thickness of the solid films has been monitored during depositions by using a thickness monitor (DTM-101) (with an uncertainty of ±30 nm). The compositions of the evaporated samples have been measured by an electron microprobe analyzer (JEOL 8600 MX) on different spots (size ~ 2μm). For the composition analysis, the constitutional elements (Ge, Se and Sb) and the bulk original alloys, i.e. $Ge_{17}Se_{83-x}Sb_x$ (x = 0, 3, 9, 12, 15) are taken as reference samples. The

composition of 2×2 cm^2 sample is uniform within the measurement accuracy of about ±1.5–2.0%. The bulk as well as the thin films of the samples prepared were characterized by the X-ray diffraction (XRD) technique (Philips PW 1710 X-ray diffractometer, Cu Kα radiation, λ = 1.540 598 Å, 40 kV and 35 mA, 2θ range from 5° to 100°, step size = 0.017°). The normal incidence transmittance and reflectance spectra in the spectral range 400–2000 nm of films were obtained by a double beam ultraviolet–visible–near infrared spectrophotometer (Perkin Elmer Lambda-750). All measurements were performed at room temperature (300 K).

7.3: Results and discussion

Figure 7.1 shows the XRD patterns of the $Ge_{17}Se_{83-x}Sb_x$ (x = 0, 3, 9, 12, 15) thin films. The absence of sharp structural peaks in these XRD traces confirmed the amorphous nature of thin films.

Figure 7.2 shows the transmittance and the reflectance spectra of the $Ge_{17}Se_{83-x}Sb_x$ (x = 0, 3, 9, 12, 15) thin films. The figure shows fringes due to interference at various wavelengths. It is apparent from the transmission spectra that there is a clear red shift in the interference free region with the addition of Sb content. Following the fundamental Kramers–Kronig relationships, the red-shift in the spectrum must necessarily give an increased refractive index value (justified later). Optical transmission (T) and reflection (R) are very complex functions and strongly depend on the absorption coefficient.

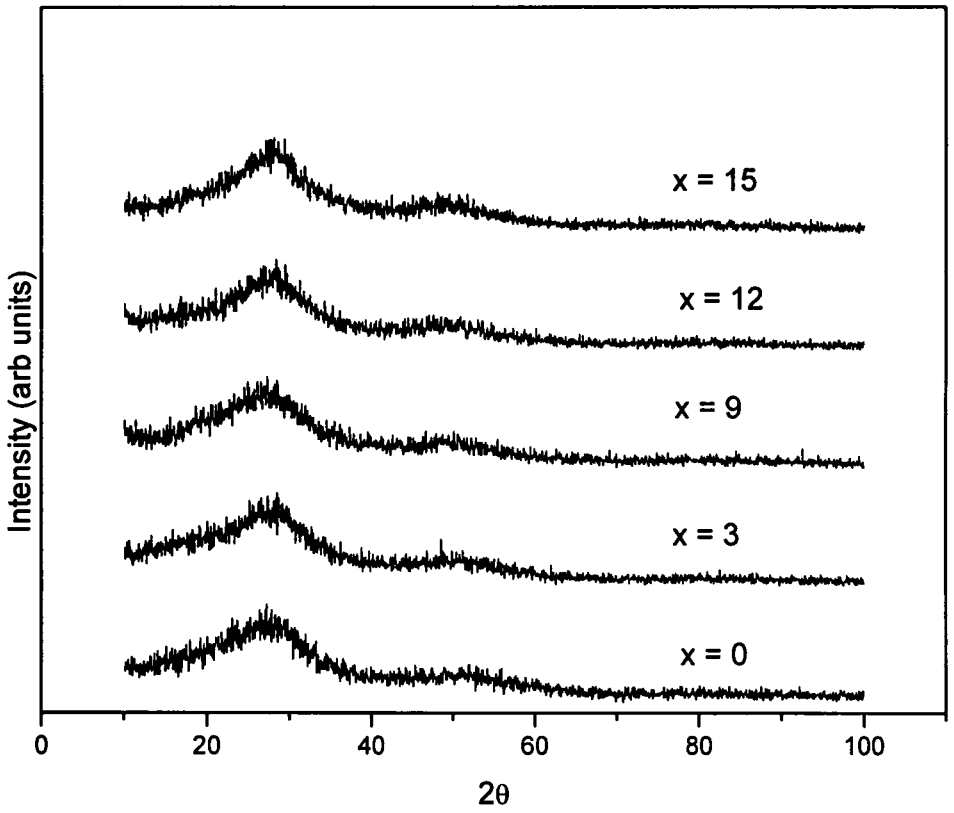

Fig. 7.1 XRD pattern for $Ge_{17}Se_{83-x}Sb_x$ (x = 0, 3, 9, 12, 15) thin films.

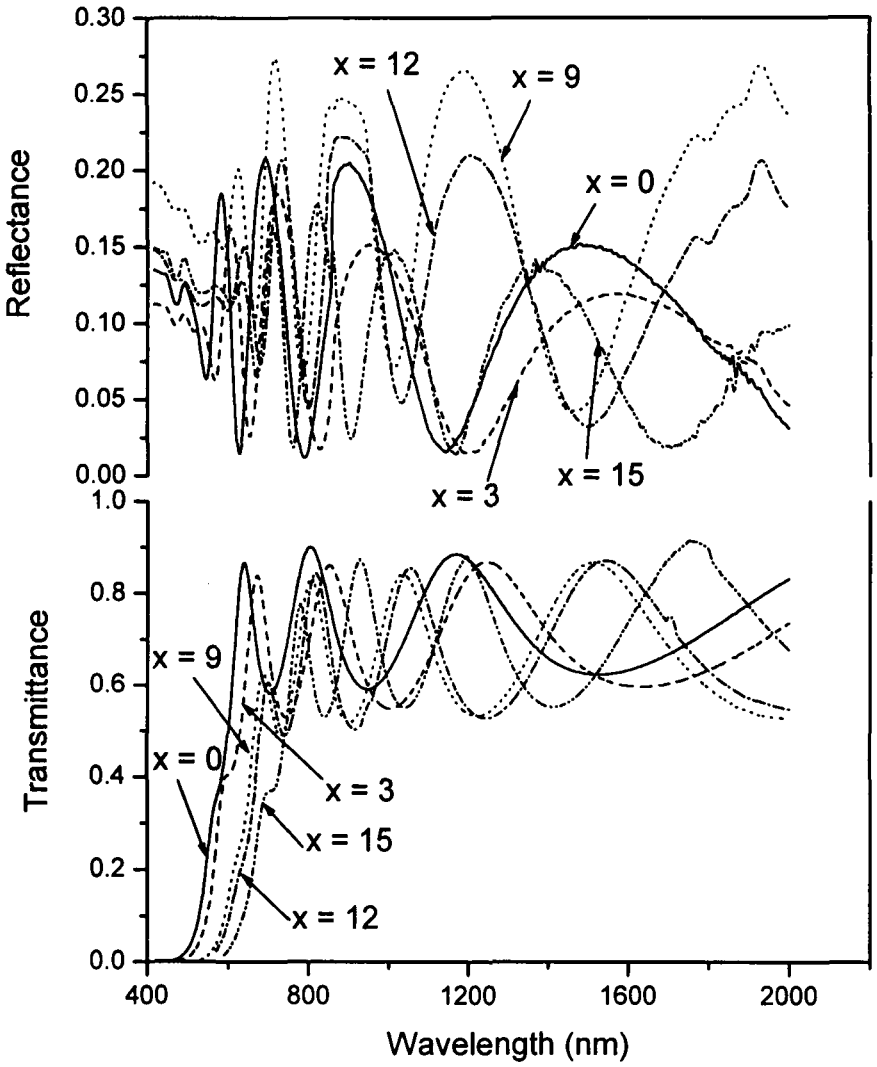

Fig. 7.2 Reflectance and transmittance spectra of $Ge_{17}Se_{83-x}Sb_x$ (x = 0, 3, 9, 12, 15) thin films.

The absorption coefficient (α) is evaluated from the relation [22]

$$\alpha = \frac{2.303}{d}\log\left(\frac{1-R}{T}\right) \qquad [1]$$

Absorption coefficient has been found to be of the order of 104 cm^{-1}. The optical energy gap $\left(E_g^{opt}\right)$ of the $Ge_{17}Se_{83-x}Sb_x$ thin films has been determined from absorption coefficient data as a function of photon energy, according to the generally accepted 'non-direct transition' model for amorphous semiconductors [23], proposed by Tauc [24]

$$\alpha h\nu = B\left(h\nu - E_g^{opt}\right)^2 \qquad [2]$$

where B is the slope of the Tauc edge called band tailing parameter.

Figure 7.3 shows the variation of $(\alpha h\nu)^{1/2}$ with hν.

The optical energy gap has been determined by the intercepts of extrapolations to zero with the photon energy axis $(\alpha h\nu)^{1/2} \rightarrow 0$ (i.e. Tauc extrapolation). The optical energy gap has been found to decrease with the increase in Sb content (see Table 7.1), from 1.92 eV for x = 0 to 1.63 eV for x = 15. This decrease in the optical energy gap $\left(E_g^{opt}\right)$ with increasing Sb content may be explained on the basis of the chemical bond approach proposed by Biecerano and Ovshinsky [25].

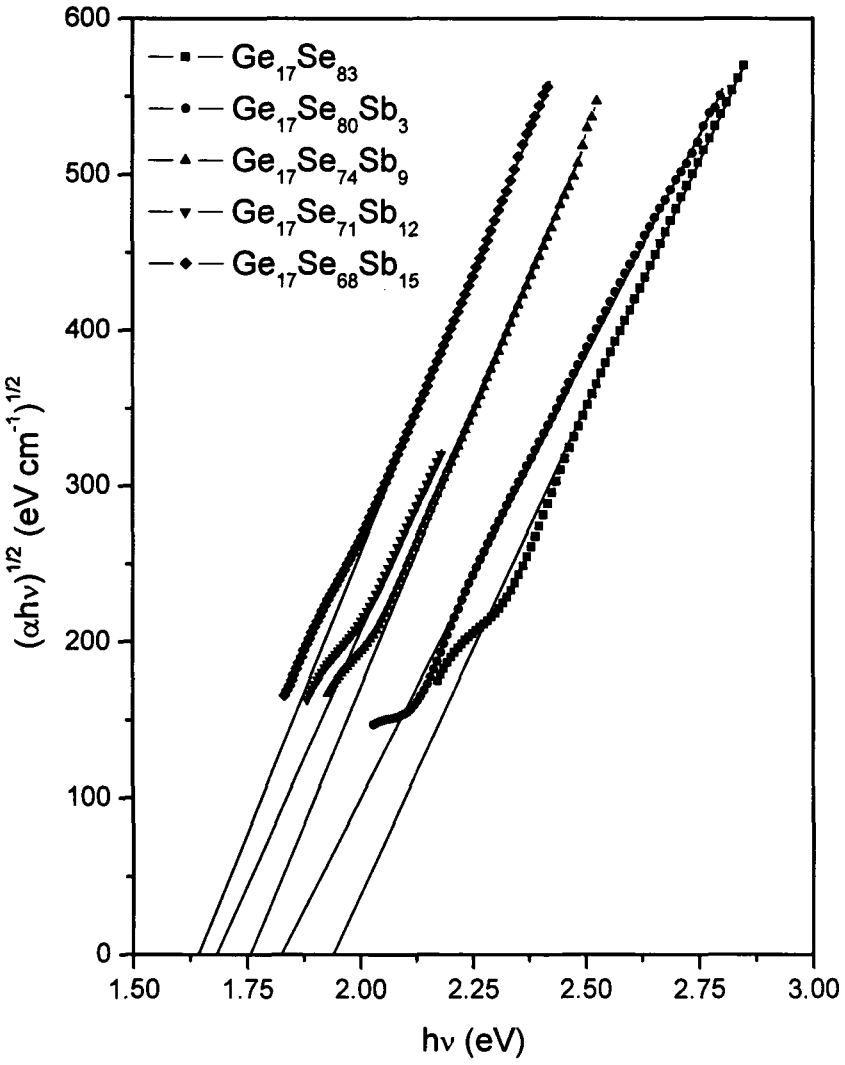

Fig. 7.3 Plot of $(\alpha h\nu)^{1/2}$ versus $h\nu$ for $Ge_{17}Se_{83-x}Sb_x$ (x = 0, 3, 9, 12, 15) thin films.

Table 7.1 Values of thickness (d), optical energy gap $\left(E_g^{opt}\right)$, energy gap $\left(E_g^{th}\right)$, oscillator strength (E_0) and dispersion energy (E_d), static refractive index (n_0) and high frequency dielectric constant (ε_∞) of $Ge_{17}Se_{83-x}Sb_x$ (x = 0, 3, 9, 12, 15) thin films.

x	d (nm)	$\left(E_g^{opt}\right)$ (eV)	$\left(E_g^{th}\right)$ (eV)	(E_d) (eV)	(E_0) (eV)	n_0	ε_∞
0	560	1.92	1.80	19.78	3.94	2.45	6.02
3	540	1.82	1.74	23.22	3.55	2.75	7.55
9	600	1.75	1.63	23.23	3.35	2.82	7.93
12	590	1.67	1.56	23.50	3.31	2.85	8.09
15	630	1.63	1.50	24.59	3.29	2.91	8.47

They assumed that heteropolar bonds have preeminence over homopolar bonds and bonds are formed in the sequences of decreasing bond energy until all the available valances of the atoms are saturated. Each constituent is coordinated by 8-N atoms, whereN is the number of electrons in the outer shell and this is equivalent to neglecting the dangling bonds and the other valence defects. Increasing Sb content at the expense of selenium leads to the formation of heteropolar Se–Sb (42.9 kcal mol^{-1}) bonds at the expense of Se–Se (44.0 kcal mol^{-1}) bonds [26]. Hence, the formation of Se–Sb bonds reduces the average energy of the system. As the optical energy gap is a bond sensitive property so the decrease in the average bond energy of the system leads to a decrease in the optical energy gap with increasing Sb content. Further decrease in optical energy gap with increase in Sb content may also be correlated with the decrease in the average single bond energy ($\overline{H}$ s/m) [21] (where $\overline{H}_s$ is the average heat of atomization and m represents coordination number) which is a measure of cohesive energy; i.e. a decrease in ($\overline{H}_s$/m) will lead to a decrease in the optical energy gap. The decrease in the optical energy gap with the increase in Sb content may also be explained on the basis of electronegativity. Since electronegativity of Sb (2.05) is less than Se (2.55), the substitution of Sb (electropositive element) for Se may raise the energy of some lone pair states and hence broaden the valence band. This will give rise to additional absorption over a wider range of energy leading to band tailing and hence shrinking the optical energy gap.

Energy gap has also been calculated theoretically for $Ge_{17}Se_{83-x}Sb_x$ (x = 0, 3, 9, 12, 15) system using the relation proposed by Shimakawa [27]

$$\left(E_g^{opt}\right)(AB) = YE_g(A) + (1 - Y)E_g(B), \qquad [3]$$

where Y is the volume fraction of element A, $E_g(A)$ and $E_g(B)$ are the optical energy gaps for elements A and B, respectively. The conversion from atomic composition (at%) or molecular composition (mol%) to volume fraction Y is made using atomic or molecular mass and density of the constituent elements. The values of the calculated energy gap are given in Table 7.1 and are in good agreement with the optical energy gap evaluated from absorption coefficient data. This leads to the anticipation that a modified virtual crystal approach for mixed crystals may be acceptable for an amorphous system.

The extinction coefficient (k) has been calculated using the relation [22]

$$k = \frac{2.303\lambda}{4\pi d}\log\left(\frac{1-R}{T}\right), \qquad [4]$$

where λ is the wavelength, R is reflectance, T is transmittance and d is the thickness of the film. The refractive index (n) has been calculated using the relation [22]

$$R = \frac{(n-1)^2 + k^2}{(n+1)^2 + k^2} \qquad [5]$$

It is observed that both the extinction coefficient and the refractive index decrease with the increase in wavelength. The decrease in the refractive index with increasing wavelength shows the normal dispersion of the system under investigation. The values of n and k are given in table 2 at 800 nm. Further, it is observed that with the increase in Sb content the refractive index increases (see Table 7.2).

Table 7.2 Values of refractive index (n), extinction coefficient (k), dielectric constant (ε_r), dielectric loss (ε_i) and optical conductivity (σ) at 800 nm of $Ge_{17}Se_{83-x}Sb_x$ (x = 0, 3, 9, 12, 15) thin films.

x	n	k	ε_r	ε_i	$\sigma x10^{12}$ (s^{-1})
0	2.62	0.0045	6.86	0.023	4.23
3	2.78	0.0079	7.73	0.044	8.20
9	2.91	0.0081	8.47	0.047	8.87
12	2.98	0.0097	8.88	0.058	10.62
15	3.05	0.0099	9.30	0.060	10.91

The high refractive index values are advantageous for strong optical field confinement, which allows small waveguide bend radii leading to compact circuit designs and enhances the optical intensities for efficient nonlinear interactions. The increase in the values of n with increasing Sb content may be explained on the basis of polarizability. The larger the atomic radius of the atom, the larger will be its polarizability and consequently, according to the Lorentz–Lorenz relation between refractive index and polarizability, the larger will be the refractive index. The Lorentz–Lorenz relation is [28]

$$\frac{n^2-1}{n^2+2}=\frac{1}{3\varepsilon_0}\sum_i N_i\alpha_{pi}\ , \qquad [6]$$

where ε_o is the vacuum permittivity, Ni is the number of polarizable units of type i per unit volume with polarizability α_{pi} . The atomic radii of Se (1.16 Å) and Sb (1.40 Å) [29]. Thus, the substitution of more polarizable Sb atoms by less polarizable Se atoms may lead to an increase in refractive index. On the other hand, a clear red-shift of the optical absorption edge is observed in Figure 7.2, with increasing Sb content to the host matrix Ge–Se. It is stressed that, following the fundamental Kramers–Kronig relationships, the red-shift in the absorption spectrum must necessarily give an increased refractive index value. It is worth quoting here the fundamental relationship, $n=1+\left(1/2\pi^2\right)\int_0^\infty \alpha_{pi}d\lambda$, which allows checking the consistency of the values of the refractive index.

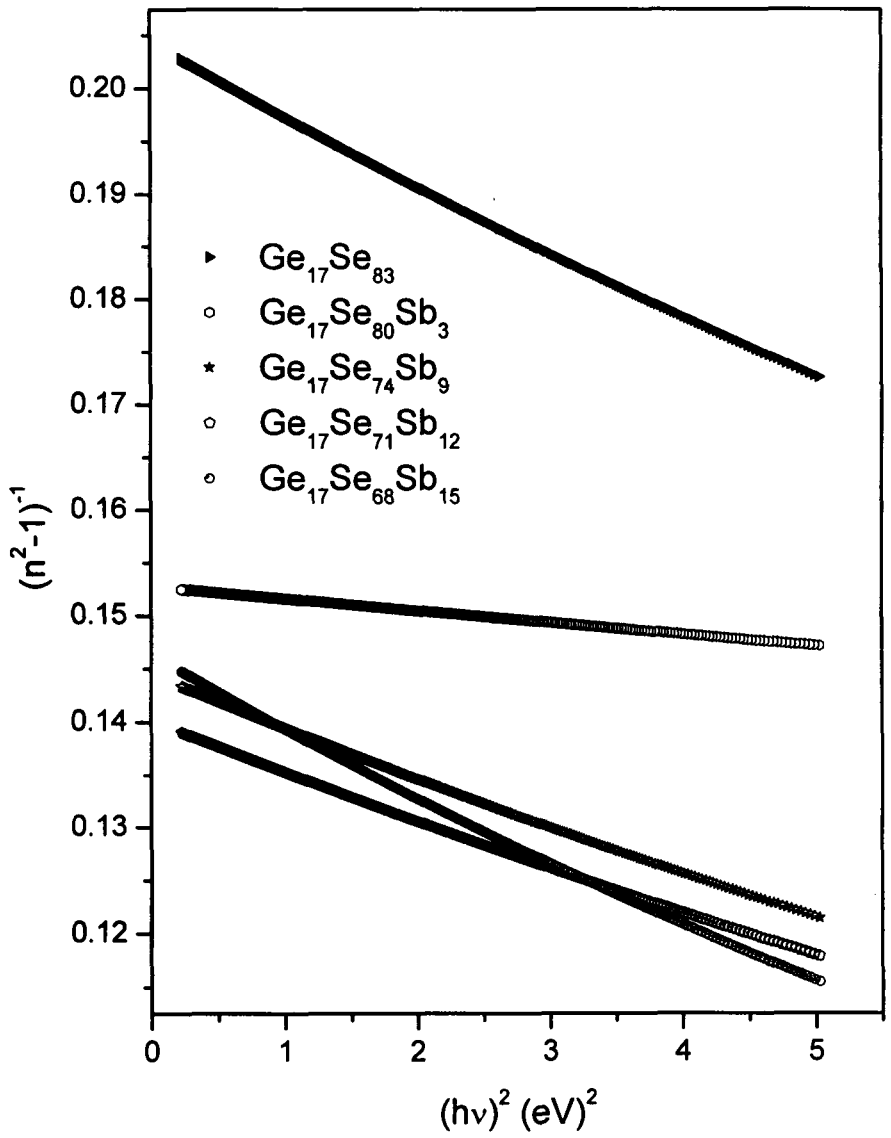

Fig. 7.4 Plot of refractive index factor $(n^2-1)^{-1}$ versus $(h\nu)^2$ for $Ge_{17}Se_{83-x}Sb_x$ (x = 0, 3, 9, 12, 15) thin films.

The high frequency properties of $Ge_{17}Se_{83-x}Sb_x$ thin films could be treated as a single oscillator. The spectral dependence of the refractive index, in the visible and nearinfrared regions, has been analysed in terms of the WDD single effective oscillator model [30],

$$n^2 - 1 = \frac{E_0 E_d}{E_0^2 - (hv)^2} \quad . \qquad [7]$$

The values of the parameters E_0 and E_d were estimated by plotting $(n^2-1)^{-1}$ versus hv (Figure 7.4) and fitting the relation to a straight line. These two parameters of the model are the dispersion energy, E_d, that measures the average strength of interband optical transitions and is associated with the changes in the structural order of the material and the effective oscillator energy, E_0, which can be directly correlated with optical energy gap by an empirical formula. It is empirically found that the dispersion parameter can be expressed by

$$E_d = \beta N_e Z_a N_c,$$

where N_e is the effective number of valence electrons per anion, Nc is the effective coordination number of the cations nearest neighbour to the anion, Z_a is the formal chemical valency of the anion, β is a two-valued constant with either an ionic or a covalent value [30]. It is observed that the variation in the dispersion energy, E_d, results primarily from changes in the nearest neighbour coordination number. Hence, the increase in the dispersion energy value is usually associated with the increase in coordination number. It has been earlier reported that coordination number increases for the $Ge_{17}Se_{83-x}Sb_x$ (x = 0, 3, 9, 12, 15) system [21]. The oscillator energy, E_0, is

independent of the scale of (ε_i) (called dielectric loss) (see tables 7.1 and 7.2) and is subsequently an average energy gap, whereas E_d depends on the scale of (ε_i) and thus serves as interband strength parameters [31].

Furthermore oscillator energy E_0 can also be used to estimate an approximate value of the optical energy gap $\left(E_g^{opt}\right)$ by using an empirical relation proposed by Tanaka [32], relating E_0 to the optical energy gap, $E_0 \approx 2 \times E_g^{opt}$. It is clear from table 7.1 that the values obtained by using the above relation are in good agreement with that obtained by using Tauc's extrapolation method. Similar results have also been reported earlier by various researchers [33, 34]. The values for the static refractive index (n_0) have been calculated from WDD dispersion parameters E_0 and E_d by using the formula

$$n_0 = \left(1 + \frac{E_d}{E_0}\right)^{1/2} . \qquad [8]$$

The values of n_0 are calculated by extrapolating the WDD dispersion equation to $h\nu \rightarrow 0$ {see equation (7)}. The values of n_0 have been given in Table 7.1. The high frequency dielectric constant (ε_∞) has been calculated from the relation $\varepsilon_\infty = (n_0)^2$ and the obtained values are reported in table 7.1. The dielectric constant (ε_r) and dielectric loss (ε_i) has been determined from $\varepsilon_r = n^2 - k^2$ and $\varepsilon_i = 2nk$ for $Ge_{17}Se_{83-x}Sb_x$ thin films. The optical conductivity calculated from $\sigma = \alpha nc/4\pi$, where α is the absorption coefficient, n is the refractive index and c is the velocity of light. Optical conductivity has been found to increase with increasing Sb content. This increase may be a

consequence of increased density of localized states in the gap itself due to the appearance of new defect states and Sb containing structural elements [35].

The dielectric constant, dielectric loss and optical conductivity directly depend on n, k and α and hence follow similar trends. The values of ε_r , ε_i and σ are given in table 2 at 800 nm.

7.4: Conclusions

Optical properties of thin films of $Ge_{17}Se_{83-x}Sb_x$ (x = 0, 3, 9, 12, 15) glassy alloys were studied using their reflection and transmission spectra in the spectral region 400–2000 nm. The interband transitions are found to be indirect type and the optical energy gap has been estimated using the Tauc method. The optical energy gap has been found to decrease from 1.92 eV for x = 0 to 1.63 eV for x = 15. The decrease in the optical energy gap is explained mainly on the basis of bond energies and on the concept of electronegativity. The energy gap calculated using Shimakawa's relation follows the same trend as the optical energy gap estimated from Tauc's method. The refractive index has been found to increase with the increase in Sb content. The increase in the refractive index with Sb content has been explained on the basis of polarizability. Dispersion of refractive index is studied using the WDD single oscillator model. The static refractive index has been found to increase with increasing Sb content from 2.45 (x = 0) to 2.91 (x = 15). The oscillator energy, E_0, follows the empirical relation with the optical energy gap.

References:

[1] V.F. Kokorina, Glasses for Infrared Optics (Boca Raton, FL: CRC Press) (1996).

[2] J.A. Savage, J. Non-Cryst. Solids **47** (1982) 101.

[3] P. Sharma and S.C. Katyal, Thin Solid Films **515** (2007) 7966.

[4] A.B. Seddon, J. Non-Cryst. Solids **184** (1995) 44.

[5] M. Frumar and T. Wagner, Curr. Opin. Solid State Mater. Sci. **7** (2003) 117.

[6] A. Znobrik, J. Stetzif, I. Kavich, V. Kavich, V. Osipenko, I. Zachko, N. Balota and O. Jakivchuk, Ukr. Phys. J. **26** (1981) 212.

[7] J.S. Sanghera and I.D. Aggarwal, J. Non-Cryst. Solids **256 & 257** (1999) 6.

[8] K. Schwartz, The Physics of Optical Recording (Berlin: Springer) (1993).

[9] A. Bradley, Optical Storage for Computers Technology and Applications (New York: Ellis Harwood Limited) (1989).

[10] J. Bradangna and S.A. Keneman, Holographic Recording Media ed H M Smith (Berlin: Springer) (1977).

[11] P.A. Thielen, L.B. Shaw, J.S. Sanghera and I.D. Aggarwal, Opt. Express **1124** (2003) 3228.

[12] J. Troles, F. Smektala, G. Boudebsa, A. Monteila, B. Bureau and J. Lucas, J. Optoelectron. Adv. Mater. **4** (2002) 729.

[13] H. Nasu, R. Kubodera, M. Kobayasi, M. Nakamura and K. Kamiya, J. Am. Ceram. Soc. **73** (1990) 1974.

[14] M.M. Hafiz, A.H. Moharram, M.A. Abdel-Rahim and A.A. Abu-Sehly, Thin Solid Films **292** (1997) 7.

[15] M.A. Majeed Khan, M. Zulfequar and M. Husain, J. Opt. Mater. **22** (2003) 21.

[16] P. Sharma and S.C. Katyal, Physica B **403** (2008) 3667.

[17] J. Vazquez, C. Wagner and P. Villares, J. Non-Cryst. Solids **235** (1998) 548.

[18] G. Fuxi, J. Non-Cryst. Solids **140** (1992) 184.

[19] H.L. Ma, Y. Guimond, X.H. Zhang and J. Lucas, J. Non-Cryst. Solids **256 & 257** (1999) 165.

[20] R. Fairman and B. Ushkov, Semiconducting Chalcogenide Glass I (Amsterdam: Elsevier) (2004)

[21] P. Sharma, V.S. Rangra, S.C. Katyal and P. Sharma, Optoelectron. Adv. Mater.—Rapid Commun. **1** (2007) 363.

[22] M.M. Abd El-Raheem, J. Phys.: Condens. Matter **19** (2007) 216209.

[23] E. Marquez, J.M. Gonzalez-Leal, A.M. Bernal-Oliva, T. Wagner and R. Jimenez-Garay, J. Phys. D: Appl. Phys. **40** (2007) 5351.

[24] J. Tauc, Amorphous and Liquid Semiconductors (New York: Plenum) (1979).

[25] J. Biecerano and S.R. Ovshinsky, J. Non-Cryst. Solids **74** (1985) 75.

[26] S.S. Fouad, A.H. Ammar and M. Abo-Ghazala, Physica B **229** (1997) 249.

[27] K. Morigaki, Physics of Amorphous Semiconductors (Singapore: World Scientific) (1999).

[28] S.R. Elliott, The Physics and Chemistry of Solids (Chichester: Wiley) (2000).

[29] C.N.R. Rao, M.V. George, J. Mahanty and P.T. Narasimhan, A Handbook of Chemistry and Physics (New Delhi: Affiliated East-West Press) (1970).

[30] S.H. Wemple, S.H. and M. DiDomenico, Phys. Rev. B **3** (1971) 1338.

[31] S.H. Wemple, Phys. Rev. B **7** (1973) 3767.

[32] K. Tanaka, Thin Solid Films **66** (1980) 271.

[33] J.M. Gonzalez-Leal, A. Ledesma, A.M. Bernal-Oliva, R. Prieto-Alcon, E. Marquez, J.A. Angel and J. Carabe, Mater. Lett. **39** (1999) 232.

[34] T.I. Kosa, T. Wagner, P.J.S. Ewen and A.E. Owen, Phil. Mag. B **71** (1995) 311.

[35] N.F. Mott, E.A. Davis, Phil. Mag. **22** (1970) 903.

Chapter-8

Summary, Discussions and Suggestions

8.1: Summary and Conclusions

Chalcogenide glasses form an important class of materials which are used in various solid state devices and in infrared optics. In this thesis the work reported is concerned with the structural, physical, thermal and optical study of $Ge_{17}Se_{83-x}Sb_x$ (x = 0, 3, 9, 12, 15) glassy system.

Ge-Se-Sb system has been studied for its structural properties using far infrared transmission spectra. The structure of the taken glassy system is based on the chain structure of selenium atoms interlinked by the tetrahedrally coordinated germanium and conceivably trivalent antimony atoms. The bond energies and probability functions conclude the least existence of bonds like Ge-Ge, Sb-Sb and Ge-Sb whose bond energies are very low. The comparison of theoretical and experimental values of the wave numbers for the stretching vibrational modes shows that the experimental wave number value for Ge-Se bond and Se-Sb bonds are greater than their corresponding theoretical values but it is just reverse for the Se-Se bonds. This may be due to the existence of more closely lying modes which leads to the broadening in the absorption bands.

Various physical parameters for $Ge_{17}Se_{83-x}Sb_x$ (x = 0, 3, 9, 12, 15) glassy system has been calculated theoretically. This study leads to the conclusion that the average coordination number, number of constraints, average heat of atomization, mean bond energy and glass transition temperature increases with the increase of Sb content while the number of lone pair of electrons decreases. The increase of glass transition has been explained on the basis of accumulation of Sb in Se-chain.

Thermal studies of the $Ge_{17}Se_{83-x}Sb_x$(x = 0, 3, 9, 12, 15) glassy system has been done by using DTA thermograms. Hruby parameter of the system under investigation is indicating not high stability against crystallization and also indicating the formation of glass of high-molecular polymer type. Also it can be seen that glass transition temperature (T_g) and glass crystallization temperature (T_c) shift towards higher temperature with increase in antimony content. This increase in the value of glass transition temperature (T_g) can be explained on the basis of CONM according to which the heteropolar bond is favoured over the homopolar bond.

Different parameters related to optical properties were calculated for vacuum evaporated thin films of $Ge_{17}Se_{83-x}Sb_x$ (x = 0, 3, 9, 12, 15) glassy system using their reflection and transmission spectra in the spectral region 400–2000 nm. The interband transitions are found to be indirect type and the optical energy gap has been estimated using the Tauc method. The optical energy gap has been found to decrease from 1.92 eV for $x = 0$ to 1.63 eV for $x = 15$. The decrease in the optical energy gap is explained mainly on the basis of bond energies and on the concept of electronegativity. The energy gap calculated using Shimakawa's relation follows the same trend as the optical energy gap estimated from Tauc's method. The refractive index has been found to increase with the increase in Sb content. The increase in the refractive index with Sb content has been explained on the basis of polarizability. Dispersion of refractive index is studied using the WDD single oscillator model. The static refractive index has been found to increase with increasing Sb content from 2.45 (x = 0) to 2.91 (x = 15). The oscillator energy, E_0, follows the empirical relation with the optical energy gap.

8.2: Suggestions for the future work

- The system under study is of ternary in nature. The work can be extended to quaternary compounds. This may enhance various optical and thermal properties.
- Various thickness related optical studies may be done by doping the present system by various dopants. This may lead to a change in refractive and transmittive properties of the system under consideration.
- The present work can be extended by doing electrical studies of the system. This helps in understanding the electrical conductivity and dielectric losses in the system.
- Raman spectroscopy, SEM may be done to furthur enhance the structural study of the system under consideration.